8-2014

Application of Membrane Processes for Concentration and Separation of Sugar Streams in Biofuel Production

Mohammadmahdi Malmali
University of Arkansas, Fayetteville

Application of Membrane Processes for Concentration and Separation of Sugar Streams in Biofuel Production

Application of Membrane Processes for
Concentration and Separation of Sugar Streams in
Biofuel Production

A dissertation submitted in partial fulfillment
of the requirements for the degree of
Doctor of Philosophy in Chemical Engineering

by

Mohammadmahdi Malmali
Razi University
Bachelor of Science in Chemical Engineering, 2007
Sharif University of Technology
Master of Science in Chemical Engineering, 2010

August 2014
University of Arkansas

This dissertation is approved for recommendation to the Graduate Council.

_____
Dr. S. Ranil Wickramasinghe
Dissertation Director

_____
Dr. Tom O. Spicer
Committee Member

_____
Dr. Ravi D. Barabote
Committee Member

_____
Dr. Ryan Tian
Committee Member

_____
Dr. Xianghong Qian
Committee Member

Abstract

The overall objective of this study was identification and development of a sugar concentration/separation membrane filtration unit to improve the bioconversion of lignocellulosic biomass into chemicals and fuels. This thesis is divided into three main parts. The first part is about our studies on the use of nanofiltration membranes for concentration of sugars in a lignocellulosic biomass hydrolysate. In addition, the feasibility of simultaneous removal of acetic acid, 5-(hydroxymethyl)furfural and furfural from the hydrolysate has also been investigated. The results obtained indicate that both concentration of sugars and removal of hydrolysis degradation products is feasible. However, careful selection of the membrane and operating conditions will be essential. Dead end filtration experiments have been used to test a number of commercially available nanofiltration membranes under a range of operating conditions. Model feed streams as well as real hydrolysates have been tested. The method developed here could be used to quickly screen membranes. Promising membranes and operating conditions could then be more rigorously tested in tangential flow operation.

The second part of this work focuses on recycle of cellulase enzyme (biocatalyst) used to catalyze the biopolymers of cellulose to monomeric soluble sugars. The enzyme represents one of the main costs in bioconversion of lignocellulosic biomass into biofuel. But exploration and development of efficient ways to reuse and recycle the enzyme are of great interest. Here we explore the use of microfiltration and ultrafiltration membranes for enzyme recycle and reuse.

Third part of this work is about modification of membranes using Layer-by-Layer (LbL) deposition of polyelectrolytes. Deposition of ultra-thin hyperbranched anionic and cationic polyelectrolytes on top of polysulfone ultrafiltration membranes results in a porous modified membrane showing nanofiltration characteristics. Deposition of polyelectrolytes on top of the

polysulfone membrane substrate is confirmed by ATR-FTIR spectra, SEM images and filtration tests. We carried out several nanofiltration tests with 20 mM model feed streams containing sucrose, glucose and xylose. Results show that these membrane are capable of separating mono- and disaccharides.

Acknowledgments

The support from my wife, Hadis, was invaluable. I could not have succeeded without her. She was a great support from the beginning until the commencement ceremony.

I would like to specially thank Dr. Wickramasinghe for all his efforts and helps during my PhD research. He introduced me to lots of members in industry and academia..

I also thank my colleagues at University of Arkansas, Membrane Separations Laboratory.

Dedication

I dedicate this work to my beloved wife, Hadis. You have sacrificed yourself to help me and to be with me during my journey towards PhD degree. I will remember all those days and night standing next to me and supporting me. You helped me to be a better person.

Table of Contents

Chapter 1: Introduction

1. Energy, the Big Picture

Energy was always a concerning global issue because it is a critical driver for growth and improvements in life standards. The picture of energy has been changed dramatically. During 1990s, long-term energy prices were estimated to be low (below $20 for a barrel of oil). Also, widespread emerging idea of gas as an energy medium was another factor that resulted in more decrease in energy price during 1990s. Industry was anticipating continual fall in gas prices since there were substantial explorations for new gas resources. Besides, there was an increasing growth in commodities and infrastructures for oil and gas explorations.

However, the picture changed quickly in 2008. Energy security becomes a significant concern. There was not enough security for a long-term supply. On the other hand, some of the environmental issues, such as climate change which leaded to more restrictive standards for energy products, increased the oil price up to $60, and spiked to $100 per barrel on 2005. Depletion of fossil fuel reserves was another threat for the long-term production of fossil fuels. Step by step, oil high prices and an energy-futuristic approach leaded to more interest in other types of energy, especially renewable. Renewables can provide a long-term secure and environmental-friendly energy resource. Since 2008, there is an ever-increasing interest for mainstream investors in renewable energies.

In 2007, there were aggressive goals set by Energy Independence and Security Act [1] (EISA): first, to move renewable fuels into the marketplace; second, reduce the nation's dependence on foreign sources of energy; third, reduce greenhouse gas (GHG) emissions. Renewable energies can significantly diminish the rate of GHG emissions, and help to decelerate global warming. Solar radiation, tide, geothermal, wind, and biomass are different types of

renewable energies, which have received significant attention during the last 10 years. Among these renewable resources, lignocellulosic biomass has specific importance to US Department of Energy (DOE). It is sufficiently abundant and can provide a sustainable source of energy for several purposes. It is also an important renewable energy for several reasons (Figure 1). Currently, the US industry and transportation system consumes 20 million barrels of crude oil every day, of which 60% is imported, and 70% of imported fuel is consumed for liquid transportations purposes [2]. Two-third of US oil consumption is in transportation sector, which accounts for one-third of the nation's GHG emissions. Biomass is also the only biorenewable feedstock that can be converted to liquid transportation fuel. Moreover, liquid fuel derived from lignocellulosic biomass can reduce the amount of GHC emission since it releases the CO2 that the plant has captured through the photosynthesis. Thus lignocellulosic biomass could represent a sustainable source of transportation fuel.

Gasoline and diesel fuels are the two important global transportation fuels. Lignocellulosic biomass can provide different transportation fuels such as: sugar ethanol, cellulosic ethanol, grain ethanol, biodiesel, pyrolysis liquids, green diesel, green gasoline, butanol, methanol, syngas liquids, biohydrogen, algae diesel, algae jet fuel, and hydrocarbons [3].

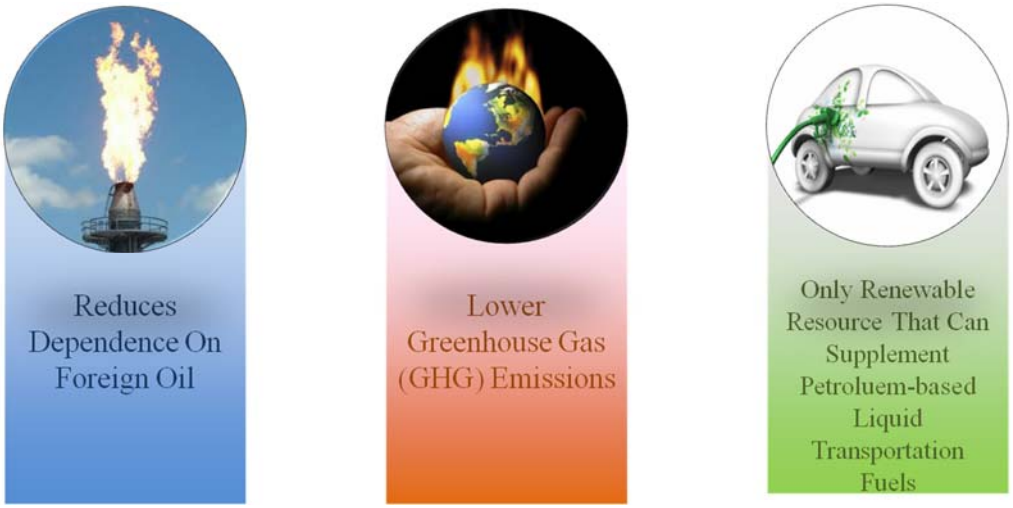

Figure 1: Factors showing the importance of biomass-derived renewable energy

2. Lignocellulosic Biomass

Lignocellulosic biomass consists of three major structural biopolymeric components: cellulose, hemicellulose and lignin [4]. Ninety percent of the plant weight is stored in the form of cellulose, hemicellulose and lignin. As it is depicted in Figure 2, lignocellulosic biomass typically contains 38-50% cellulose, 23-32% hemicellulose, 15-25% lignin and 5-13% extraneous substances. The structure of these constituents forming lignocellulosic biomass is shown in Figure 3. Lignocellulosic biomass includes wood remains, hard wood and softwood (dead tree, branches, tree stumps), yard clippings, perennial grasses, crop (corn, switchgrass, sorghum, sugarcane, bamboo, willow) residues, wood chips, and municipal solid waste (food waste).

Hemicellulose and cellulose can be used in biofuel production, whereas lignin is being removed and burned as an additional source of energy. Biochemical conversion (enzymatic hydrolysis), thermochemical conversion, and catalytic (acid or base) conversion are three most widely-used methods applied for biomass conversion to fermentable feedstock. Different methods of biomass processing for production of biofuels are shown in Figure 4.

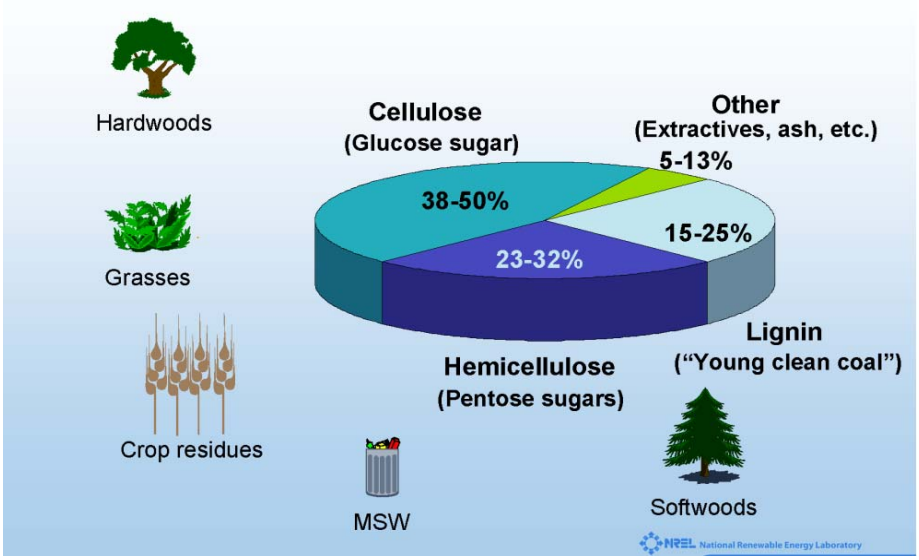

Figure 2: Lignocellulosic biomass constituents and sources [courtesy of NREL]

2.1. Cellulose

Cellulose is an abundant carbohydrate available in nature, and it is continually produced by photosynthesis. It is a linear homopolymer of (1, 4)- β-D-glucopyranosyl units and composed of crystalline and amorphous component with the degree of polymerization in the range of 10,000 to 15,000. Top and bottom of the cellulose chain is hydrophobic, while the side of the polymer chain is hydrophilic. These glucopyranosyl units have a great tendency to form hydrogen bonds [5].

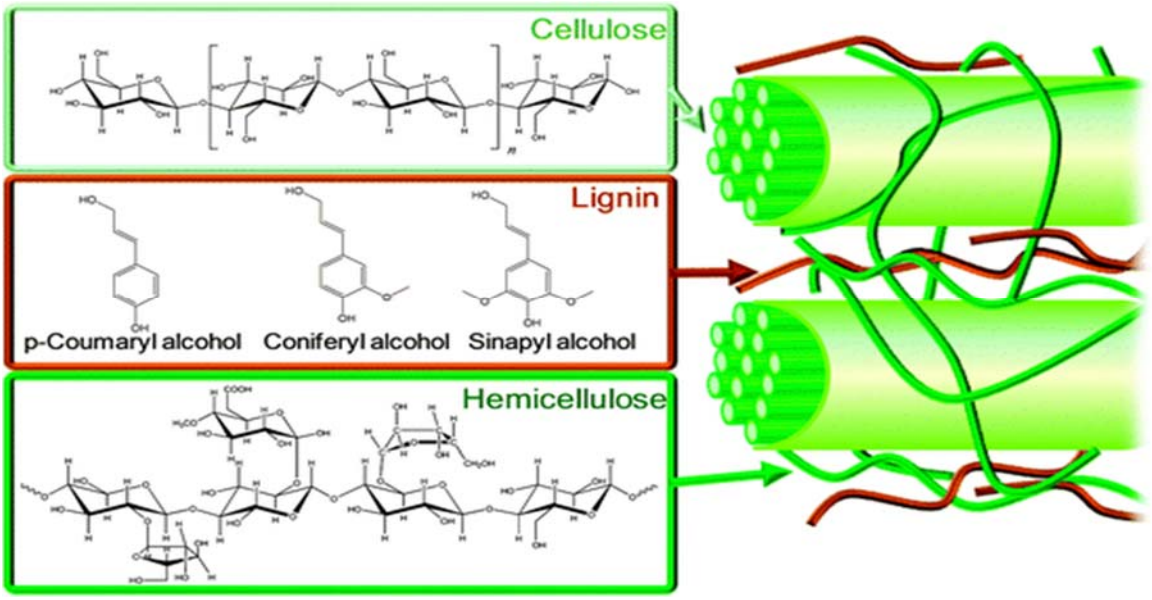

Figure 3: Biomass structure [6]

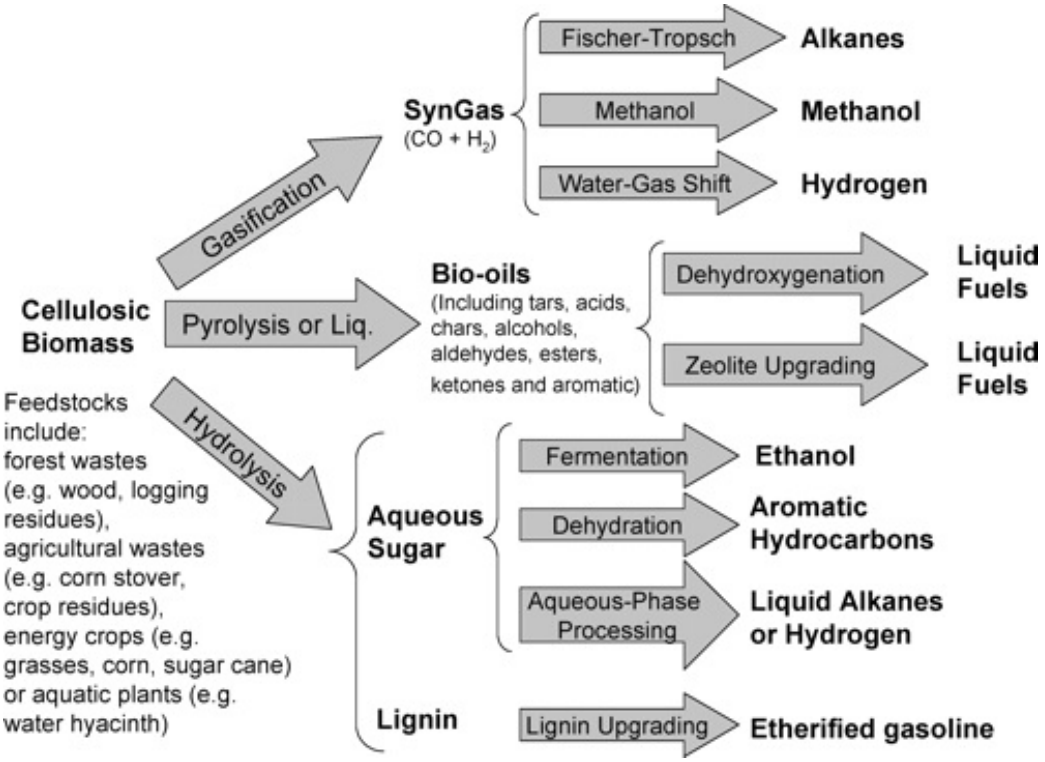

Figure 4: Strategies for biomass-derived biofuel production [7]

2.2. Hemicellulose

Hemicellulose is composed of shorter chains of polysaccharides. Hemicellulose is a polymer chain of five different carbon sugars [8]: xylose and arabinose, which are five-carbon sugars and galactose, glucose, and mannose, which are six-carbon sugars. These compounds make the carbohydrate structure of hemicellulose. The main hemicellulose feature that differs from cellulose is that hemicellulose has branches with short lateral chains consisting pentose and sugar acids. Hemicellulose is relatively easier to hydrolyze because of its amorphous branched structure [7].

2.3. Lignin

Lignin is the most complex and recalcitrant part of the lignocellulosic biomass. Also it is the least well characterized component in lignocellolusic biomass. It is primarily found in secondary cell wall and gives the structural rigidity to the plant. As a result, it is a critical component of lignocellulosic biomass for protection of plant cell against degradation by bacteria and fungi [9]. After cellulose, lignin is the most abundant organic natural product. Lignin has a very complex network with polyphenolic polymer that consists of aromatic compounds such as phenylpropanoids, hydroxycinnamoyl alcohol, and monolignols [10]. Monolignols are p-coumaryls, coniferyl, and sinapyl alcohols which give rise to p-hydroxyphenyl, guaiacyl, and syringyl. Majority of lignin in softwood is composed of guaiacyl units while in hardwood it is composed of guaiacyl and syringyl units [5]. Lignin is covalently bound and crosslinked to polysaccharides. Hydrogen bonding, ionic bonding with Ca^{+} ions, covalent ester linkages, ether linkages, and van der Waals interactions are the most important lignin-polysaccharide interaction that has direct influence one digestibility of lignocellulosic biomass [11].

2.4. Extraneous Material

Extraneous components of lignocellulosic biomass are the non-cell wall material. These material belong to a wide range of chemicals. Based on their solubility in organic and inorganic solvent they are classified as extractives and non-extractives [12]. Extractives fall into three main categories: terpens, resins, and phenols. Non-extractives are inorganic material mostly present in ash, and consist of alkali and alkali earth carbonates and oxalates [8].

3. Biorefinery

A biorefinery is a facility that integrates biomass conversion processes and equipment to co-produce value added chemicals, fuels, heat, and power from various biomass resources. It is a large integrated processing facility that produces chemical and biochemical from plant feedstocks. Biorefinery refers to the conversion of biomass feedstock into a host of valuable chemicals and energy with minimal waste and emissions [13–15]. There are there different type of biorefineries based on biomass feedstock: corn-to-ethanol, basic lignocellulosic biomass-to-ethanol, and integrated lignocellulosic biomass-to-ethanol [16]. The schematic diagram of a common lignocellulosic biomass biorefinery is depicted in Figure 5.

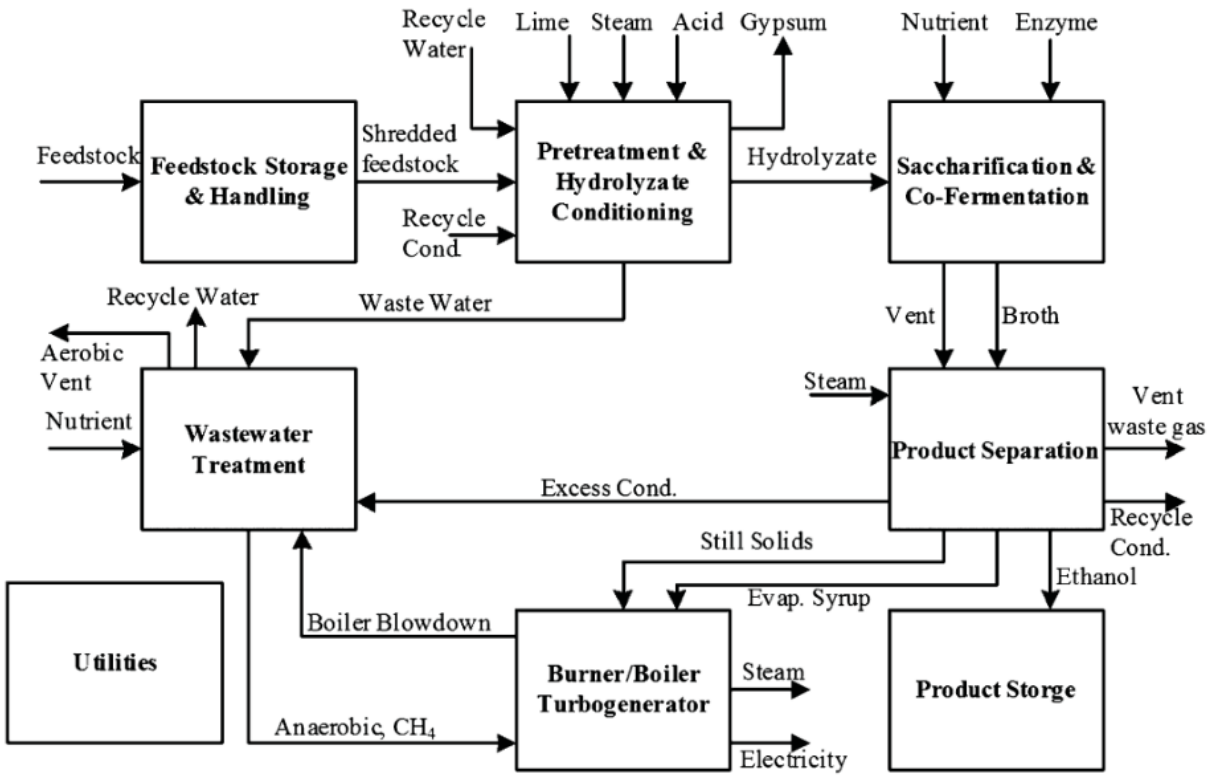

Figure 5: Process diagram of a lignocellulosic biorefinery [16]

3.1. Corn-to-ethanol Biorefinery

There are two different processes applied in corn-to-ethanol biorefineries: dry grind and wet mill. In wet mill biorefineries, there are several high-value added products derived though capital costs are higher. Schematic process diagram of dry mill and wet mill corn-to-ethanol biorefinery is shown in Figure 6.

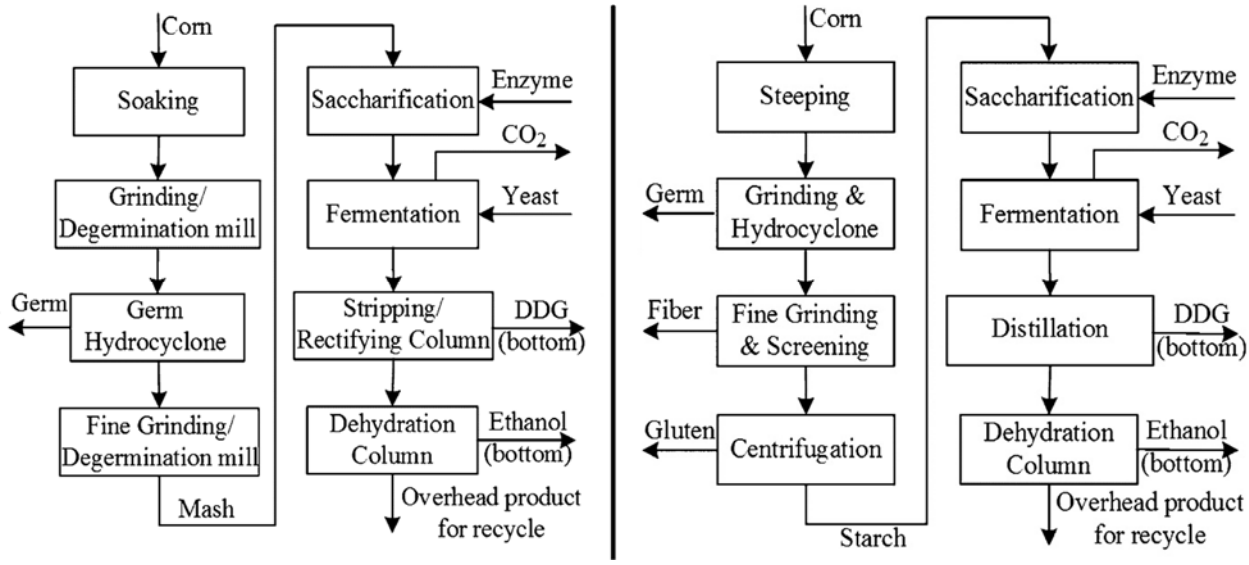

Figure 6: Corn-to-ethanol biorefinery: dry grind (left hand side) and wet mill (right hand side) [16]

3.2. Lignocellulosic Biomass-to-ethanol Biorefinery

The feedstock for this type of biorefinery is lignocellulosic biomass, such as agricultural residue (corn stover, crop straw, and sugarcane bagasse), herbaceous crops (alfalfa, switchgrass), forestry wastes, wood (hardwoods, softwoods), wastepaper, and other wastes. This feedstock is the largest potential feedstock for ethanol production. Overall, process consists of handling, pretreatment, saccharification, fermentation, product recovery and separation, wastewater treatment, product storage, and lignin combustion. However, this type of biorefinery is not widely commercialized because there are many technical, economic, and commercial barriers. A process diagram of a lignocellulosic biorefinery is shown in Figure 7.

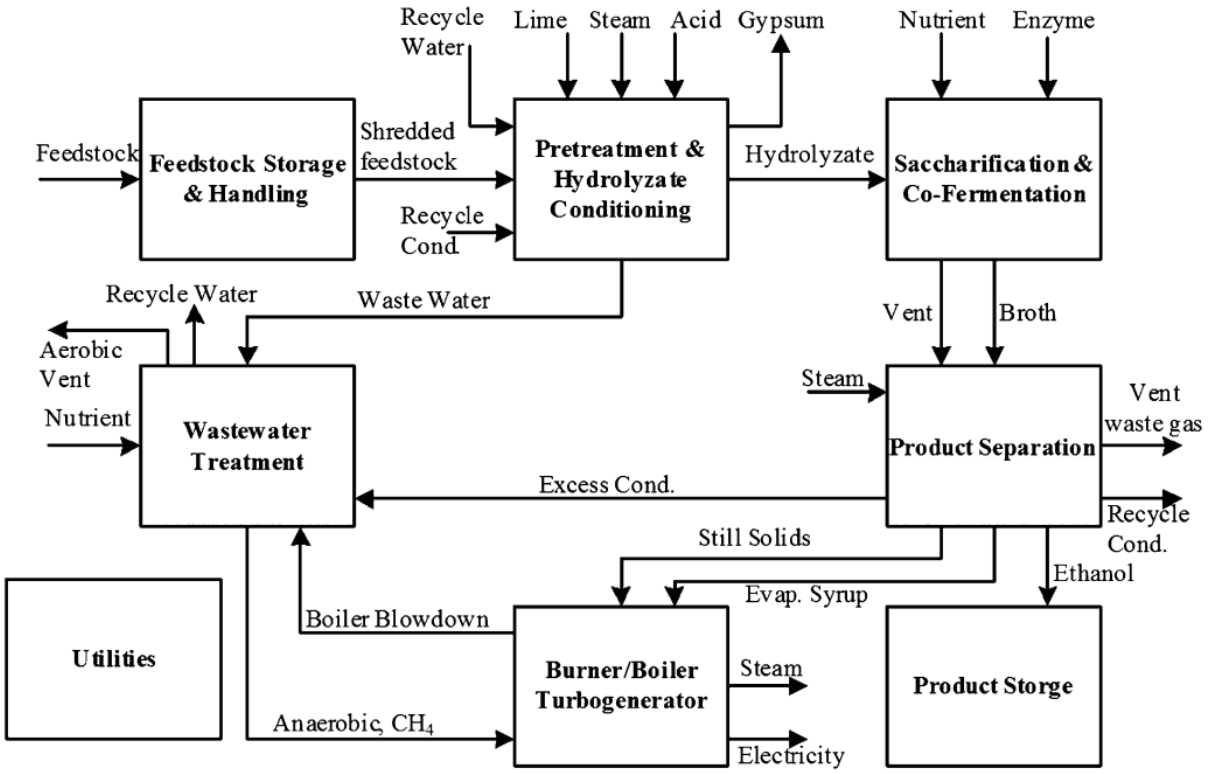

Figure 7: Process diagram of a lignocellulosic biorefinery [16]

3.3. Integrated Lignocellulosic Biorefinery

The feedstock of a so-called integrated lignocellulosic biorefinery is pulp mill which can be used to produce fuel, high value chemicals, together with pulp and paper. Hemicellulosic sugars should be extracted before pulping. Isolation of short and long fibers helps to use short fibers for sugar and long fibers for paper production. The process diagram of an integrated lignocellulosic biorefinery is shown in Figure 8.

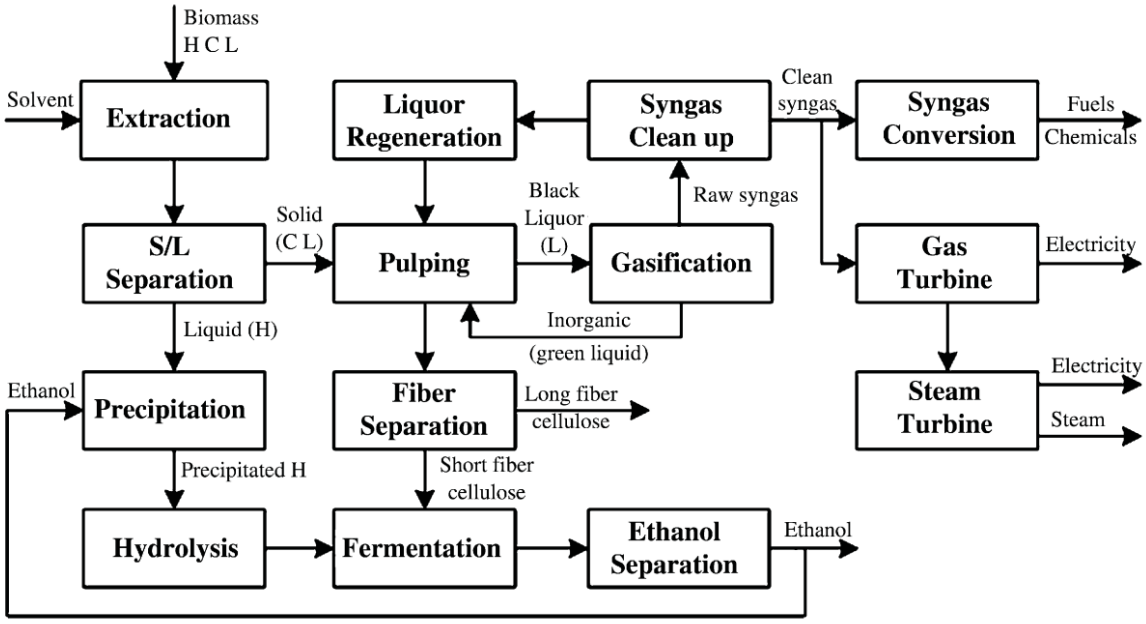

Figure 8: Flow diagram of an integrated lignocellolusic biorefinery [16]

For all biorefineries, fermentation of sugars released during hydrolysis is key. Consequently maximization of sugar yield is essential. Continuous removal of glucose, as it is produced by enzymatic hydrolysis, will minimize product inhibition and maximize glucose yields. Concentration of the sugars prior to fermentation is essential to optimize ethanol yields and fermentation conditions. Chapter 2 and some parts of chapter 4 of this thesis are about the concentration and separation of sugars present in hydrolysate, respectively.

4. Bioconversion of Lignocellulosic Biomass to Ethanol Fuel

Conversion of lignocellulosic biomass to ethanol consists of four main processes: pretreatment, hydrolysis, fermentation, and product recovery. The overall process for bioconversion of biomass to ethanol is depicted in Figure 9. During the pretreatment, majority of polymer chains of hemicellulose are hydrolyzed to monomeric sugars, mostly pentose sugars. Afterwards, during hydrolysis, cellulose is hydrolyzed to produce six-carbon sugars. Then the microorganisms will be added to hydrolysate and they digest fermentable sugars to ethanol.

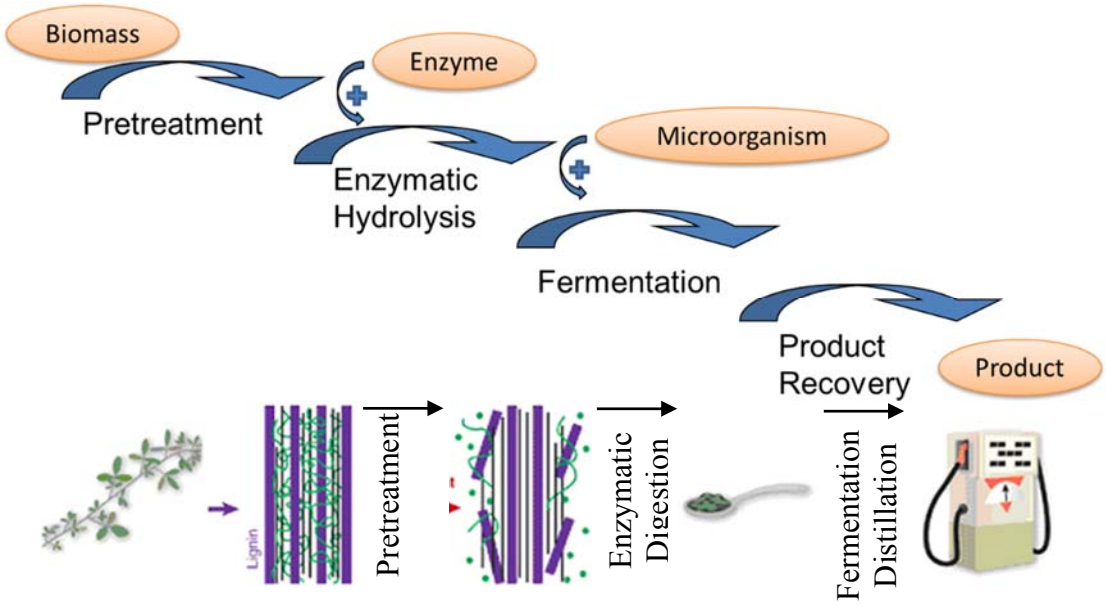

Figure 9: Bioconversion of biomass to ethanol [17]

4.1. Pretreatment

In the structural conformation of lignocellulosic biomass cellulose, hemicellulose, and lignin are woven together. This structural conformation of lignocellulosic biomass makes it very recalcitrant [18]. Cellulose is the major source of fermentable sugars. To have a high yield during the bioconversion process, it is very important to break down the polymeric structure of cellulose and release sugars. Hydrolysis occurs due to the catalytic effect of enzyme or acid, and fermentation is carried out by applying yeasts or bacteria [19]. To have an efficient hydrolysis, it is critical that cellulose be accessible to enzyme or catalyst.

An efficient pretreatment step is a necessary requirement for bioconversion lignocellulosic biomass [20]. Pretreatment is often one of the most expensive steps of a lignocellulosic biomass conversion to ethanol process [21]. Pretreatment affects the hydrolysis of cellulose by changing (1) crystallinity (higher porosity), (2) lignin content, (3) acetyl linkage, and (4) complex hemicellulose-lignin shield that surrounds cellulose in the plant cell wall [22]. Decreased

crystallinity and increased porosity makes the cellulose more accessible towards enzyme and acid, and it increases surface area. The purpose of pretreatment is to: (1) improve sugar depolymerization; (2) decrease the amount of degradation; (3) avoid byproduct formation; (4) improve the efficiency of the process. Pretreatment strategies fall into following categories: Physical (mechanical comminution, pyrolysis); physiochemical (steam explosion, ammonia fiber explosion, carbon dioxide explosion, liquid hot water); chemical (ozonolysis, acid hydrolysis, alkaline hydrolysis, oxidative delignification, organosolv process); biological; pulsed-electric-field. One of the most frequently used methods for pretreatment is dilute acid and hydrothermal pretreatment. Advantages and disadvantages of different pretreatment methods of lignocellulosic biomass is summarized in Table 1 [19,23].

Table 1: Different methods of pretreatment, their advantages and disadvantages

Pretreatment Method	Advantages	Disadvantages
Mechanical Comminution	Reduces cellulose crystallinity	Power consumption usually higher than inherent biomass energy
AFEX	Increase accessible surface area; remove lignin and hemicellulose to some extent; does not produce inhibitors for downstream processes	Not efficient for biomass with high lignin content
Steam explosion	Causes hemicellulose degradation and lignin transformation; Cost-effective; Higher yield of cellulose and hemicellulose solubilization	Generation of toxic compounds; Partial hemicellulose degradation; Incomplete disruption of the lignin-carbohydrate matrix
CO2 Explosion	Increase accessible surface area; Cost-effective; Does not cause formation of inhibitory compounds	Does not affect lignin hemicellulose; Very high pressure requirements

Cont. Table 2: Different methods of pretreatment, their advantages and disadvantages

Pretreatment Method (Cont.)	Advantages (Cont.)	Disadvantages (Cont.)
Ozonolysis	Reduces lignin content; Does not produce toxic residues	Large amount of ozone required; Expensive
Dilute acid	Less corrosion problem than concentrated acid; Less formation of inhibitors	Generation of degradation products; Low sugar concentration in exit stream; Equipment corrosion
Concentrated acid	High glucose yield; Ambient temperatures	High cost of acid and need to be recovered; Reactor corrosion problems; Formation of inhibitors
Alkaline	Removes hemicellulose and lignin; Increases accessible surface area	Long residence time; Irrecoverable salts from and incorporate to biomass stream
Orgonosolve	Hydrolyze lignin and hemicellulose	High cost; Solvents need to be drained and recovered
Pyrolysis	Produces gas and liquid products	High temperature; Ash production
Pulse electrical field	Ambient conditions; Disrupt plant cells; Simple equipment	Process needs more research
Biological	Degrades lignin and hemicellulose; Low energy requirements	Rate of hydrolysis is low

4.1.1. Degradation Products and Inhibition

There is a range of compounds produced during pretreatment of lignocellulosic biomass which are inhibitory to enzymes during hydrolysis, as well as microorganisms during fermentation process. Formation of degradation products during pretreatment depends on biomass and operating conditions such as temperature, pressure, time, pH, and concentration of catalyst. Overall,

concentration of inhibitory compounds depends on severity of pretreatment and loading of lignocellulosic biomass into the reactor [24,25].

During pretreatment or (acid) hydrolysis, hemicellulose degrades to xylose, mannose, acetic acid, and galactose, glucose and amorphous cellulose degrades to glucose. Under harsher operating conditions (high temperature, pressure or acid loading) xylose is degraded to furfural. Simultaneously, hexose sugars can degrade to form 5-hydroxymethyl furfural (HMF). In addition, lignin compounds can partially break down and produce phenolic compounds. Further degradation of furfural and HMF results in production of formic acid. Levulinic acid can also be formed through degradation of HMF [25]. The diagram for degradation of biomass substrate (spruce wood) is depicted in Figure 10.

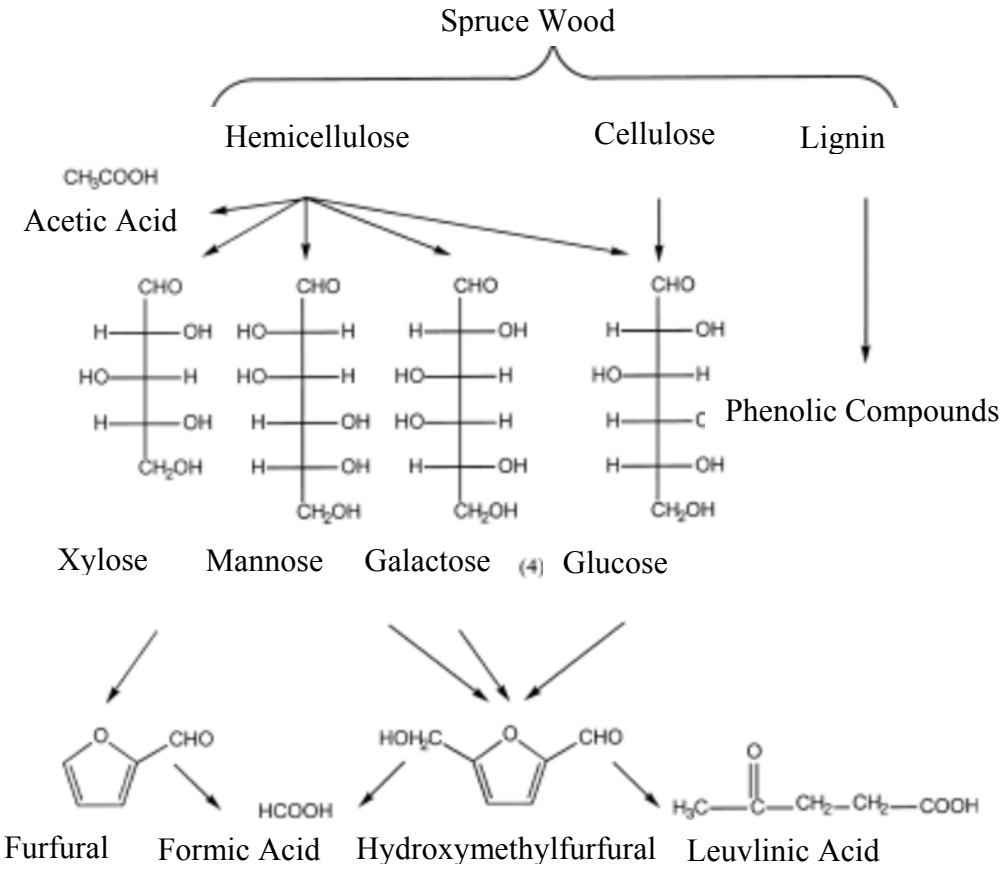

Figure 10: Reactions occurring during hydrolysis of lignocellulosic materials

Each of these toxic compounds is able to inhibit hydrolysis or fermentation with different mechanisms. Weak acids, produced through degradation reactions, inhibits cell growth. In addition, lower pHs due to existence of weak acids also results in lower fermentation rates. Two mechanisms have been proposed to explain the inhibitory effect of weak acid: uncoupling and intracellular anion accumulation. Furfural and HMF are metabolized by S. cerevisiae. Furfural is reported to reduce to furfuryl alcohol with high yields, which is inhibitory to fermentation microorganisms. Furfural also reduces specific growth rate [26]. A mechanism for reduction of furfural to furfuryl alcohol, which inactivate cell growth is proposed. HMF is also following a similar mechanism.

4.2. Hydrolysis

The mechanism for hydrolysis of cellulose biopolymer to six-carbon monomeric sugars is shown in Equation 1. Since there is multitude hydrogen bonding in the cellulose structure, hydrolysis of this polymeric structure is more difficult. Acid or enzyme can catalyze depolymerization of this sturdy structure. Typically, there are three hydrolysis processes widely employed to liberate fermentable sugars: dilute acid, concentrated acid, and enzymatic hydrolysis. Acid hydrolysis results in some degree of degradation of monomeric sugars. Also there will be mass transfer limitations in acid hydrolysis due to the heterogeneous characteristic of reaction [7]. The mechanism of hydrolysis for cleavage of C-O-C bond involves protonation of glucoside bond. This protonation can occur for either the oxygen bond between two monomeric sugars or cyclic oxygen [8]. Cellulose hydrolysis mechanism is depicted in Figure 11. A rapid intermediate complex structure will occur followed by splitting of the glucosidic bond.

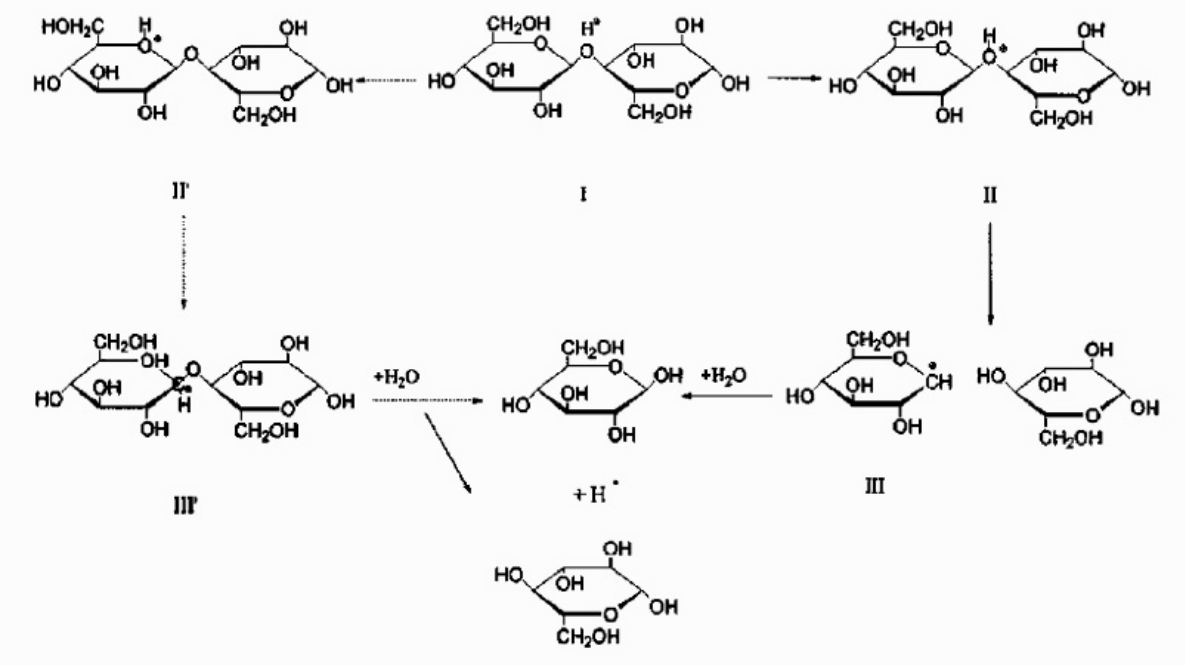

Figure 11: Hydrolysis of glucoside bond [8]

Enzymatic hydrolysis can release monomeric sugars with more than 95% yield. It requires a proper pretreatment step to open up the cellulose structure and make it more accessible towards enzyme. However, a disadvantage of this process is cellobiose and glucose inhibitory effects on the enzyme activity.

4.2.1. Dilute Acid Hydrolysis

Dilute acid is used to hydrolyze hemicellulose and break down this biopolymer to pentose and hexose monomeric and oligomeric sugars. However, cellulose hydrolysis requires harsher conditions. Dilute acid hydrolysis is carried out at higher temperatures and pressures. The process conditions requires the acid loading with concentration in the range of 2-5% and high temperature (160-230 ˚C) and pressure (~ 10 atm) [23,27].

4.2.2. Concentrated Acid Hydrolysis

Concentrated acid hydrolysis requires higher acid loadings in the range of 10-30%, while it operates in lower temperature (<50 ˚C) and pressure (atmospheric) [28]. Disadvantage of this technique is high costs of acid recovery, and extensive operating and capital costs.

4.2.3. Enzymatic Hydrolysis

Enzymatic hydrolysis is the process of depolymerization of cellulose polymer, which is facilitated by cellulase. Product of enzymatic hydrolysis are reduced monomeric or oligomeric sugars. Economically speaking, enzymes are expensive, however, utility cost in enzymatic hydrolysis is less in comparison acid hydrolysis [29]. Enzymatic hydrolysis is preferred because of higher conversion yields and less corrosive and toxic conditions compared to acid hydrolysis [4]. So lower capital and operating cost is an advantage of this process.

4.2.3.1.Enzyme Inhibition

Reduction of the enzyme activity occurs in different ways. One of these ways is the reduction in hydrolysis kinetics because of the inhibition by products such as glucose and cellobiose. The effect of these products on the enzyme activity can be easily quantified. To best understand the effect of each of these compounds on the hydrolysis, we can check the influence of each of them separately. Based on the literature [30], an increase in glucose concentration from 7.5 g/L to 48 g/L reduces the conversion rate by 94%. Selective removal of the products while retaining enzyme is an appropriate approach that leads to higher biomass conversion, at the end of the process. There are several investigations on the application of the membrane reactor for the removal of the product inhibitory compounds [31–36]. Most literatures have reported ultrafiltration membranes as a right choice for retaining the cellulase. Knutsen et al. [35,36] have

reported that MF membrane can also effectively retain cellulase. Chapter 3 of this thesis is about application of MF and UF membranes to retain and reuse enzyme, while diluting glucose.

4.2.3.2.Enzyme

Currently, enzymatic hydrolysis is conducted using a cocktail of enzymes consisting of three main enzyme groups: endo-glucanase, exo-glucanase, and beta-glucosidases. The endo-gluconases attacks the β-1-4 linkages randomly and hydrolyze β-1-4 glucosidic linkage of radical chains. Afterwards, exo-glucanases attack free radicals and depolymerize the free end chain to produce cellobiose. Finally, β-glucosidases enzyme hydrolyze the disaccharide to release the hexose sugars. A schematic of this process is illustrated in Figure 12.

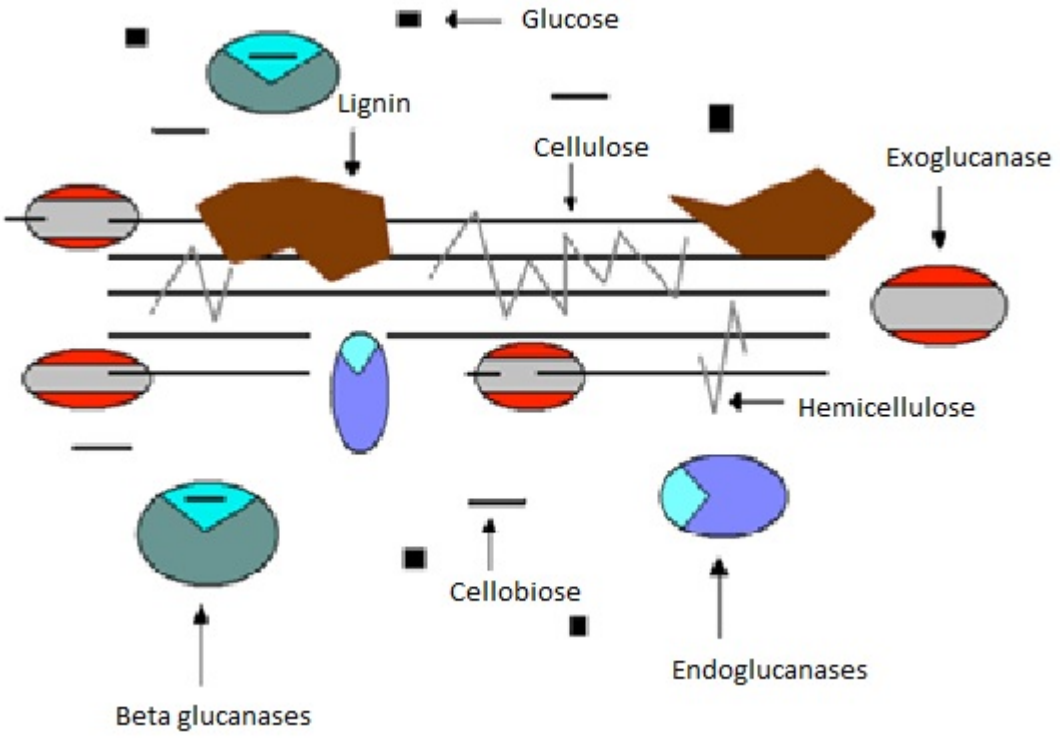

Figure 12: Hydrolysis of lignocellulosic biomass using an enzyme cocktail containing Exoglucanase, endoglucanases, and beta glucanases [4]

4.3. Fermentation

Fermentation is a process in which microorganisms (generally yeast strains) metabolize sugars to ethanol. To achieve the economistic vision set by Department of Energy (DOE) Biomass Program, fermentation of both hexose sugars (such as glucose, mannose, and galactose) and pentose sugars (such as xylose and arabinose) released during hydrolysis of biomass is critical to gain high ethanol yields. For ethanol production, saacharomyces cerevisiae, known as baker's yeast, is preferred since it is highly resistant towards metabolic inhibitory compounds. However, this specific yeast is incapable of fermenting pentose sugars. During the last few decades, there has been a great deal of research devoted to study xylose-fermentation microorganisms (bacteria, yeast, and filamentous fungi) [37–39]; however, pentose-fermenting anaerobic bacteria is inhibited due to high concentrations of ethanol and sugars; pentose-fermenting yeasts are not tolerant towards inhibitory compounds produced during pretreatment of lignocellulosic biomass; filamentous fungi are too slow for industrial processes.

Although fermentation of mixed sugar slurries (hexose and pentose) is a prerequisite for an economically viable bioconversion process, it still does not show high ethanol yields [40]. Currently, there are three main strategies investigating to improve the fermentation of lignocellulosic biomass (Figure 13): 1) Pentose sugar fermentation; 2) Direct cellubiose fermentation; 3) Improving microorganisms more tolerant towards temperature and inhibitory compounds [40]. Dutta et al. [41] have investigated an economic study on different hydrolysis and fermentation protocols. They found out separate hexose and pentose sugars fermentation leads to higher ethanol yields.

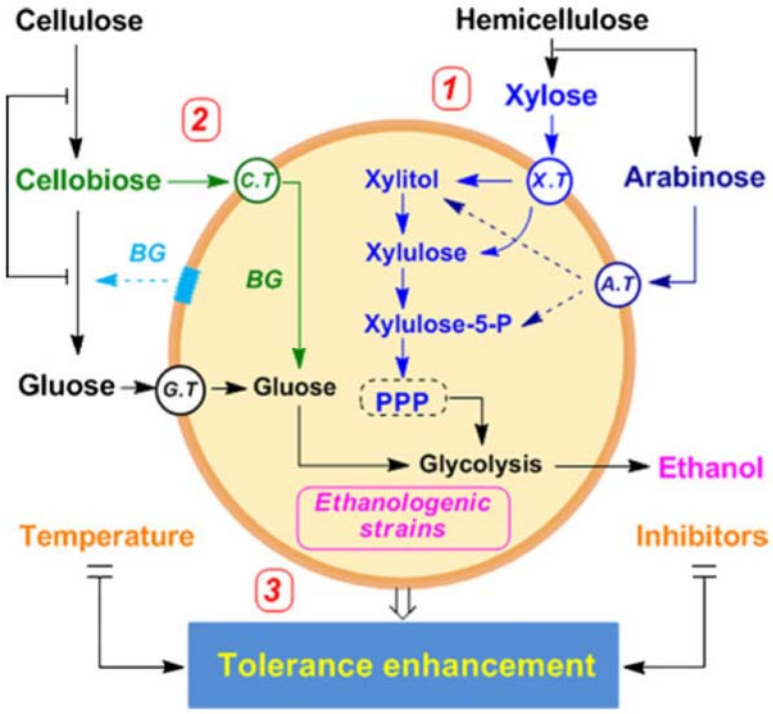

Figure 13: Strategies to improve ethanol fermentation: 1) pentose sugars fermentation; 2) direct cellubiose fermentation; 3) Developing microorganism strains tolarable towards inhibitors [42]

5. Current NREL Lignocellulosic Bioconversion Process

This section is prepared upon a previous report written by NREL scientists (Golden, CO) and Harris Group Inc. (Seattle, WA) [43]. The process developed in the report consists of a co-current dilute-acid pretreatment of lignocellulosic biomass (corn stover) followed by enzymatic hydrolysis of cellulose, and then continued by fermentation of the fermentable sugar. The process has 9 Unit Areas. The schematic diagram of the process is shown in Figure 1 of reference 41.

5.1. Brief Review of Biochemical Conversion Process

This process is divided into nine areas:

Area 100 is designed for feedstock storage, handling and conveying the incoming biomass.

Area 200 is for pretreatment and conditioning of biomass. In this area most of hemicellulose is converted to soluble sugars, and then pH is adjusted to ~5.

Area 300 is designed for enzymatic hydrolysis to convert cellulose content of biomass to soluble glucose sugars, using cellulase. We will talk about this step in detail. Fermentation also happens in this area to convert sugars to ethanol.

Area 400 is an on-site enzyme production section.

Area 500 is for liquid-liquid and solid-liquid separations.

Area 600 is the wastewater treatment section. Wastewater streams from different areas are collected and treated at Area 600. Afterwards, the water is distributed to other areas.

Area 700 provides storage needed for the chemicals and products.

Area 800 provides the majority of the steam and heat demand for the process by combusting the solids remaining from distillation.

Area 900 includes the utility of overall process.

As discussed earlier, our research is specifically focuses on the Area 300, where enzymatic hydrolysis of biomass is occurring. The economics of enzymatic hydrolysis is the bottleneck of the process. The Department of Energy's Office of Biomass target for enzyme cost was specified as $ 0.12/gal ethanol by 2012. This value is one-third of what is mentioned in the NREL report on 2012 ($ 0.34/ gal). These numbers show that there should be more investigations to decrease the enzyme's cost contribution to this process.

The NREL report shows that enzymatic hydrolysis occurs in 12 batch reactors in parallel. First, hydrolysate stream mixes with the cellulase enzyme stream in an in-line mixer. Then, enzymatic hydrolysis is initiated in a continuous vertical high-solid plug flow reactor. This continuous reactor has a 24-hour retention time. The reactor's incoming stream contains around

20% solids (10.8% insoluble and 9.7% soluble). This initial step is essential to help hydrolysate to be pumped to the batch reactors. Afterwards, there are 12 batch 3600-m^3 CSTR reactors. Enzymatic hydrolysis is conducted in these CSTR reactors for another 60 hours at 48 ˚C. Afterwards, the saccharified slurry is cooled down by the pump-around loop and the heat exchanger. As soon as the temperature gets close to 32 ˚C, recombinant Zymomonas mobilis bacterium is added as an ethanologen. This bacterium can simultaneously ferment glucose and xylose to ethanol. Fermentation is followed and conducted in one of the 12 CSTR reactors. Total holding time during fermentation is modeled for 36 hours. At the end of fermentation, produced beer has an ethanol concentration of 5.4%. The flow diagram of the area 300 is shown in Figure 14.

Our approach to improve the hydrolysis reaction efficiency is to design a continuous enzymatic hydrolysis, and substitute the batch process with the continuous one. The main idea behind this new approach is to replace the 12 CSTR batch reactors with membrane assisted reactors to enable a cost-effective continuous enzymatic hydrolysis. We also aim to add a sugar concentration step, to remove some of the water content of the saccharified slurry, before starting the fermentation step. We believe replacing the 12 batch stirred reactors with the membrane-assisted reactor will be beneficial for the process, because:

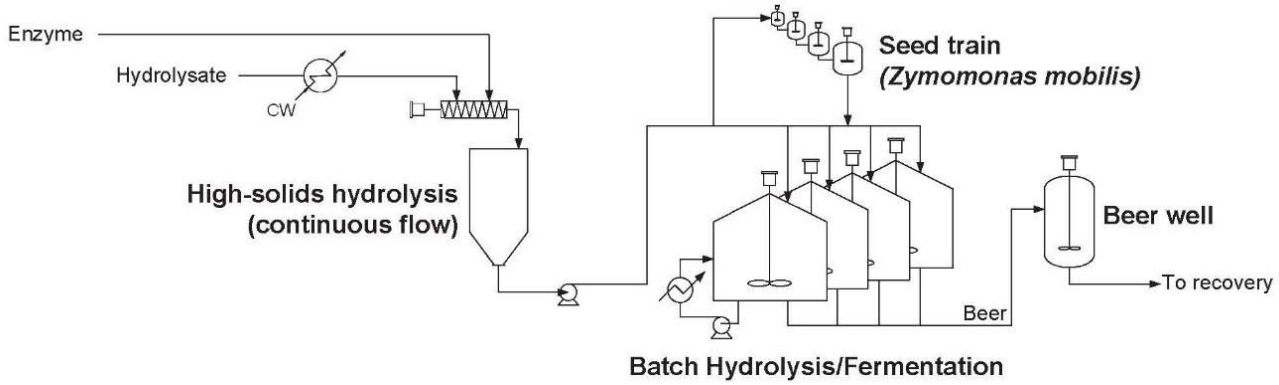

Figure 14: Flow diagram of area 300 [43]

1- A membrane bioreactor will help us to retain and reuse most of the enzyme, and it will result in a decrease in enzyme loading during the process. It will be very helpful since enzyme contribution is still a major component of the final minimum ethanol selling price (MESP).

2- A membrane bioreactor will help us to decrease the concentration of released sugars inside the hydrolysis reactor. These soluble sugars can pass through the membrane and leave the reactor through the permeation stream. As a result, we will always have low concentration of sugars in the membrane bioreactor. This is important because glucose has an inhibitory effect on the kinetics of the hydrolysis process. Thus, the membrane reactor will help us to have a faster reaction with lower enzyme inhibition.

3- A membrane bioreactor will help us to decrease the unit operation costs since it reduces the amount of insoluble solids in the hydrolysate stream. Reduction of insoluble solids results in lower viscosity, lower corrosion rate, and we may be able to replace some of the equipment (such as pumps) with cheaper ones.

Sugar concentration step will help us to remove and recycle a significant amount of water. It is important because we can remove 90% of the saccharified slurry water content, before starting

the fermentation step. This huge change in the size of saccharified slurry stream will result in reduced production cost associated with the reduction of equipment size and energy consumption for heating, cooling, and mixing.

By concentration of sugars, at the fermentation step, we are having a much higher ratio of sugar to microorganisms. It means that we can have faster fermentation with lower amount of microorganisms. Chapter 3 and 2 of this thesis talks about the continuous enzymatic hydrolysis of biomass and concentration of sugars in the hydrolysate, respectively.

6. Motivation

It is known that in most of chemical engineering processes 60-80 % of capital costs accounts for separations, and 15% of the energy consumed worldwide was invested in different forms of separation and purification. Membranes are relatively less energy-intensive and application of membrane processes for future biorefineries leads to lower production costs and higher efficiencies.

Here membrane applications in the production of biofuels from lignocellulosic biomass will be studied. Specifically the focus is on enzymatic hydrolysis. Enzymatic hydrolysis of polysaccharides, e.g. cellulose, starch, is usually conducted in a batch reactor [44]. Disadvantages of the classical batch reactor are: product variation from batch to batch, higher overall investment costs due to larger reactor volumes, higher running costs due to frequent startup/shut down, one time use of enzymes as well as catalyst/enzyme separation costs. Development of a continuous saccharification process overcomes the limitations of batch operation. Additional potential advantages include: recovery and reuse of enzymes, improvement of product yield and kinetics,

and reduction in inhibition of enzymes [45]. Continuous saccharification reactors have been described in the past [46,47].

Membrane reactors or bioreactors have been developed for numerous applications since the 1980s [48]. One embodiment of a membrane bioreactor involves the use of a semipermeable membrane (usually an ultrafiltration membrane) which selectively allows passage of a product species while retaining catalyst and reactants. Thus separation and reaction are conducted in the same step. Membrane bioreactors could be ideally suited for hydrolysis of polysaccharides. The polysaccharide (cellulose) and enzyme is rejected by the membrane while the product (glucose) passes through the membrane pores. Thus continuous addition of substrate and removal of the product is possible.

Besides catalyst recovery, it is also economically favorable to obtain a high concentration sugar product stream that could be used in the subsequent fermentation step. Thus if membranes are to be used it is likely that multiple membrane filtration steps will be required for catalyst /enzyme recovery and for sugar concentration. Here we focus on sugar concentration using nanofiltration and reverse osmosis membranes. Nanofiltration, which originated in the 1970s, is one of the newest pressure driven membrane filtration processes [49]. Low pressure reverse osmosis membranes came to be known as nanofiltration membranes with some of the earliest applications being described in the 1980s [50]. Characteristics of nanofiltration membranes include greater than 99% rejection of multivalent ions, 0-70% rejection of monovalent ions and greater than 90% rejection of small organic compounds with molecular weights in the range 150-300.

We will also investigate the application of modified membranes for separation and fractionation of mono and oligosaccharides. One of the interesting topics in food industry and

biofuel production is separation and concentration of sugars. Fractionation of the sugar and larger oligosaccharide streams has been investigated [51–55]. Among the mono- and oligosaccharides, fractionation of streams containing glucose, xylose, sucrose and fructose is more challenging and interesting. There are different structural carbohydrates such as glucan, xylan, galactan, arabinan, and mannan present in the hydrolysate, and composition of the structural carbohydrates existing in hydrolysate. The sucrose component of the hydrolysate stream will 100% hydrolyze to fructose and glucose during pretreatment [43].

7. References

[1] US department of energy biomass program, Biomass program overview, 2012.

[2] How much petroleum does the United States import and from where? - FAQ - U.S. Energy Information Administration (EIA), (n.d.).

[3] D. Lee, Composition of herbaceous biomass feedstocks, North Central Sun Grant Center South Dakota State University, Brookings S.D., 2007.

[4] J. MacLellan, Innovative Strategies to Enhance Enzymatic Hydrolysis: A Review, MMG 445 Basic Biotechnol. eJournal. 6 (2010).

[5] Y. Pu, F. Hu, F. Huang, B.H. Davison, A.J. Ragauskas, Assessing the molecular structure basis for biomass recalcitrance during dilute acid and hydrothermal pretreatments., Biotechnol. Biofuels. 6 (2013) 15.

[6] D.M. Alonso, S.G. Wettstein, J.A. Dumesic, Bimetallic catalysts for upgrading of biomass to fuels and chemicals., Chem. Soc. Rev. 41 (2012) 8075–98.

[7] G.W. Huber, S. Iborra, A. Corma, Synthesis of transportation fuels from biomass: chemistry, catalysts, and engineering., Chem. Rev. 106 (2006) 4044–98.

[8] L. Fan, M.M. Gharpuray, Y.-H. Lee, Cellulose Hydrolysis, Springer Berlin Heidelberg, Berlin, Heidelberg, 1987.

[9] S. Haghighi Mood, A. Hossein Golfeshan, M. Tabatabaei, G. Salehi Jouzani, G.H. Najafi, M. Gholami, et al., Lignocellulosic biomass to bioethanol, a comprehensive review with a focus on pretreatment, Renew. Sustain. Energy Rev. 27 (2013) 77–93.

[10] L. Laureano-Perez, F. Teymouri, H. Alizadeh, B.E. Dale, Understanding Factors that Limit Enzymatic Hydrolysis of Biomass: Characterization of Pretreated Corn Stover, Appl. Biochem. Biotechnol. 124 (2005) 1081–1100.

[11] A. Crozier, Y. Kamiya, G. Bishop, T. Yokota, Biosynthysis of hormones and elicitor molecules, in: B.B. Buchanan, W. Gruissem, R.L. Jones (Eds.), Biochem. Mol. Biol. Plants, American Society of Plant Physiologists, Rockville, MD, USA, 2000.

[12] J.R. L., The Pulping of Wood, 2nd ed., McGraw-Hill, New York, 1969.

[13] Y. Chen, M.A. Stevens, Y. Zhu, J. Holmes, G. Moxley, H. Xu, Reducing acid in dilute acid pretreatment and the impact on enzymatic saccharification., J. Ind. Microbiol. Biotechnol. 39 (2012) 691–700.

[14] A. Demirbas, Biorefineries: Current activities and future developments, Energy Convers. Manag. 50 (2009) 2782–2801.

[15] A. Demirbas, Biorefinery Technologies for Biomass Upgrading, Energy Sources, Part A Recover. Util. Environ. Eff. 32 (2010) 1547–1558.

[16] H.-J. Huang, S. Ramaswamy, U.W. Tschirner, B.V. Ramarao, A review of separation technologies in current and future biorefineries, Sep. Purif. Technol. 62 (2008) 1–21.

[17] C. Chapple, M. Ladisch, R. Meilan, Loosening lignin's grip on biofuel production., Nat. Biotechnol. 25 (2007) 746–8.

[18] T.H. Kim, Pretreatment of Lignocellulosic Biomass, in: S.-T. Yang, H.A. El-Enshasy, N. Thongchul (Eds.), Bioprocess. Technol. Biorefinery Sustain. Prod. Fuels, Chem. Polym., John Wiley & Sons, Inc., Hoboken, NJ, USA, 2013.

[19] P. Alvira, E. Tomás-Pejó, M. Ballesteros, M.J. Negro, Pretreatment technologies for an efficient bioethanol production process based on enzymatic hydrolysis: A review., Bioresour. Technol. 101 (2010) 4851–61.

[20] J. Luo, M. Cai, T. Gu, Pretreatment of Lignocellulosic Biomass Using Green Ionic Liquids, in: T. Gu (Ed.), Green Biomass Pretreat. Biofuels Prod., Springer Netherlands, Dordrecht, 2013: pp. 127–153.

[21] A. Brandt, M.J. Ray, T.Q. To, D.J. Leak, R.J. Murphy, T. Welton, Ionic liquid pretreatment of lignocellulosic biomass with ionic liquid–water mixtures, Green Chem. 13 (2011) 2489.

[22] A.T.W.M. Hendriks, G. Zeeman, Pretreatments to enhance the digestibility of lignocellulosic biomass, Bioresour. Technol. 100 (2009) 10–18.

[23] P. Kumar, D.M. Barrett, M.J. Delwiche, P. Stroeve, Methods for Pretreatment of Lignocellulosic Biomass for Efficient Hydrolysis and Biofuel Production, Ind. Eng. Chem. Res. 48 (2009) 3713–3729.

[24] E. Palmqvist, B. Hahn-Hägerdal, Fermentation of lignocellulosic hydrolysates. I: inhibition and detoxification, Bioresour. Technol. 74 (2000) 17–24.

[25] E. Palmqvist, B. Hahn-Hägerdal, Fermentation of lignocellulosic hydrolysates. II: inhibitors and mechanisms of inhibition, Bioresour. Technol. 74 (2000) 25–33.

[26] Z.L. Liu, J. Moon, B.J. Andersh, P.J. Slininger, S. Weber, Multiple gene-mediated NAD(P)H-dependent aldehyde reduction is a mechanism of in situ detoxification of furfural and 5-hydroxymethylfurfural by Saccharomyces cerevisiae., Appl. Microbiol. Biotechnol. 81 (2008) 743–53.

[27] J. Iranmahboob, F. Nadim, S. Monemi, Optimizing acid-hydrolysis: a critical step for production of ethanol from mixed wood chips, Biomass and Bioenergy. 22 (2002) 401–404.

[28] J.D. Broder, J.W. Barrier, K.P. Lee, M.M. Bulls, Biofuels system economics, World Resour. Rev. (1995) 560–569.

[29] Y. Sun, J. Cheng, Hydrolysis of lignocellulosic materials for ethanol production: a review, Bioresour. Technol. 83 (2002) 1–11.

[30] B.T. Smith, J.S. Knutsen, R.H. Davis, Empirical evaluation of inhibitory product, substrate, and enzyme effects during the enzymatic saccharification of lignocellulosic biomass., Appl. Biochem. Biotechnol. 161 (2010) 468–82.

[31] M. Zhang, R. Su, Q. Li, W. Qi, Z. He, Enzymatic saccharification of pretreated corn stover in a fed-batch membrane bioreactor, BioEnergy Res. 4 (2010) 134–140.

[32] Q. Gan, S.. Allen, G. Taylor, Design and operation of an integrated membrane reactor for enzymatic cellulose hydrolysis, Biochem. Eng. J. 12 (2002) 223–229.

[33] S.G. Lee, H.S. Kim, Optimal operating policy of the ultrafiltration membrane bioreactor for enzymatic hydrolysis of cellulose., Biotechnol. Bioeng. 42 (1993) 737–46.

[34] K. Bélafi-Bakó, A. Koutinas, N. Nemestóthy, L. Gubicza, C. Webb, Continuous enzymatic cellulose hydrolysis in a tubular membrane bioreactor, Enzyme Microb. Technol. 38 (2006) 155–161.

[35] W.D. Mores, J.S. Knutsen, R.H. Davis, Cellulase Recovery via Membrane Filtration, Appl. Biochem. Biotechnol. 91-93 (2001) 297–310.

[36] J.S. Knutsen, R.H. Davis, Cellulase Retention and Sugar Removal by Membrane Ultrafiltration During Lignocellulosic Biomass Hydrolysis, Appl. Biochem. Biotechnol. 114 (2004) 585–600.

[37] K. Skoog, B. Hahn-Hägerdal, Xylose fermentation, Enzyme Microb. Technol. 10 (1988) 66–80.

[38] T.W. Jeffries, Engineering yeasts for xylose metabolism., Curr. Opin. Biotechnol. 17 (2006) 320–6.

[39] B.S. Dien, M.A. Cotta, T.W. Jeffries, Bacteria engineered for fuel ethanol production: current status., Appl. Microbiol. Biotechnol. 63 (2003) 258–66.

[40] R. Huang, R. Su, W. Qi, Z. He, Bioconversion of Lignocellulose into Bioethanol: Process Intensification and Mechanism Research, BioEnergy Res. 4 (2011) 225–245.

[41] A. Dutta, N. Dowe, K.N. Ibsen, D.J. Schell, A. Aden, An economic comparison of different fermentation configurations to convert corn stover to ethanol using Z. mobilis and Saccharomyces., Biotechnol. Prog. 26 (n.d.) 64–72.

[42] T. Lindén, B. Hahn-Hägerdal, Fermentation of lignocellulose hydrolysates with yeasts and xylose isomerase, Enzyme Microb. Technol. 11 (1989) 583–589.

[43] D. Humbird, R. Davis, L. Tao, C. Kinchin, D. Hsu, A. Aden, et al., Process design and economics for biochemical conversion of lignocellulosic biomass to ethanol dilute-acid pretreatment and enzymatic hydrolysis of corn stover, National Renewable Energy Laboratory, Golden, CO, 2011.

[44] D. Paolucci-Jeanjean, M.-P. Belleville, G.M. Rios, N. Zakhia, Why on Earth Can People Need Continuous Recycle Membrane Reactors for Starch Hydrolysis?, Starch - Stärke. 51 (1999) 25–32.

[45] S. Yang, W. Ding, H. Chen, Enzymatic hydrolysis of rice straw in a tubular reactor coupled with UF membrane, Process Biochem. 41 (2006) 721–725.

[46] K.A. Sims, M. Cheryan, Hydrolysis of liquefied corn starch in a membrane reactor., Biotechnol. Bioeng. 39 (1992) 960–7.

[47] L. Slomińska, W. Grajek, A. Grześkowiak, M. Gocalek, Enzymatic Starch Saccharification in an Ultrafiltration Membrane Reactor, Starch - Stärke. 50 (1998) 390–396.

[48] S.L. Matson, J.A. Quinn, Membrane Reactors in Bioprocessing, Ann. N. Y. Acad. Sci. 469 (1986) 152–165.

[49] B. Van der Bruggen, J. Geens, Nanofiltration in advanced membrane technology and applications, in: N.N. Li, A.G. Fane, W.S.W. Ho, T. Matsuura (Eds.), Adv. Membr. Technol. Appl., Hoboken, NJ, USA, 2008.

[50] P. Eriksson, Nanofiltration extends the range of membrane filtration, Environ. Prog. 7 (1988) 58–62.

[51] J.J. Harris, J.L. Stair, M.L. Bruening, Layered Polyelectrolyte Films as Selective, Ultrathin Barriers for Anion Transport, Chem. Mater. 12 (2000) 1941–1946.

[52] E. Tsakalidou, E. Alichanidis, D.L. Oliveira, R.A. Wilbey, A.S. Grandison, L.C. Duarte, et al., Separation of oligosaccharides from caprine milk whey, prior to prebiotic evaluation, Int. Dairy J. 24 (2012) 102–106.

[53] N. V. Patil, A.E.M. Janssen, R.M. Boom, The potential impact of membrane cascading on downstream processing of oligosaccharides, Chem. Eng. Sci. 106 (2014) 86–98.

[54] C. Nobre, J.A. Teixeira, L.R. Rodrigues, New trends and technological challenges in the industrial production and purification of fructo-oligosaccharides, Crit. Rev. Food Sci. Nutr. (2013) 131011062919009.

[55] A. Giacobbo, A.M. Bernardes, M.N. de Pinho, Nanofiltration for the Recovery of Low Molecular Weight Polysaccharides and Polyphenols from Winery Effluents, Sep. Sci. Technol. 48 (2013) 2524–2530.

[56] S. Mondal, S.R. Wickramasinghe, Produced water treatment by nanofiltration and reverse osmosis membranes, J. Memb. Sci. 322 (2008) 162–170.

[57] N.D. Weiss, J.J. Stickel, J.L. Wolfe, Q.A. Nguyen, A simplified method for the measurement of insoluble solids in pretreated biomass slurries., Appl. Biochem. Biotechnol. 162 (2010) 975–87.

[58] G. Decher, Fuzzy Nanoassemblies: Toward Layered Polymeric Multicomposites, Science (80-.). 277 (1997) 1232–1237.

[59] J.C. Yang, M.J. Jablonsky, J.W. Mays, NMR and FT-IR studies of sulfonated styrene-based homopolymers and copolymers, Polymer (Guildf). 43 (2002) 5125–5132.

[60] N.A. Kotov, S. Magonov, E. Tropsha, Layer-by-Layer Self-Assembly of Alumosilicate−Polyelectrolyte Composites: Mechanism of Deposition, Crack Resistance, and Perspectives for Novel Membrane Materials, Chem. Mater. 10 (1998) 886–895.

[61] S.S. Shiratori, M.F. Rubner, pH-Dependent Thickness Behavior of Sequentially Adsorbed Layers of Weak Polyelectrolytes, Macromolecules. 33 (2000) 4213–4219.

[62] E. Sjöman, M. Mänttäri, M. Nyström, H. Koivikko, H. Heikkilä, Separation of xylose from glucose by nanofiltration from concentrated monosaccharide solutions, J. Memb. Sci. 292 (2007) 106–115.

Chapter 2: Sugar Concentration and Detoxification of Clarified Biomass Hydrolysate by Nanofiltration1

[1] This chapter is version of a paper submitted to Separation and Purification Technology by Mohammadmahdi Malmali, Jonathan J Stickel and S. Ranil Wickramasinghe. It is under review.

Sugar Concentration and Detoxification of Clarified Biomass Hydrolysate by Nanofiltration

Mohammadmahdi Malmali[*], Jonathan J. Stickel[#], S. Ranil Wickramasinghe[*]

[*] Ralph E. Martin Department of Chemical Engineering, University of Arkansas, Fayetteville, AR 72701, USA

[#] National Renewable Energy Laboratory, National Bioenergy Center, Golden, CO 80401, USA

1. Abstract

Development of efficient unit operations is critical in order to design economically viable processes for conversion of lignocellulosic biomass into chemicals and fuels. Here the use of nanofiltration membranes for concentration of sugars in a lignocellulosic biomass hydrolysate has been explored. In addition, the feasibility of simultaneous removal of acetic acid, 5-(hydroxymethyl)furfural and furfural from the hydrolysate has also been investigated. The results obtained here indicate that both concentration of sugars and removal of hydrolysis degradation products are feasible. However careful selection of the membrane and operating conditions are essential. Dead-end filtration experiments have been used to test a number of commercially available nanofiltration membranes under a range of operating conditions. Model feed streams as well as real hydrolysates have been tested. By using design-of-experiments software the number of experiments has been minimized. The introduction of a nanofiltration step for concentration of sugars and removal of hydrolysis degradation products could enable the development of a continuous process for biomass hydrolysis.

Key-words: acetic acid, biomass, fouling, permeability, rejection

2. Introduction

Today, production of 1st generation biofuels such as bioethanol from sugar cane and corn starch is well established [1]. Manufacturing processes that include the use of membrane-based unit operations have been described [2]. However increasing competition between food and energy production has led to significant efforts to convert lignocellulosic biomass into 2nd generation biofuels. Unlike 1st generation biofuels, production of 2nd generation biofuels is far more complex. Development of efficient separation and purification operations are essential for production of competitive 2nd generation drop-in biofuels. Membrane based separation processes are attractive as they could lead to significant process intensification and hence reduced operating costs [3].

Three main strategies exist for conversion of lignocellulosic biomass into liquid fuels and chemical intermediates: gasification, pyrolysis and hydrolysis [4]. Here we focus on hydrolysis of lignocellulosic biomass followed by fermentation. Dilute-acid pretreatment is a leading technology for initial hydrolysis [5]. Dilute sulfuric acid has been shown to effectively hydrolyze the hemicellulose component of the biomass to its monomeric sugars as well as enhance the enzymatic digestibility of cellulose [6]. Next, cellulose is enzymatically hydrolyzed to glucose. Prior to fermentation, the hydrolysate is conditioned or detoxified to remove byproducts and sugar degradation products (toxic compounds). These compounds inhibit subsequent bioconversion of the solubilized sugars[6]. In addition, the maximum glucose concentration is limited by product inhibition during enzymatic hydrolysis. However increasing the sugar concentration in the fermentation reactor is desirable in order to increase the fermentation product yield e.g. ethanol. In this work we focus on the development of a pressure driven membrane filtration step to remove toxic compounds as well as concentrate the soluble sugars prior to fermentation.

Abels et al. [1] recently reviewed membrane based separation processes for biorefinery applications. Several investigators have considered the use of ultrafiltration membranes for removal of glucose during enzymatic hydrolysis thus avoiding product inhibition [7-10]. Carstensen et al. [11] have reviewed membrane bioreactors for in situ product recovery. However, here the focus is concentration of sugars and removal of toxic compounds. Thus it is assumed that suspended solids and enzymes have already been removed from the feed stream.

In more recent studies, a few investigators have considered the use of nanofiltration membranes. Nanofiltration, or low-pressure reverse osmosis membranes were initially developed for softening of surface and ground waters [12][49]. These membranes typically exhibit over 99% rejection of multivalent ions but less than 70% rejection of monovalent ions. In addition they exhibit over 90% rejection of dissolved organic compounds with molecular weights over 150-300. Weng et al. [13] investigated separation of acetic acid, a toxic compound produced during dilute acid hydrolysis of rice straw [6] from xylose. They indicated a separation factor of acetic acid over xylose of 49. Higher separation factors were also obtained for acetic acid over glucose. Their work indicates that the actual separation factor depends on many variables such as pH and the presence of other species in the feed. Our recent work indicates the importance of pH on the flux, rejection and selectivity of nanofiltration membranes [14]. Qi et al. [15] have investigated separation of furfural (a xylose degradation product) from model feed streams containing glucose, xylose and furfural. Their result also indicated the importance of feed pH and the presence of other species on glucose and xylose rejection. In real hydrolysates it is likely that the presence of other dissolved species could have a significant effect on membrane performance.

Maiti et al. [16] conducted a far more detailed study where they investigated separation of a number of toxic compounds from rice straw hydrolysates by several commercially available

nanofiltration membranes. Model and real hydrolysate feed streams were investigated. Their study indicates that removal of toxic compounds and concentration of monomeric sugars is possible using nanofiltration membranes. However, as nanofiltration membrane performance depends on size exclusion as well as surface interactions between the membrane and dissolved species, feed pH, ionic strength and the concentration of the various dissolved solutes will have a significant effect on membrane performance.

Development of a nanofiltration step to detoxify the hydrolysate and concentrate the monomeric sugars could be economically beneficial. In order to mitigate product inhibition and high viscosities, a continuous hydrolysis process will likely result in dilute concentrations of sugars, and hence a sugar concentration step will be needed before fermentation. Selection of an appropriate membrane and operating conditions will be essential in order to determine the feasibility of such a step. The purpose of this work was to develop a method to screen a number of membranes under a range of conditions. All experiments have been conducted in dead-end filtration mode. In industrial practice, nanofiltration is conducted in tangential flow filtration mode. However dead-end filtration experiments provide much more control over operating conditions and are well suited for comparing the performance of different membrane and feed conditions [17]. Five commercially available nanofiltration and low pressure reverse osmosis membranes were tested. The effect of feed pH and pressure, total glucose and xylose (monomeric sugar) concentration as well as the total concentration of acetic acid, 5-(hydroxymethyl)furfural (HMF) and furfural (toxic compounds) were determined for model feed streams. In addition, the filtration of real hydrolysates through selected membranes was performed. Design of experiments software was used to minimize the number of experiments. Finally, membrane surfaces were

characterized by X-ray photoelectron spectroscopy (XPS), contact angle and zeta potential measurements.

3. Experimental

3.1. Material and Methods

Unless otherwise noted, all chemical were ACS reagent grade. D-glucose and D-xylose were purchased from Sigma Aldrich (St. Louis, MO). 5-(hydroxymethyl)furfural (HMF) 99% and 2-furaldehyde (furfural) 99% were purchased from Thermo Fisher Scientific (Waltham, NJ). Sodium azide 5% w/v, acetic acid and sulfuric acid were purchased from Seastar Chemicals Inc. (Sidney, BC, Canada). Sodium hydroxide was purchased from J. T. Baker (Philipsburg, NJ). Deionized water (conductivity < 10 μScm^{-1} and resistance > 18.5 MΩ) was obtained from a Labconco (Kansas City, MO) water purification system (Water Pro RO and Water Pro PS Polishing Stations).

Three commercially available Alpha Laval (Wood Dale, IL) membranes (RO90, RO98 and RO99) and two Dow Filmtec (Edina, MN) membranes (NF90 and NF270) were tested. The Alpha Laval membranes are marketed as low pressure (brackish water) reverse osmosis membranes while the Dow Filmtec membranes are marketed as nanofiltration membranes. Table 1 gives further information on the 5 membranes tested here. As can be seen the Alpha Laval membranes are generally tighter (lower NMWCO). All experiments were conducted using a stirred cell HP4750, Strelitech Corporation (Kent, WA). The cell is designed to operate at a maximum feed pressure of 69 bar using 49 mm membrane discs with 14.6 cm^2 active membrane area.

Table 1: Membranes tested together with manufactures specifications

Membrane	NF270 [18]	NF90 [19]	RO90 [20]	RO98 [21]	RO99 [22]
Manufacturer	Dow Filmtec, Edina, MN	Dow Filmtec, Edina, MN	Alpha Laval, Lund, Sweden	Alpha Laval, Lund, Sweden	Alpha Laval, Lund, Sweden
Structure	Thin film composite polyamide, polysulfone and polyester support	Thin film composite polyamide, polysulfone and polyester support,	Thin film composite polyamide and polyester support	Thin film composite polyamide and polypropylene support	Thin film composite polyamide and polyester support
Molecular weight cut off and rejection	250-300 Da 50% NaCl >98% $MgSO_4$	200 Da 90-96 % NaCl >98% $MgSO_4$	>90% NaCl	>97% NaCl	>98% NaCl
Charge at pH 7.0	Negative	Negative	Negative	Negative	Negative
Operating range	5-45 °C 3-10 pH up to 41 bar	5-45 °C 3-10 pH up to 41 bar	5-50 °C 3-10 pH up to 55 bar	5-60 °C 2-11 pH up to 55 bar	5-50 °C 3-10 pH up to 55 bar

A virgin membrane was used for each experiment. Prior to testing with model and real hydrolysate, the DI water flux of the membrane was determined. All membranes were washed in DI water for 24 hrs. The membrane was then placed in the filtration cell and precompacted at a pressure of 40 bar and a temperature of 42℃ for 60 min. DI water fluxes were then measured at 20, 30 and 40 bar over a period of 1 hour and the values compared to the manufacturer's values. If the flux was outside the specified range, the membrane was discarded. Next, 160 mL of model or real hydrolysate was loaded into the nanofiltration cell. Permeate samples (1.5 mL) were collected at regular intervals for HPLC analysis.

3.2. Statistical Design of Experiments

Design Expert 7.1.3 (Stat-Ease, Minneapolis, MN) was used to design a set of experiments to determine and optimize the experimental conditions for concentration of model feed solutions.

Table 2 lists the parameters investigated for model feed streams. Four membranes were investigated. NF270 was not tested as it displayed very low rejection of glucose and xylose during our preliminary experiments with model feed streams. Three levels of total sugar concentrations (5, 12 and 20 g L^{-1}) were investigated where the ratio of xylose to glucose was 1:3. Three concentrations of toxic compounds (0, 0.9 and 1.8 g L^{-1}) were investigated where the ratio of the three toxic compounds acetic acid: HMF: furfural was 6: 2: 1. The various compounds were dissolved in DI water. These concentrations and concentration ratios were selected in order to model the range of concentrations expected in corn stover hydrolysates in a continuous hydrolysis and fermentation process. The pH was adjusted using sulfuric acid or sodium hydroxide. A total of 40 experiments were conducted as listed in Table 2. A few experiments marked (*) were run in duplicate as suggested by the design of experiments software. The operating temperature was 42℃. This temperature was chosen as it is between the possible operating temperatures for enzymatic hydrolysis (50℃) and fermentation (30℃). A total of seven responsive variables namely xylose recovery (R1), glucose recovery (R2), acetic acid rejection (R3), furfural rejection (R4), HMF rejection (R5), flux flow (R6) and flux decline (R7) were chosen as responses for analyzing. Analysis of variance (ANOVA) was used to estimate the statistical parameters during response surface model. Optimum values of the selected factors for sugars rejection and inhibitors removal were determined by analyzing the response-surface contour plots.

Table 2: Experimental conditions for model hydrolysate solutions (*) denotes experiments that were run in duplicate

Run #	Total sugar concentration (g/L)	Total toxic compound concentration (g/L)	Transmembrane pressure (bar)	pH	Membrane
1	5.0	0	40	5.75	NF90
2	5.0	0.90	40	3.00	NF90
3	5.0	0.90	20	8.50	NF90

Cont. Table 2: Experimental conditions for model hydrolysate solutions (*) denotes experiments that were run in duplicate

Run (Cont.)#	Total sugar concentration (g/L) (Cont.)	Total toxic compound concentration (g/L) (Cont.)	Transmembrane pressure (bar) (Cont.)	pH (Cont.)	Membrane (Cont.)
4	5.0	1.80	30	3.00	NF90
5	12.5	0	20	3.00	NF90
6	12.5	1.80	40	8.50	NF90
7	20.0	0	30	8.50	NF90
8	20.0	0	40	3.00	NF90
9	20.0	1.80	20	5.75	NF90
10	20.0	1.80	40	3.00	NF90
11	5.0	0	20	8.50	RO90
12	5.0	0	40	3.00	RO90
13	5.0	1.80	20	3.00	RO90
14	5.0	1.80	40	8.50	RO90
15	20.0	0	40	8.50	RO90
16	20.0	0	20	3.00	RO90
17	20.0	1.80	20	8.50	RO90
18	20.0	1.80	40	3.00	RO90
19*	5.0	0	20	3.00	RO98
20*	5.0	0	40	8.50	RO98
21	5.0	1.80	40	3.00	RO98
22	5.0	1.80	20	8.50	RO98
23*	12.5	0.90	30	5.75	RO98
24	20.0	0	20	8.50	RO98
25	20.0	0	40	3.00	RO98
26*	20.0	1.80	20	3.00	RO98
27*	20.0	1.80	40	8.50	RO98
28	5.0	0	30	8.50	RO99
29	5.0	0.90	20	3.00	RO99
30	5.0	1.80	40	5.75	RO99
31	12.5	0	40	3.00	RO99
32	12.5	1.80	20	8.50	RO99
33	20.0	0	20	5.75	RO99
34	20.0	0.90	40	8.50	RO99
35	20.0	1.80	30	3.00	RO99

* Tests were run in duplicate

Corn stover hydrolysate from a batch pretreatment and enzymatic hydrolysis process was obtained from the National Renewable Energy Laboratory (Golden, CO). Table 3 provides the

concentration of glucose, xylose, acetic acid, furfural and HMF after pretreatment with dilute sulfuric acid and enzymatic hydrolysis. The hydrolysate was centrifuged to remove particulate matter, and the pH of the hydrolysate was 4.75. As can be seen, residual acetic acid, HMF and furfural are present in the hydrolysate. The hydrolysate was diluted 5 to 10 fold so that the total sugar concentration was in the range 14 to 27 g/L, and the xylose to glucose ratio was 1:1.3. Hence, the ratio of xylose to glucose is different to the model feed streams and the highest sugar concentration was higher than the highest sugar concentration (20 g/L) in the model feed streams. The total concentration of toxic compounds was 0.8 to 1.6 g/L. The ratio of acetic acid: HMF: furfural is 0.76: 0.02: 1.0. Thus while the total concentration of toxic compounds is within the range investigated using model feed streams, the ratio of the three compounds investigated is different.

Table 3: Characteristics of corn stover hydrolysate

Compound	Concentration (g/L)
Glucose	77.872
Xylose	58.791
Acetic Acid	3.445
HMF	0.093
Furfural	4.508

The concentration of sugars and toxic compounds in the model feed streams were chosen to bracket the expected concentrations in a continuous process. No attempt was made to adjust the ratio of these various dissolved solutes in the actual hydrolysate obtained from batch processing. Based on the result of the experiments using model feed streams, a further 16 experiments were conducted using the real hydrolysate as given in Table 4. The same pressures were used as for the model feed streams. The feed pH was adjusted using sulfuric acid or sodium hydroxide. pH values in the range 3 to 5.75 were investigated. RO90 and RO98 were replaced by

NF270 as they displayed very high rejection of toxic compounds and low fluxes for model feed streams. Design Expert 7.1.3 was again used to select experimental conditions.

Table 4: Experimental conditions for hydrolysate feed streams

Membrane	Pressure (bar)	Dilution Factor	pH
NF270	40	5	4.66
NF270	30	5	5.75
NF270	30	5	3.30
NF270	30	5	2.95
RO99	40	10	4.20
RO99	20	10	4.20
RO99	40	10	5.75
RO99	40	5	4.30
RO99	40	5	4.30
NF90	20	10	4.20
NF90	40	10	3.00
NF90	40	5	4.20
NF90	40	7	4.70
NF90	40	5	5.75
NF90	40	5	4.66
NF90	40	5	3

3.3. Analytical Methods

The concentration of glucose, xylose, acetic acid, HMF and furfural were determined using an Agilent 1200 series HPLC (Agilent Technologies, Palo Alto, CA) equipped with a Biorad Aminex HPX-87 H column (Hercules, CA) and Agilent refractive index detector. The mobile phase consisted of 12 N sulfuric acid diluted to 0.001 N with HPLC grade water and filtered using a 0.2 μm filter. A series of calibration standards and calibration verification standards (CVS) were obtained from Absolute Standards Inc., Hamden, CT. The flow rate was set at 0.6 mL min^{-1} at a column temperature of 55℃ and injection volume of 15 μL. All measurements were taken in triplicate and average results are reported.

3.4. Membrane Characterization

Membrane contact angles were determined using a contact angle goniometer (Model 100, Rame-Hart Instrument Company, Netcong, NJ) using the sessile drop method at room temperature and pressure. Virgin membranes were rinsed twice with 10 mL DI water. They were then placed in a 100 mL beaker containing 50 mL DI water for 10 min with slow stirring. The membranes were again rinsed twice with 10 mL DI water and air dried for 15 min and then dried overnight in vacuum oven at 30˚C. A 3 μL drop of DI water at a rate of 1 μL/s was applied to the surface of the membrane using a syringe. Using the circle fitting method, the angle made between the water drop and the membrane surface was measured every 0.1 seconds. Data were collected for 5 seconds at five locations and averaged for each membrane.

Membrane zeta potential was measured using a Beckman Coulter DelsaNano HC (Brea, CA). The DelsaNano HC machine was also equipped with DelsaNano AT auto-titrator which automatically adjusts the pH of the liquid solution passing tangentially over the membrane surface. For pH titration, 1 M sulfuric acid and sodium hydroxide was used. Virgin membranes were washed and dried as described for contact angle measurement. Two samples (1×2.5 cm) of each commercial membrane were tested. Zeta potential measurements were conducted at a minimum of 6 different pH values. For each sample the zeta potential was determined twice at the same pH value. Thus each zeta potential measurement represents the average of 4 values.

X-ray Photoelectron Spectroscopy XPS is useful for studying membrane surface chemistry since it provides chemical binding information for the top 1-10 nm of the sample. Membranes were washed and dried as described for contact angle measurement. For each sample, 5 survey

scans over the range 0-1000 eV with a resolution of 0.2 eV were averaged using a Versa Probe station from Physical Electronics (PHI) (Chanhassen, MN).

4. Results and Discussion

As indicated in Table 5, a large range of surface contact angles was observed. NF270 displayed the lowest contact angle (most hydrophilic). Previous studies indicate a range of contact angles for NF270 [23,24]. The value obtained here is in agreement with previous values. The range in reported surface contact angles is not surprising as the measured contact angle will depend on the experimental conditions as well as the roughness of the membrane where the contact angle is measured. Table 5 indicates that RO90 and RO98 display the highest surface contact angles (most hydrophobic).

Table 5: Membrane contact angles

Membrane	Contact angle
NF90	84.4±3.4
NF270	33±6.1
RO90	104.6±4.2
RO98	116.1±4.7
RO99	56.8±5.3

Table 6 gives the ratio of carbon, oxygen and nitrogen from XPS analysis. The theoretical O: N ratio for a fully aromatic polyamide layer that is fully cross-linked is expected to be 1.0 while the ratio for a corresponding linear polyamide layer is expected to be 2.0 where the polyamide layer is formed by reaction of trimesoyl chloride and 1,3-benzenediamine (m-phenyl-diamine) [25]. However the actual theoretical ratio for a given polyamide barrier layer will depend on the monomers used. The barrier layer of NF270 for example consists of a piperazine-based semi-aromatic polyamide. The XPS data for NF90, RO90 and RO98 indicate similar C: N: O ratios. It appears these membranes are heavily cross-linked [25]. NF270, and RO99 display O: N ratios

greater than 2. This increase in the ratio of oxygen present is most likely due to proprietary modifications to the basic polymerization reaction or the presence of a coating such as polyvinyl alcohol [25]. Comparing Tables 5 and 6 it can be seen that increasing the ratio of oxygen to nitrogen tends to reduce the surface contact angle (more hydrophilic surface).

Table 6: Elemental compositions of carbon, oxygen and nitrogen for the barrier layer of the membranes tested. Elemental composition are based on C(1s), O(1s) and N(1s) peaks. Data for NF 270 are from Mondal and Wickramasinghe [56].

Membrane	C (%)	O (%)	N (%)	C:O:N ratio
NF270	64.4	22.3	7.58	8.49 : 2.94 : 1.00
NF90	73.82	15.14	11.04	7.09 : 1.37 : 1.00
RO90	74.37	12.86	12.77	5.82 : 1.01 : 1.00
RO98	73.9	14.27	11.83	6.24 : 1.20 : 1.00
RO99	72.99	22.79	4.22	17.29 : 5.40 : 1.00

Figure 1 gives membrane zeta potential as a function of pH. RO90 and NF90 display a similar variation in zeta potential with pH. Tables 5 and 6 indicate that they display similar contact angles and O: N ratios. Similarly RO98 and RO99 also display a similar variation of zeta potential with pH even though they display different contact angles and have different O: N ratios. It can also be seen that the variation of zeta potential for these two membranes is much less than for RO90 and NF90 over the same range of pH. Since nanofiltration depends strongly on surface properties these differences in membrane surface properties are likely to have a significant effect on membrane performance. Tang et al. [25] provided a detailed discussion on how to relate membrane surface properties and chemical composition to the structure of the polyamide barrier layer and any additional coating that may be present. Next we discuss our results for model feed streams and real hydrolysates.

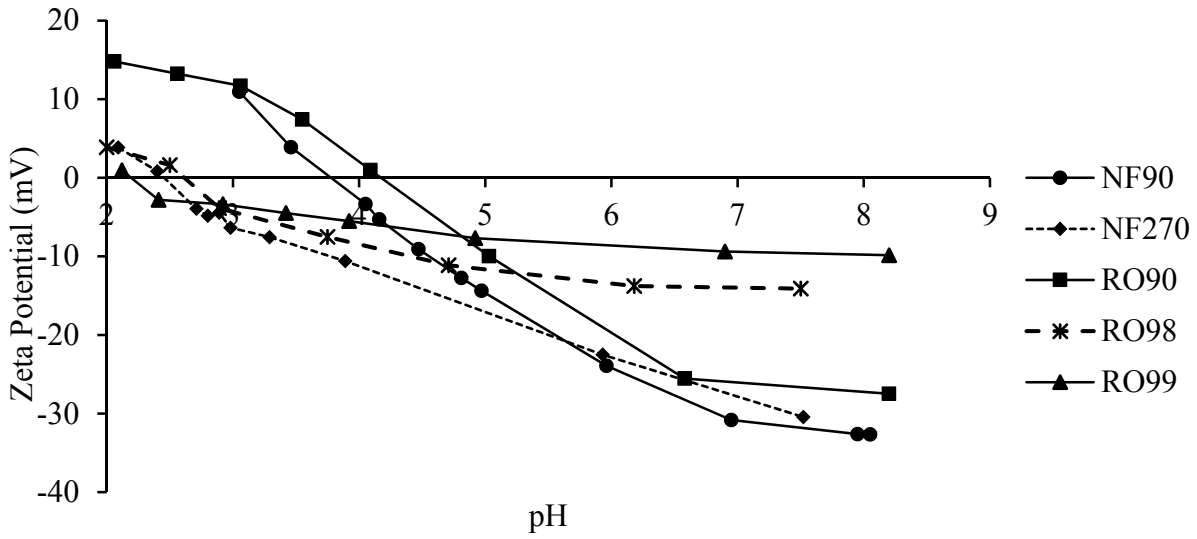

Figure 1: Variation of membrane zeta potential with pH

Figures 2-5 give the variation of permeability with feed conditions for NF90, RO90, RO98 and RO99, respectively. In each figure the data are presented in order of decreasing permeability. Results are shown after 20 min of operation. It was observed that for all membranes an approximately steady flux was obtained between 15 and 25 min of operation. At shorter run times some start-up transient effects were frequently observed. For longer run times, a steady decrease in permeate flux was observed due to the changing feed conditions. Thus the permeability after 20 min of operation was used to compare membrane performance. Permeability is defined as the permeate flux divided by the feed pressure.

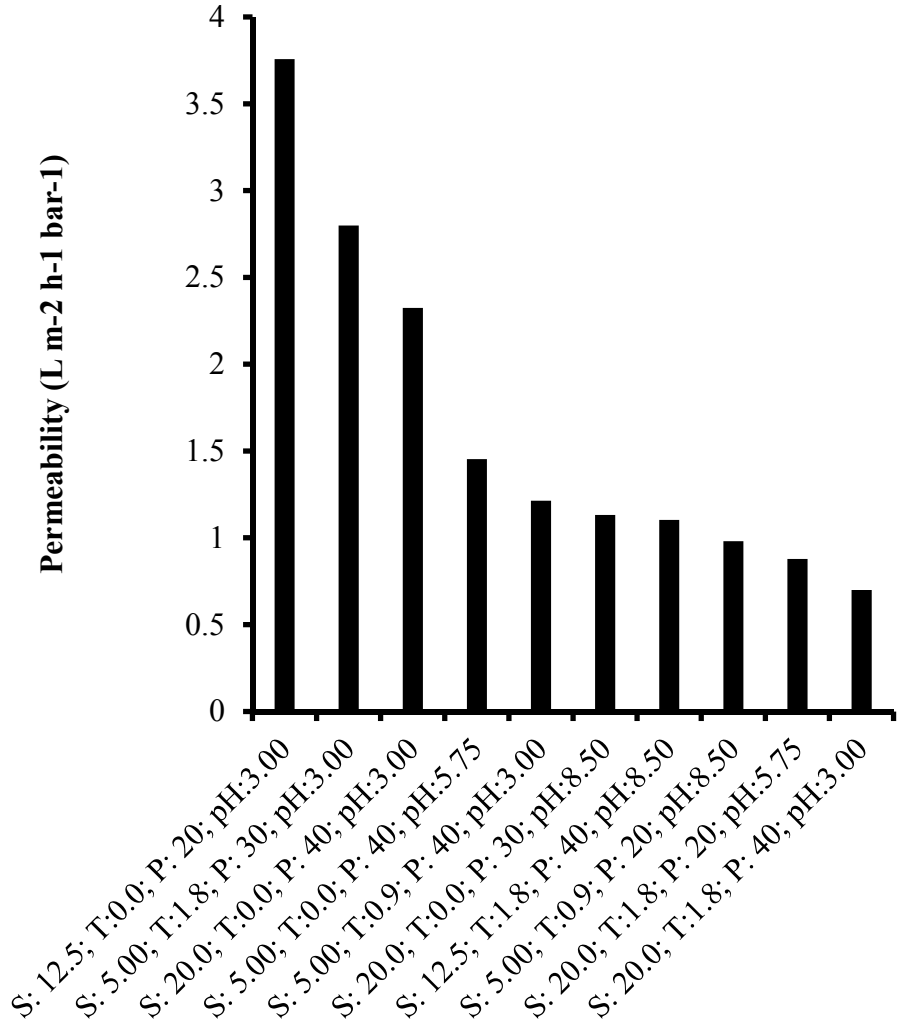

Figure 2: NF90 permeability under the experimental conditions tested. S: total sugar concentration (g/L) (glucose and xylose), T: total toxic compound concentration (g/L) (acetic acid, HMF and furfural); P; pressure (bar).

Figures 2-5 indicate that the feed conditions have a significant influence on the permeate flux. In general NF90 displayed the highest permeability of the four membranes. This is not surprising as it has a large nominal molecular weight cut off and relatively low NaCl rejection. RO90 and RO98 displayed permeabilities that were similar over the range of operating conditions tested. However, according to the manufacturer, RO98 has much higher NaCl rejection rating. Interestingly, RO99 which has the highest rated NaCl rejection, does display permeabilities higher than RO90 and RO98. Table 5 indicates that RO99 is much more hydrophilic than RO90 and

RO98. The permeability of nanofiltration membranes depends on a combination of convection through the membrane pores and diffusion through the polyamide barrier layer, which depends on the free volume present in the polymer network [26]. With the exception of very loose nanofiltration membranes, these membranes contain few real pores [27-29]. Consequently permeability does not depend entirely on the nominal molecular weight with cut off of the membrane. As the nominal molecular weight cut off decreases, the diffusive contribution to the permeate flux becomes more significant.

Figure 2 indicates that NF90 displayed the highest permeability at pH 3.0 in the absence of any toxic compounds at a feed pressure of 20 bar. Higher pressures reduce the membrane permeability. For an approximately incompressible membrane, in the absence of any concentration polarization and membrane fouling, the permeability should be independent of feed pressure. The results obtained here indicate that this is not the case when the feed stream contains dissolved solutes that are partially rejected by the membrane.

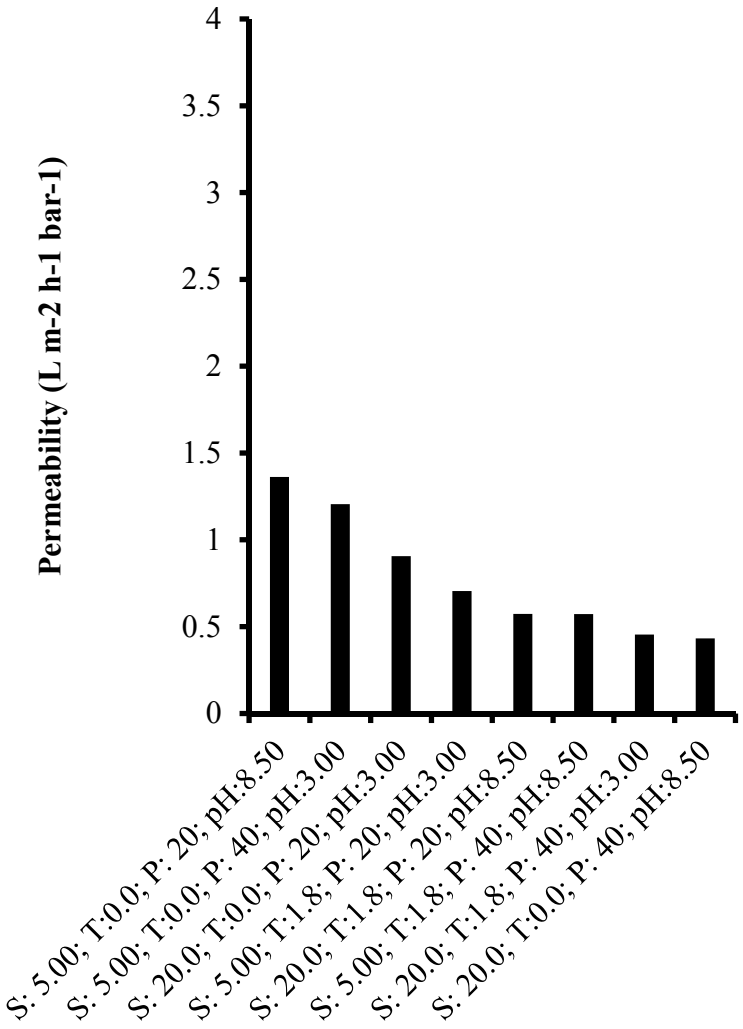

Figure 3: RO90 permeability under experimental conditions tested. S: total sugar concentration (g/L) (glucose and xylose), T: total toxic compound concentration (g/L) (acetic acid, HMF and furfural); P; pressure (bar).

Comparing Figure 2 with Figures 3 (RO90) it can be seen that the highest permeability for RO90 occurs at pH 8.5. Further, over the range of operating conditions tested, the variation of permeability is less than for NF90. In the case of RO98 (Figure 4) the variation in permeability is also much lower than that for NF90 but the highest permeability occurs at pH 3.0. Finally RO99 (Figure 5) displays a much larger variation in permeability over the range of feed conditions investigated compared to RO90 and RO98. The maximum permeability occurs at a feed pH of 8.5.

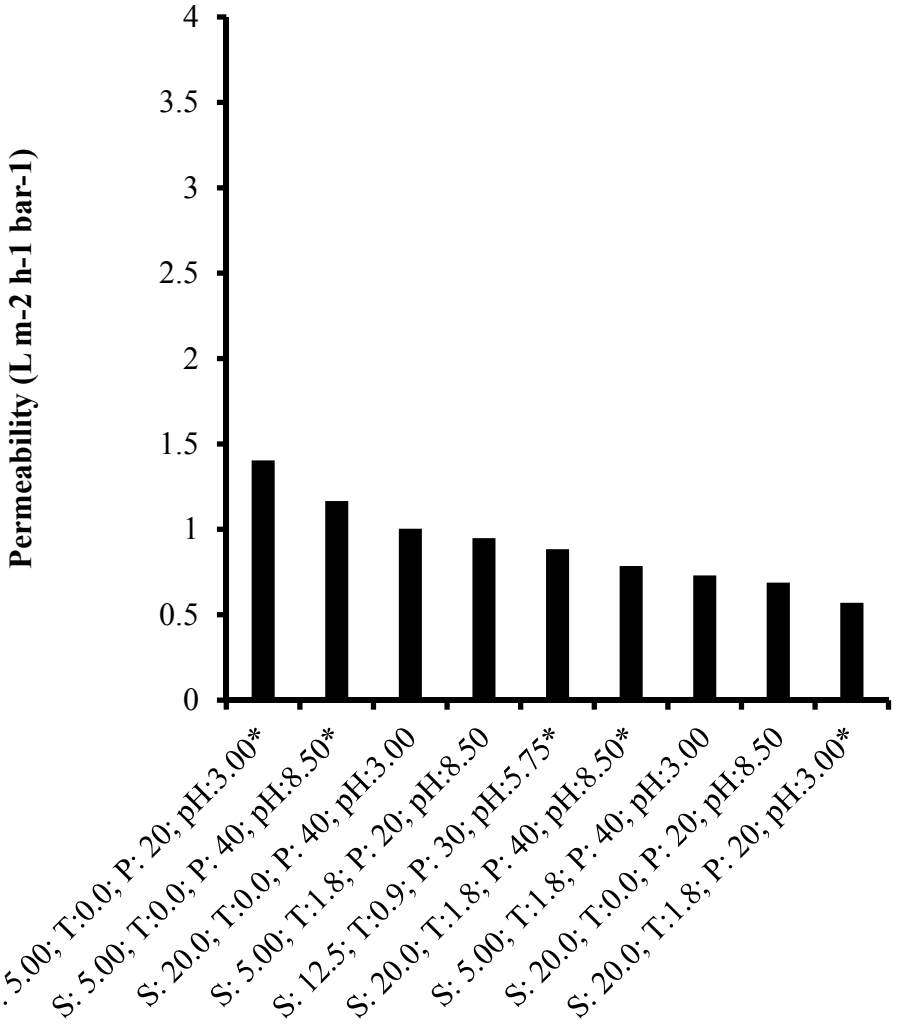

Figure 4: RO98 permeability under experimental conditions tested. (*) These tests were conducted in duplicate based on the design of experiments software output. Average results are shown. S: total sugar concentration (g/L) (glucose and xylose), T: total toxic compound concentration (g/L) (acetic acid, HMF and furfural); P; pressure (bar).

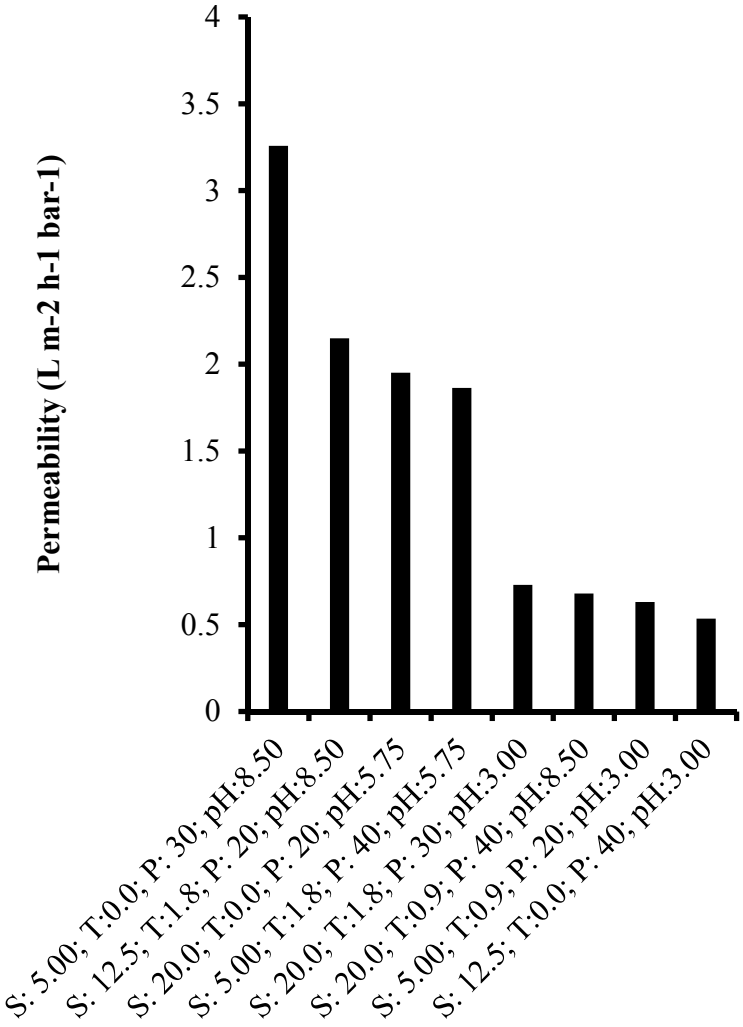

Figure 5: RO99 permeability under experimental conditions tested. S: total sugar concentration (g/L) (glucose and xylose), T: total toxic compound concentration (g/L) (acetic acid, HMF and furfural); P; pressure (bar).

The feed pH can affect both the membrane and dissolved solutes present. The toxic compounds investigated here interact with the membrane. For all four membranes the highest permeability occurs in the absence of the toxic compounds. Glucose and xylose will not be affected by pH over the range 3.0-8.5. Manttari et al. [26] observed an increase in permeate flux for NF270 for feed pH values above 8.0. The polyamide barrier layer in the membranes tested here consist of a three dimensional network of polymer chains and associated free volume. Minor changes in free volume can lead to observable changes in permeability. Under alkaline conditions

proton dissociation of residual carboxylic groups in the barrier layer will lead to swelling of the cross linked polymer barrier layer and consequently an increase in free volume, which results in higher observed permeabilities [17,30,31]. However the amount of swelling that occurs depends on the number of carboxylic groups present, which in turn depends on the actual monomer used and the polymerization conditions. In addition, swelling will be affected by the degree of cross-linking. Table 6 suggests that the polyamide layer in RO90 and RO98 are heavily cross-linked. This could explain the much lower variation in permeability observed for the experimental conditions tested. The increase in permeability at alkaline pH values depends on the membrane and will vary for membranes with similarly permeability and rejection ratings from different manufacturers.

Figures 6 to 9 provide rejection data for NF90, RO90, RO98 and RO99 respectively. The data are presented in order of decreasing permeability. Thus the ordering of the data in Figures 6-9 is the same as in Figures 2-5 respectively. Figures 6-9 indicate that all 4 membranes display very high rejection of glucose and xylose under all the operating conditions tested. The molecular weights of glucose and xylose are 180 and 150 respectively. According to information from the manufacturers (Table 1), very high rejection by RO90, RO98 and RO99 is expected. In the case of NF90 it appears better than expected rejection is observed based on the manufacturer's listed nominal molecular weight cut-off. However the nominal molecular weight cut-off given by the manufacturer is for tangential flow filtration under specified conditions. The observed rejection will be different in dead-end filtration.

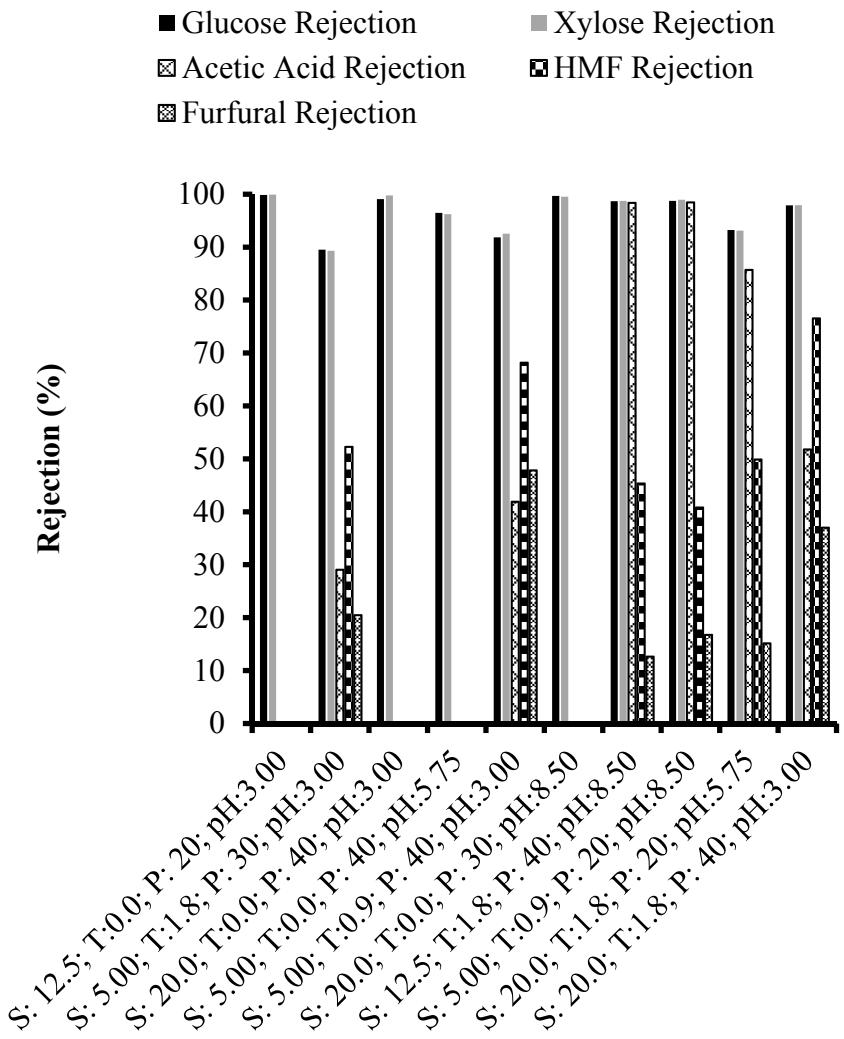

Figure 6: Rejection of glucose, xylose, acetic acid, HMF and furfural by NF90 under the experimental conditions tested. S: total sugar concentration (g/L) (glucose and xylose), T: total toxic compound concentration (g/L) (acetic acid, HMF and furfural); P; pressure (bar).

Figure 6 indicates a tremendous variation in acetic acid rejection for the NF90 membrane. Rejection increases dramatically at pH 5.75 and 8.0. The molecular weight of acetic acid is 60, much lower than either glucose or xylose. Thus the observed rejection of acetic acid is due to interactions with the membrane. Figure 1 indicates that above pH 4.0, NF 90 is negatively charged. The pKa of acetic acid is 4.76. Thus at pH 5.75 and 8.5 it will be deprotonated and negatively charged. At pH 5.75 only about 10% of the acetic acid molecules will be present in the protonated form while at pH 8.75 essentially all the acetic acid molecules will be deprotonated. Electrostatic

repulsion of the negatively charged acetate anion by the negatively charged membrane could explain the observed high rejection at high pH values. Some rejection of acetic acid is observed at pH 3.0 when the membrane is positively charged. Because the acetic acid molecule is polar, it could interact with the other dissolved species present as well as with the membrane surface, contributing to the observed rejection. It is important to note that the observed rejection of a particular species depends on feed and operating conditions as well as the membrane properties.

Similar results are observed for acetic acid rejection by RO90 (Figure 7) and RO99 (Figure 9). Figure 1 indicates that the variation of membrane zeta potential for RO90 is similar to NF90. However RO99 remains slightly negatively charged at pH 3.0. Nevertheless acetic acid will be present mainly in its protonated form at pH 3.0. Acetic acid rejection by RO98 appears to follow a similar trend though low rejection is observed at pH 8.5 at the highest concentration of toxic compounds and the highest feed pressure. It should however be noted that high feed pressure and feed concentration will tend to maximize passage of acetic acid.

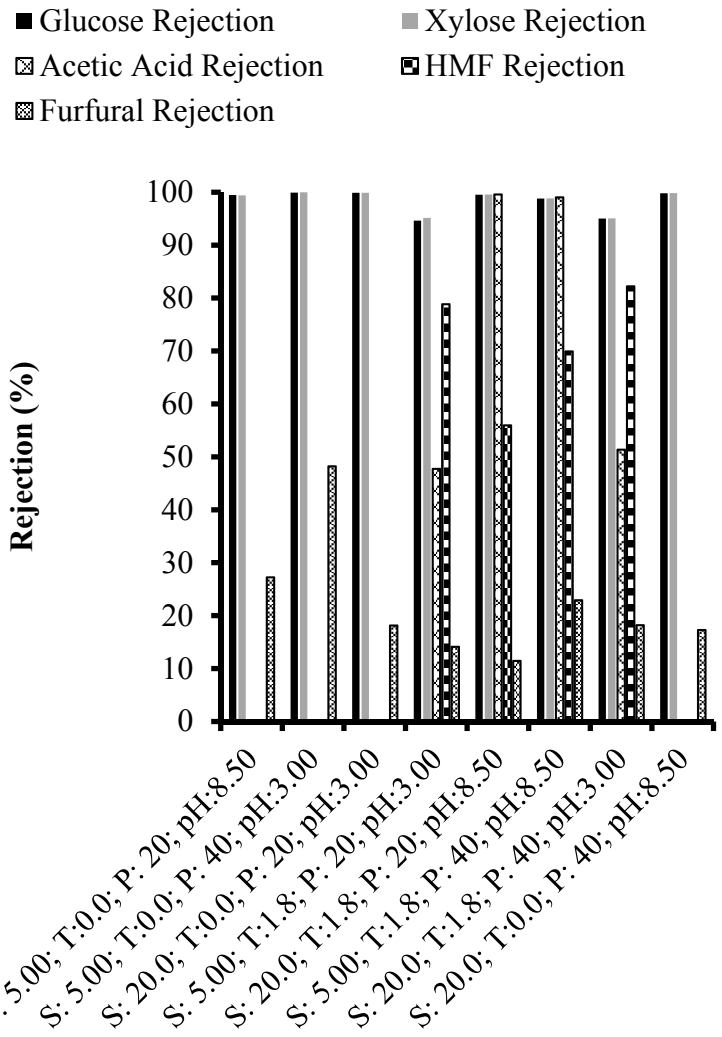

Figure 7: Rejection of glucose, xylose, acetic acid, HMF and furfural by RO90 under the experimental conditions tested. S: total sugar concentration (g/L) (glucose and xylose), T: total toxic compound concentration (g/L) (acetic acid, HMF and furfural); P; pressure (bar).

Figures 6-9 indicate that for all four membranes under the conditions tested, rejection of furfural is less than HMF. The molecular weight of furfural is 96 while HMF is 126. It is interesting to note that though the difference in molecular weight is small, the difference in rejection is significant. By comparison, the difference in molecular weight between glucose and xylose is similar, and their rejection is also similar. The presence of an additional –HC=O group on HMF makes it more hydrophilic. It is likely that HMF interacts with other dissolved solutes as well as the membrane more than furfural, leading to the higher observed rejection.

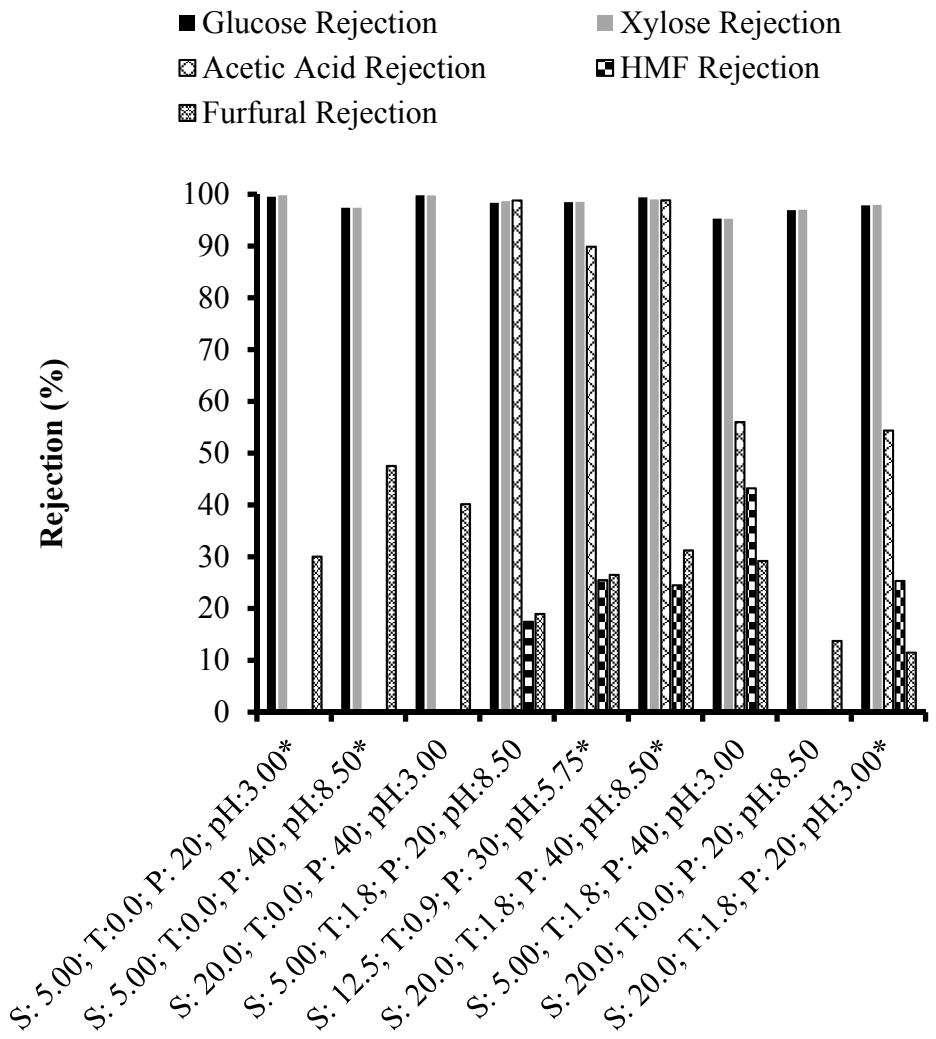

Figure 8: Rejection of glucose, xylose, acetic acid, HMF and furfural by RO98 under the experimental conditions tested. (*) These tests were conducted in duplicate based on the design of experiments software output. Average results are shown. S: total sugar concentration (g/L) (glucose and xylose), T: total toxic compound concentration (g/L) (acetic acid, HMF and furfural); P; pressure (bar).

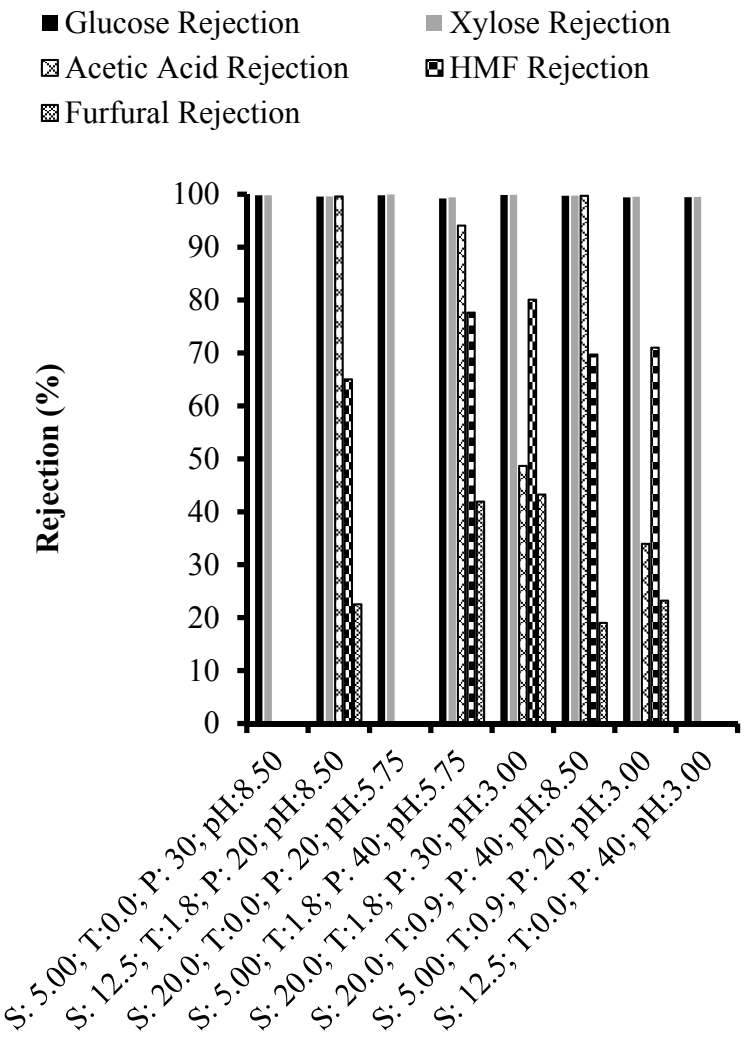

Figure 9: Rejection of glucose, xylose, acetic acid, HMF and furfural by RO99 under the experimental conditions tested. S: total sugar concentration (g/L) (glucose and xylose), T: total toxic compound concentration (g/L) (acetic acid, HMF and furfural); P; pressure (bar).

Comparing Figures 2-5 with 6-9, it can be seen that while the highest permeability occurs in the absence of any toxic compounds, it is not the case that the absence of toxic compounds always leads to higher permeabilities for the same operating conditions. This observation highlights the importance of feed and operating conditions on membrane performance. It also highlights the importance of screening membranes with model feed streams, thus avoiding the variability that exists with real hydrolysates.

Results for real hydrolysates are presented in Figures 10 and 11. Analogous to model feed streams, membrane permeability (Figure 10) and rejection (Figure11) results are given after 20 minutes of operation. As was the case for model feed streams, results are given in order of decreasing permeability. Based on the results for model feed streams, RO90 and RO98, which showed the lowest permeabilities, were replaced by NF270. The observed permeabilities for real hydrolysates are less than for model feed streams. The presence of dissolved and suspended solutes in the real hydrolysate will lead to lower permeabilities than for the model feed streams.

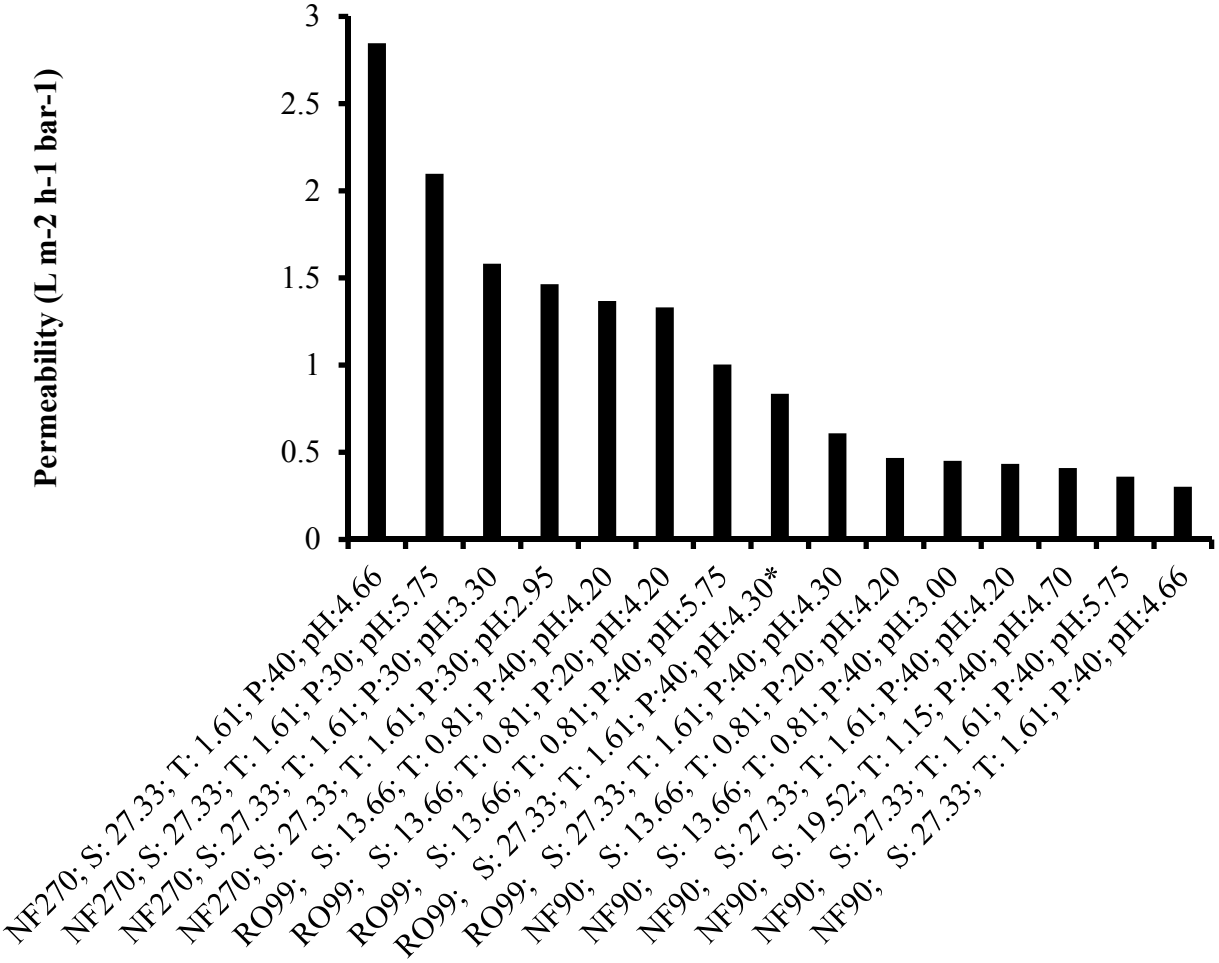

Figure 10: Permeability of NF270, NF90 and RO99 for feed streams consisting of real hydrolysates. (*) These tests were conducted in duplicate. Average results are shown. S: total sugar concentration (g/L) (glucose and xylose), T: total toxic compound concentration (g/L) (acetic acid, HMF and furfural); P; pressure (bar).

Figure 10 indicates that under the experimental conditions tested, NF270 always displayed the highest permeability. Table 1 indicates that this is not unexpected given the high nominal molecular weight cut off and low NaCl rejection of this membrane. Interestingly the permeability of NF90 is always less than RO99 under the experimental condition tested here. For model feed streams however, though the two membranes displayed similar permeabilities, NF90 often displayed slightly higher permeabilities than RO99. NF270 displays decreasing permeabilities with decreasing pH. This is most likely due to the changing surface charge on the membrane (see Figure 1), which in turn leads to changed interactions between the membrane and the dissolved species in the hydrolysate. Permeabilities for RO99 decrease with increasing concentration of toxic compounds, which is not unexpected as these compounds together with other species present in the feed will interact with the membrane surface. Finally NF90 displayed the lowest permeabilities and the lowest variation in permeability over the experimental conditions investigated. These results indicate the importance of testing membranes that performed well using model feed streams with real hydrolysates, as the presence of other species, absent in the model feed streams, can have a significant effect on membrane performance.

Figure 11 gives rejection data in order of decreasing permeability. As expected, NF270 generally displayed the lowest rejection of glucose and xylose. Rejection of all toxic compounds is low except at pH 2.95. As Figure 1 indicates that NF270 is negatively charged at all the pH values tested, the much higher rejection at pH 2.95 could be due to interactions between the toxic compounds, sugars and other dissolved and suspended solutes in the feed at pH 2.95. This result is different to the general observation for the other membranes that acetic acid rejection increases at pH value above its pKa. However as noted by Manttari et al. [26] at higher pH values, deprotonation of residual carboxylic groups in the polyamide barrier layer leads to swelling of the

NF270 membrane resulting in higher permeate fluxes. This could explain the higher rejection of toxic compounds at lower pH values.

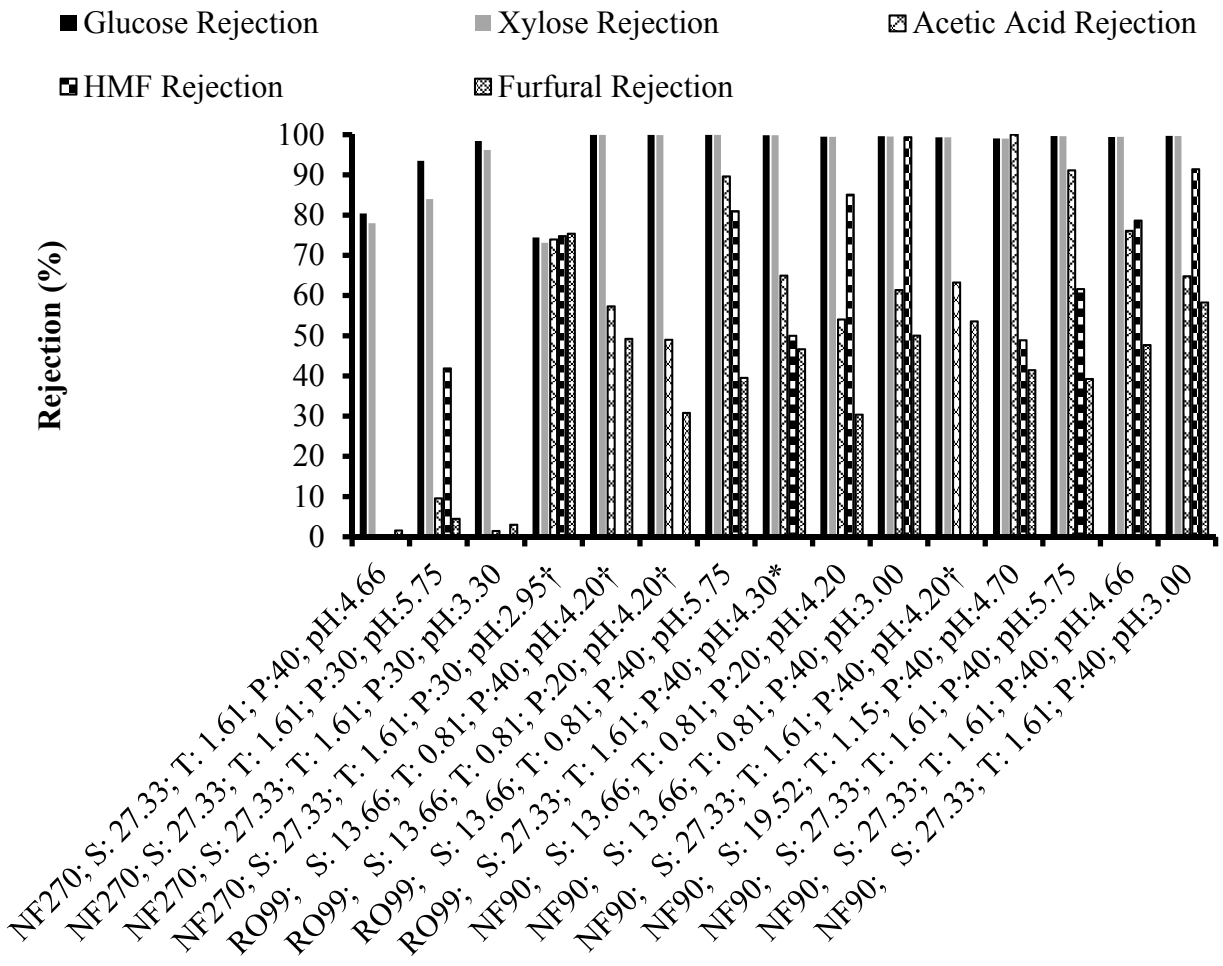

Figure 11: Rejection of glucose, xylose, acetic acid, HMF and furfural by NF270, NF90 and RO99 for feed streams consisting of real hydrolysates. (*) These experiments were conducted in duplicate. Average results are shown. (†) In these experiments, HMF concentration was below the limit of detection. S: total sugar concentration (g/L) (glucose and xylose), T: total toxic compound concentration (g/L) (acetic acid, HMF and furfural); P; pressure (bar).

Figure 11 indicates that at pH values above the pKa of acetic acid, rejection of acetic acid is generally higher, in agreement with the results for model feed streams. Further HMF rejection is generally higher than furfural rejection. In some experiments, no HMF rejection is reported. This is due to the very low HMF concentration in the feed stream. Consequently it was not detected in the retentate.

Our results indicate that nanofiltration membranes could be used to concentrate biomass hydrolysates and remove residual hydrolysis degradation products. Our results suggest that NF270 and RO99 give the best performance; highest fluxes, highest rejection of sugars and greatest passage of toxic compounds into the permeate. Membrane performance was quickly determined under a number of experimental conditions using dead end filtration. Because design of experiments software was used, not all experimental conditions were investigated. The next step would be to test NF270 and RO99 in tangential flow mode over a range of operating conditions that bracket the expected conditions in a real continuous process.

4.1. Analysis of Variance Using Surface Response Model

Conditions for the rejection of sugars and elimination of inhibitors from the synthetic feed while concentrating the sugars solution were optimized. The goal of the optimization was to assess the best pool of conditions for maximal rejection of sugars and elimination of inhibitors from the feed. Process variables and their range have been shown in Table 2. The optimization of selected parameters within the given ranges was designed to obtain the concrete information on the impact on rejection of sugars molecules in conjunction with elimination of the inhibitors from simulated feed. Figure 2 shows the response surface model desirability plots depicting the effect of total sugars concentration (mg/L) and feed pressure (bar) on desirability using four different membranes i.e. NF90, RO90, RO98 and RO99. NF90 and RO99 membrane showed the highest desirability toward sugar concentration (Fig. 1 a, d).

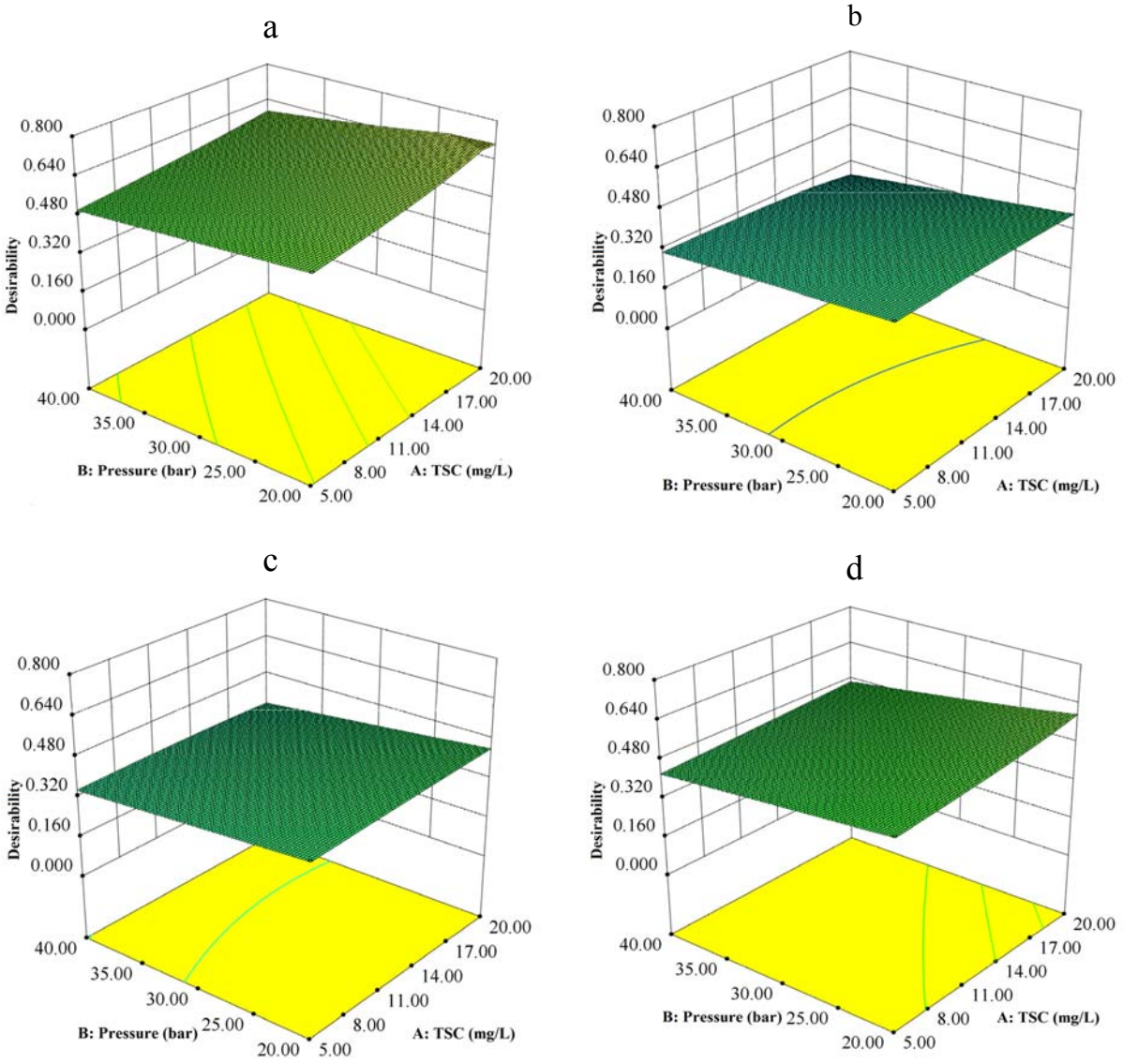

Figure 12: Response surface model desirability for: a) NF90; b) RO90; c) RO98; d) RO99

Analysis of RSM results showed the most influential parameters and their interactions such as type of membrane versus xylose/glucose rejection, pH versus xylose, glucose and acetic acid rejection and the interaction of flux decline with total sugars concentration (Figure 13). Other response surface plots showing the interactions of variables were also plotted (supplementary figures and tables are provided in Appendix 1 C). However, their effects were not found significant.

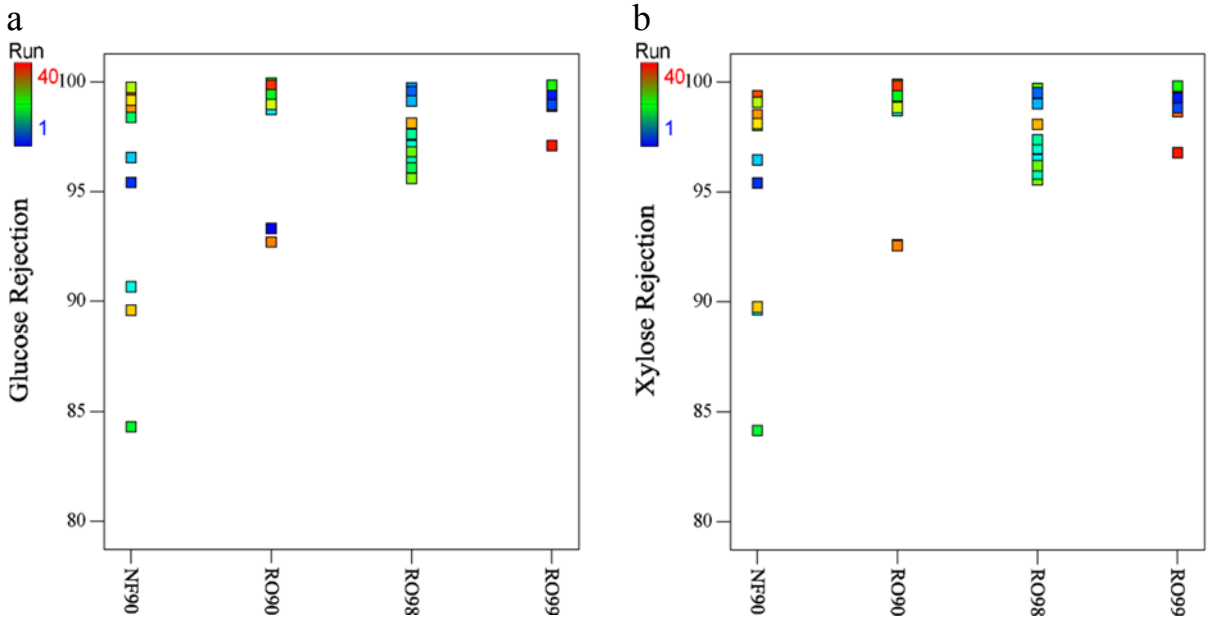

Figure 13: Analysis of Experimental Results Obtained from Software: a) Membrane vs. Glucose Rejection; b) Membrane vs. Xylose Rejection

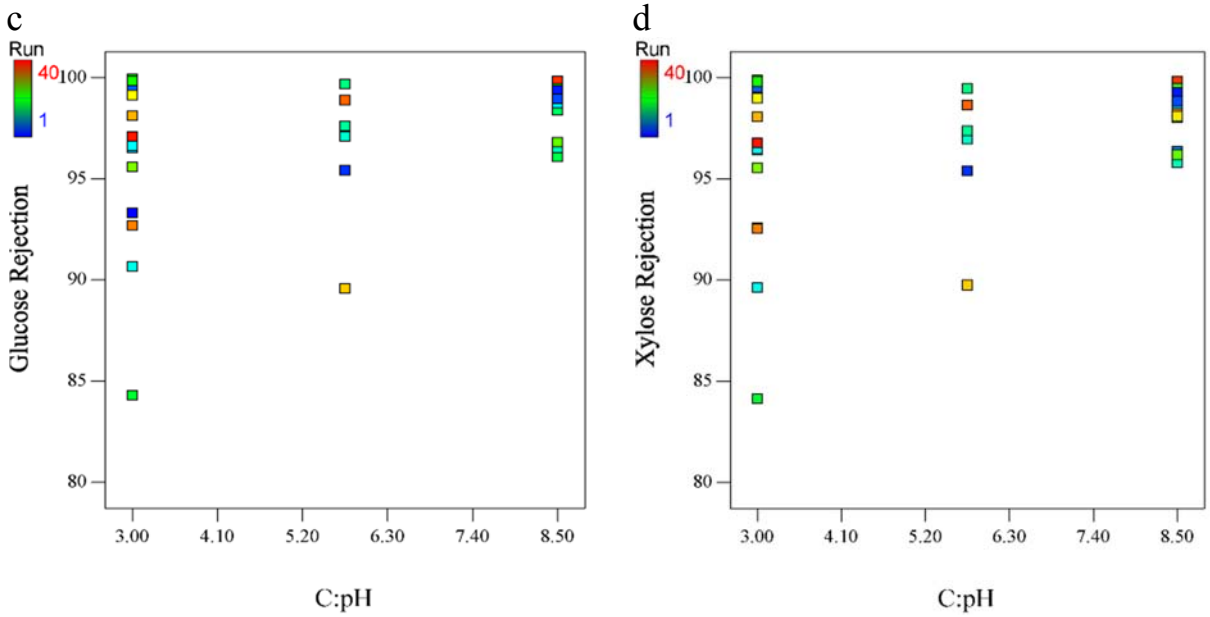

Figure 13: Analysis of Experimental Results Obtained from Software: c) pH vs. Glucose Rejection; d) pH vs. Xylose Rejection

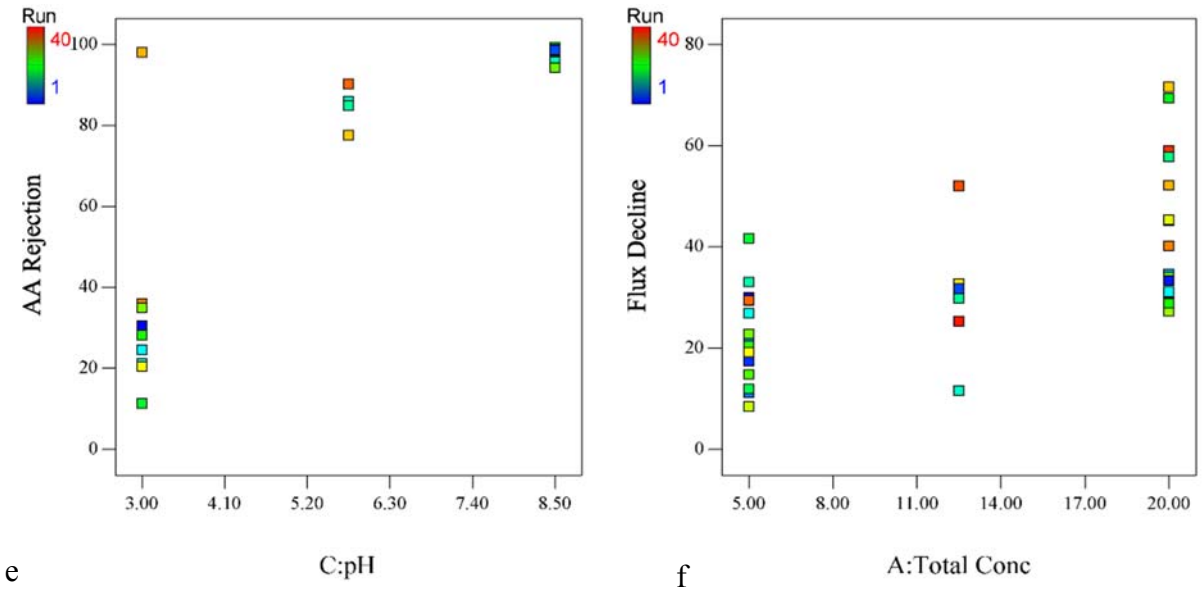

Figure 13: Analysis of Experimental Results Obtained from Software: e) pH vs. Acetic Acid Rejection; f) Flux Decline vs. Total Sugar Concentration

The effect of all five process variables (total sugars concentration, feed pressure, pH, toxic compounds concentration and type of membrane) on responsive variables i.e. sugars rejection, elimination of toxic compounds, flux flow and flux decline have been correlated with their respective p-values (Table D 1). From comparing the p-values, toxic compounds concentration had maximum impact on xylose recovery ($p>0.0094$) and glucose recovery ($p>0.0121$). Acetic acid, furfural and HMF rejection was more influenced with the pH of feed solution ($p>0.0009$), ($p>0.0001$) and ($p>0.0013$) respectively. Flux flow showed maximum influence with type of membrane ($p>0.0152$) while flux decline was influenced maximally on the sugars concentration ($p>0.0002$).

5. Conclusion

Dead-end filtration experiments have been conducted using model and real hydrolysate to screen a number of commercially available membranes under a range of conditions. Design of experiments software enabled minimization of the number of experiments while yet indicating the effect of the various variables that were investigated on membrane performance. This work highlights the fact that nanofiltration could be a viable process for sugar concentration in biomass hydrolysates while reducing the load of toxic compounds prior to fermentation. Often selection of an appropriate membrane and optimum operating conditions is complex and time consuming. The method developed here could be used to quickly screen membranes. Promising membranes and operating conditions could then be more rigorously tested in tangential flow operation.

6. Acknowledgements

This work was funded by the U.S. Department of Energy (Contract No. DE-AC36-08-GO28308) and the National Renewable Energy Laboratory via subcontract AFA-1-11658-01. We gratefully acknowledge Dr. Frank Lipinzki from Alfa Laval for sampling us with free membranes.

7. References

[1] C. Abels, F. Carstensen, M. Wessling, Membrane processes in biorefinery applications, J. Memb. Sci. 444 (2013) 285–317.

[2] Z. Qiu, L. Zhao, L. Weatherley, Process intensification technologies in continuous biodiesel production, Chem. Eng. Process. Process Intensif. 49 (2010) 323–330.

[3] E. Drioli, A. Brunetti, G. Di Profio, G. Barbieri, Process intensification strategies and membrane engineering, Green Chem. 14 (2012) 1561.

[4] G.W. Huber, S. Iborra, A. Corma, Synthesis of transportation fuels from biomass: chemistry, catalysts, and engineering., Chem. Rev. (2006) 4044–4098.

[5] H.-J. Huang, S. Ramaswamy, U.W. Tschirner, B.V. Ramarao, A review of separation technologies in current and future biorefineries, Sep. Purif. Technol. 62 (2008) 1–21.

[6] D.L. Grzenia, D.J. Schell, S.R. Wickramasinghe, Membrane extraction for removal of acetic acid from biomass hydrolysates, J. Memb. Sci. 322 (2008) 189–195.

[7] Q. Gan, S.. Allen, G. Taylor, Design and operation of an integrated membrane reactor for enzymatic cellulose hydrolysis, Biochem. Eng. J. 12 (2002) 223–229.

[8] S. Kinoshita, J.W. Chua, N. Kato, T. Yoshida, H. Taguchi, Hydrolysis of cellulose by cellulases of Sporotrichum cellulophilum in an ultrafilter membrane reactor, Enzyme Microb. Technol. 8 (1986) 691–695.

[9] I. Ohlson, G. Trägårdh, B. Hahn-Hägerdal, Enzymatic hydrolysis of sodium-hydroxide-pretreated sallow in an ultrafiltration membrane reactor., Biotechnol. Bioeng. 26 (1984) 647–53.

[10] K. Bélafi-Bakó, A. Koutinas, N. Nemestóthy, L. Gubicza, C. Webb, Continuous enzymatic cellulose hydrolysis in a tubular membrane bioreactor, Enzyme Microb. Technol. 38 (2006) 155–161.

[11] F. Carstensen, A. Apel, M. Wessling, In situ product recovery: Submerged membranes vs. external loop membranes, J. Memb. Sci. 394-395 (2012) 1–36.

[12] B. Van der Bruggen, J. Geens, Nanofiltration in advanced membrane technology and applications, in: N.N. Li, A.G. Fane, W.S.W. Ho, T. Matsuura (Eds.), Adv. Membr. Technol. Appl., Hoboken, NJ, USA, 2008.

[13] Y.-H. Weng, H.-J. Wei, T.-Y. Tsai, T.-H. Lin, T.-Y. Wei, G.-L. Guo, et al., Separation of furans and carboxylic acids from sugars in dilute acid rice straw hydrolyzates by nanofiltration., Bioresour. Technol. 101 (2010) 4889–94.

[14] H.H. Himstedt, H. Du, K.M. Marshall, S.R. Wickramasinghe, X. Qian, pH Responsive Nanofiltration Membranes for Sugar Separations, Ind. Eng. Chem. Res. 52 (2013) 9259–9269.

[15] B. Qi, J. Luo, X. Chen, X. Hang, Y. Wan, Separation of furfural from monosaccharides by nanofiltration., Bioresour. Technol. 102 (2011) 7111–8.

[16] S.K. Maiti, Y. Lukka Thuyavan, S. Singh, H.S. Oberoi, G.P. Agarwal, Modeling of the separation of inhibitory components from pretreated rice straw hydrolysate by nanofiltration membranes., Bioresour. Technol. 114 (2012) 419–27.

[17] H.H. Himstedt, K.M. Marshall, S.R. Wickramasinghe, pH-responsive nanofiltration membranes by surface modification, J. Memb. Sci. 366 (2011) 373–381.

[18] Dow FilmTec product information for NF270, 2012.

[19] Dow FilmTec product information for NF90, 2012.

[20] Alfa Laval product information for RO90, 2012.

[21] Alfa Laval product information for RO98, 2012.

[22] Alfa Laval product information for RO99, 2012.

[23] K. Boussu, Y. Zhang, J. Cocquyt, P. Van der Meeren, A. Volodin, C. Van Haesendonck, et al., Characterization of polymeric nanofiltration membranes for systematic analysis of membrane performance, J. Memb. Sci. 278 (2006) 418–427.

[24] S. Mondal, S.R. Wickramasinghe, Produced water treatment by nanofiltration and reverse osmosis membranes, J. Memb. Sci. 322 (2008) 162–170.

[25] C. TANG, Y. KWON, J. LECKIE, Probing the nano- and micro-scales of reverse osmosis membranes—A comprehensive characterization of physiochemical properties of uncoated and coated membranes by XPS, TEM, ATR-FTIR, and streaming potential measurements, J. Memb. Sci. 287 (2007) 146–156.

[26] M. Mänttäri, A. Pihlajamäki, M. Nyström, Effect of pH on hydrophilicity and charge and their effect on the filtration efficiency of NF membranes at different pH, J. Memb. Sci. 280 (2006) 311–320.

[27] G. Bargeman, J.M. Vollenbroek, J. Straatsma, C.G.P.H. Schroën, R.M. Boom, Nanofiltration of multi-component feeds. Interactions between neutral and charged components and their effect on retention, J. Memb. Sci. 247 (2005) 11–20.

[28] S. Kimura, S. Sourirajan, Transport Characteristics of Porous Cellulose Actate Membranes for Reverse Osmosis Separation of Sucrose in Aqueous Solutions, Ind. Eng. Chem. Process Des. Dev. 7 (1968) 548–554.

[29] C. Rodrigues, A.I. Cavaco Morão, M.N. de Pinho, V. Geraldes, On the prediction of permeate flux for nanofiltration of concentrated aqueous solutions with thin-film composite polyamide membranes, J. Memb. Sci. 346 (2010) 1–7.

[30] N. Aydoğan, T. Gürkan, L. Yilmaz, Effect of Operating Parameters on the Separation of Sugars by Nanofiltration, Sep. Sci. Technol. 33 (1998) 1767–1785.

[31] C.Y. Tang, Y.-N. Kwon, J.O. Leckie, Effect of membrane chemistry and coating layer on physiochemical properties of thin film composite polyamide RO and NF membranes, Desalination. 242 (2009) 168–182.

8. Appendix

Appendix 1 A: Design of Experiments

Table B 1: Model sugar solution design of experiments

Run #	Total sugar concentration (g/L)	Total toxic compound concentration (g/L)	Transmembrane pressure (bar)	pH	Membrane
1	5.0	0	40	5.75	NF90
2	5.0	0.90	40	3.00	NF90
3	5.0	0.90	20	8.50	NF90
4	5.0	1.80	30	3.00	NF90
5	12.5	0	20	3.00	NF90
6	12.5	1.80	40	8.50	NF90
7	20.0	0	30	8.50	NF90
8	20.0	0	40	3.00	NF90
9	20.0	1.80	20	5.75	NF90
10	20.0	1.80	40	3.00	NF90
11	5.0	0	20	8.50	RO90
12	5.0	0	40	3.00	RO90
13	5.0	1.80	20	3.00	RO90
14	5.0	1.80	40	8.50	RO90
15	20.0	0	40	8.50	RO90
16	20.0	0	20	3.00	RO90
17	20.0	1.80	20	8.50	RO90
18	20.0	1.80	40	3.00	RO90
19*	5.0	0	20	3.00	RO98
20*	5.0	0	40	8.50	RO98
21	5.0	1.80	40	3.00	RO98
22	5.0	1.80	20	8.50	RO98
23*	12.5	0.90	30	5.75	RO98
24	20.0	0	20	8.50	RO98
25	20.0	0	40	3.00	RO98
26*	20.0	1.80	20	3.00	RO98
27*	20.0	1.80	40	8.50	RO98
28	5.0	0	30	8.50	RO99
29	5.0	0.90	20	3.00	RO99
30	5.0	1.80	40	5.75	RO99
31	12.5	0	40	3.00	RO99
32	12.5	1.80	20	8.50	RO99
33	20.0	0	20	5.75	RO99
34	20.0	0.90	40	8.50	RO99
35	20.0	1.80	30	3.00	RO99

Appendix 1 B: Real Hydrolysate Filtrations

Table B 1: Actual hydrolysate filtration design of experiments

Run #	Membrane	Pressure (bar)	Dilution Factor	pH
1	NF90	40	5	4.66
2	NF90	40	7	4.7
3	NF270	40	5	4.68
4	BW30	40	5	4.68
5	NF90	40	5	3
6	NF90	40	5	5.75
7	NF90	40	10	3
8	NF270	30	5	3.3
9	NF270	30	5	2.95
10	NF270	30	5	5.75
11	RO99	40	5	4.3
12	RO99	40	5	4.3
13	NF90	40	5	4.2
14	RO99	40	10	4.2
15	RO99	20	10	4.2
16	RO99	40	10	5.75
17	NF90	20	10	4.2

Appendix 1 C: Software Results from Surface Response Model

Table 1 C:

Collection of p-values after the statistical analysis of response surface method

Source (R1)	R1: p-value Prob>F	R2: p-value Prob>F	R3: p-value Prob>F	R4: p-value Prob>F	R5: p-value Prob>F	R6: p-value Prob>F	R7: p-value Prob>F	Sum of Squares	df	Mean Square	F	p-value Prob>F
Model	0.0152	0.0258	0.0216	<0.0001	0.0356	0.0213	0.0015	170.24	7	24.32	3.01	0.0152
A- Total Concentration	0.1061	0.1401	0.2286	0.7584	0.5177	0.1588	0.0002	22.36	1	22.36	2.76	0.1061
B-Pressure	0.8008	0.8367	0.99	0.0715	0.2314	0.6161	0.0668	0.52	1	0.52	0.065	0.8008
C- pH	0.2128	0.2073	0.0009	<0.0001	0.0013	0.6745	0.2041	13.07	1	13.07	1.62	0.2128
D- Additive Concentration	0.0094	0.0121	0.6932	0.1651	0.5936	0.0511	0.4308	61.74	1	61.74	7.63	0.0094
E- Membrane	0.045	0.069	0.4541	0.00007	0.1798	0.0152	0.1433	72.82	3	24.27	3	0.045
Residual								258.86	32	8.09		
Lack of Fit	0.0127	0.0063	0.4168	0.293	0.7987	<0.0001	0.6367	253.32	27	9.38	8.46	0.0127
Pure Error								5.54	5	1.11		
Cor. Total								429.1	39			

College of Engineering

Ralph E. Martin Department of Chemical Engineering

Appendix 2 D: Multiple Author Documentation

To whom it may concern,

Hereby, I confirm that Mr. Malmali has done more than 51% of the work for chapter 2 of this dissertation. The list of authors is as follow:

Mohammadmahdi Malmali

Jonathan Stickel

S. Ranil Wickramasinghe

S. Ranil Wickramasinghe, PhD

Professor, Ross E Martin Chair in Emerging Technologies
Ralph E Martin Department of Chemical Engineering
University of Arkansas
3202 Bell Engineering Center

Chapter 3: Submerged Membrane Reactor for Continuous Biomass Hydrolysis

Submerged Membrane Reactor for Continuous Biomass Hydrolysis

Mohammadmahdi Malmali[*], Jonathan J. Stickel[#], S. Ranil Wickramasinghe[*2]

[*] Ralph E. Martin Department of Chemical Engineering, University of Arkansas, Fayetteville, AR 72701, USA

[#] National Renewable Energy Laboratory, National Bioenergy Center, Golden, CO 80401, USA

1. Abstract

The second part of this work focuses on recycle of cellulase enzyme (biocatalyst) used to catalyze the biopolymers of cellulose to monomeric soluble sugars. The enzyme represents one of the main costs in bioconversion of lignocellulosic biomass into biofuel. But exploration and development of efficient ways to reuse and recycle the enzyme are of great interest. Here we explore the use of microfiltration and ultrafiltration membranes for enzyme recycle and reuse.

2. Introduction

Increasing world energy usage as well as increasing environmental concerns relating to greenhouse gas emission combined with the limited fossil fuel reserves has led to considerable interest in the development of economical and energy efficient processes for sustainable production of fuels and chemicals [1]. Plant biomass represents the only sustainable source of organic carbon [2]. Unlike 1st generation biofuels, production of 2nd generation biofuels from

[2] Corresponding author: Tel: +1 479 575 8475; Fax: +1 479 575 4940; email: ranil.wickrmasinghe@uark.edu

lignocellulosic biomass is far more complex. Development of new efficient separation and purification operations that lead to process intensification are essential for production of competitive 2nd generation drop-in biofuels. Membrane-based separation processes are attractive as they could lead to significant process intensification and hence reduced operating costs [3].

Here, we focus on hydrolysis of lignocellulosic biomass followed by fermentation. Dilute sulfuric acid has been shown to effectively hydrolyze the hemicellulose component of the biomass to its monomeric sugars as well as enhance the enzymatic digestibility of cellulose [4]. Next, cellulose is enzymatically hydrolyzed to glucose. A cocktail of cellulase enzymes is used to break down cellulose synergistically [5]. However, the cost of the enzymes has been an inhibitory factor for the commercialization of biomass conversion technology [6]. Thus, development of a continuous enzymatic hydrolysis process where the cellulose enzymes may be reused is of considerable interest.

A further complication with batch hydrolysis of cellulose is that the conversion rate is often limited by inhibition due to glucose and cellobiose. Using Celluclast, Novozymes A/S (Bagsvaerd, Denmark) cellulose enzyme, Andrić et al. [7] indicate that the presence of glucose significantly reduced enzymatic hydrolysis rates. Removal of glucose lead to increased glucose yields and rates of production. Combination of a membrane separation unit with a hydrolysis reactor could enable continuous removal of glucose and recycle of cellulose enzyme and residual cellulose. Here, we focus on development of a combined membrane separation unit with a hydrolysis reactor that could enable continuous enzymatic hydrolysis of lignocellulosic biomass. Further by recycling the enzyme and continuously removing glucose, enzyme usage glucose production rates and glucose yields are increased potentially leading to a more cost-effective process.

Abels et al. [8] provide an excellent review of membrane processes for biorefinery applications. Several studies [9-14] have focused on the use of ultrafiltration membranes for continuous removal of glucose in the permeate. The retentate containing residual cellulose and cellulase enzyme is recycled to the enzyme reactor. Mores et al. [15] have considered the use of sedimentation and microfiltration for recovery of cellulase enzyme.

Andrić et al. [16] provide several insights into the design of membrane bioreactor for enzymatic hydrolysis of lingnocellulosic biomass. Since cellulose is insoluble, pumping high solids concentration feed streams is problematic due to the high solution viscosity. Further membrane fouling is a serious concern at high solids loadings. In addition, the glucose concentration in the permeate is too low for direct flow into the fermentation reactor. Finally, one needs to remove lignin and other non-hydrolysable components of the lignocellulosic biomass.

Carstensen et al. [8] have reviewed the use of membranes for in situ product recovery. Two modes of operation exist: external loop membranes and submerged membranes. External loop membranes involve pumping the contents of the enzyme reactor through a membrane module. Retentate is recycled back to the reactor while the permeate containing glucose is continuously removed. Submerged membranes on the other hand involve placing the membrane inside the enzymatic hydrolysis reactor. Then, there is no need to pump the contents of the enzyme reactor through an external loop. Numerous configurations have been described for both external loop [17-23] and submerged membranes [24-27] The reactor volume is kept constant by adding fresh feed (cellulose enzyme and biomass) at the same rate at which permeate is removed. Carstensen et al. [28] describes the advantages and disadvantages of external loop versus submerged membranes.

Use of a submerged membrane overcomes the need to pump aqueous streams containing high cellulose concentration through a membrane module. This is a significant benefit as these high viscosity feed streams are difficult to pump. By ensuring rapid mixing we minimize membrane fouling due to deposition of cellulose and cellulose enzyme on the member surface. We use a modified dead-end stirred cell as the enzyme rector. Thus, the bottom surface of the reactor contains the membrane. Batch, semi-batch and continuous enzymatic hydrolysis experiments have been conducted using alfa-cellulose. Both ultrafiltration and microfiltration membranes have been tested. The results obtained here indicate that a submerged membrane rector may be feasible for continuous enzymatic hydrolysis of lignocellulosic biomass.

3. Experimental

3.1. Materials and Method

Unless otherwise noted all chemicals were ACS reagent grade. D-glucose, D-cellobiose, α-cellulose and grade 1 Whatman filter paper were purchased from Sigma Aldrich (St. Louis, MO). Sodium azide 5% w/v, acetic acid and sulfuric acid were purchased from Seastar Chemicals Inc. (Sidney, BC, Canada). Sodium hydroxide and citric acid were purchased from J. T. Baker (Philipsburg, NJ). Polysulfone UFX5 with 5 kDa MWCO and 0.65 μm polyethersulfone membranes were received from Alfa Laval Inc. (Wood Dale, IL) and Pall Corporation (Port Washington, NY), respectively. Sodium potassium tartrate and 3,5 dinitrosalicylic acid from Alfa Aesar (Ward Hill, MA), phenol and sodium metabisulfite from Amresco (Solon, OH) were purchased to measure the cellulose activity. Deionized water (conductivity < 10 μScm^{-1} and resistance > 18.5 MΩ) was obtained from a Labconco (Kansas City, MO) water purification system (Water Pro RO and Water Pro PS Polishing Stations).

A commercial cellulase enzyme, Cellic CTec 2 was used in all experiments. Cellic CTec 2 is a multi-enzyme cocktail produced by Trichoderma reesei, and it was generously supplied by Novozymes North America (Franklinton, NC). Cellulase activity was 145 FPU/mL, measured as mentioned by Ghose 1987 [29].

3.2. Analytical Methods

Samples collected from the permeate stream were analyzed by an Agilent 1200 series HPLC (Agilent Technologies, Palo Alto, CA) equipped with an Agilent 6.5×300 mm Hi-Plex Ca (Duo) column and Agilent refractive index detector (RID). RID sample cell was set at 55 ℃. The mobile phase appropriate for this column was HPLC grade water with flow rate set at 0.6 mL min^{-1}. Auto sampler was set for an injection volume of 15 μL and the column was kept at 80℃ using a thermostatted column compartment. A series of calibration standards and calibration verification standards (CVS) were obtained from Absolute Standards Inc., Hamden, CT. All measurements were taken in triplicate and average results are reported.

4. Enzymatic Hydrolysis Experiments

For enzymatic hydrolysis tests, the α-cellulose was diluted in a 50 mM citric acid buffer at pH 4.8 containing 0.01% w/v sodium aizde to suppress microbial contamination. The cellulase enzyme was diluted in the buffer. We tested the performance of membrane bioreactor with different agitation speeds, enzyme loading and biomass concentration. The biocatalytical conversion of cellulose to soluble sugars is carried out through the following stoichiometries:

$$(\text{Glucan})_n + n\ H_2O \rightarrow n\ \text{Glucose} \quad (1)$$

$$2(\text{Glucan})_n + n\ H_2O \rightarrow n\ \text{Cellubiose} \quad (2)$$

All hydrolysis experiments were carried at 50 °C. The reactor was incubated in a jacketed thermostatic bath to control the temperature.

4.1. Batch Experiments

Our purpose of batch experiments was to investigate the effect of temperature, pH, and hydrolysis time. We loaded several centrifuge tubes with 4 g of α-cellulose, 0.4 mL enzyme, and 38.5 ml of 50 mM citric acid buffer with pH in the range of 3.8-5.5. The pH was adjusted using 0.1 M sodium hydroxide and sulfuric acid. Then, we sealed and incubated the centrifuge tubes in a thermostatic shaker at 40, 50 and 60 ˚C for 48 and 96 hours. Shaker was set at 150 rpm to provide the required mixing during hydrolysis experiment.

Mixing and handling high streams containing high lignocellulosic substrate concentration is proved to be challenging [30,31], and it does present several difficulties. This is why we were interested to run enzymatic hydrolysis tests in a larger scale (1000 mL) reactor to investigate kinetics of the enzymatic saccharification, enzyme inhibition and operating conditions in larger scale. We used a 1 L flask as our hydrolysis reactor. We also used a RZR1 Brinkmann Heidolph (Elk Grove Village, IL) mechanical overhead stirrer equipped with a Heidolph PR30 pitched blade impeller to provide the required agitation.

For batch experiments, we loaded the reactor with 50 mM citric acid buffer and a predetermined amount of cellulose a night before. Then, the reactor was incubated for about 12 hours in a thermostatic bath with 100 rpm mixing. We started the experiments by addition of the enzyme to the reactor cell. Each experiment took place at least for 85 hours until glucose production reached an insignificant rate.

4.2. Semibatch Experiments

In semibatch operation, fresh cellulose and enzyme were added intermittently while the solvent (water plus dissolved compounds) are removed from the reactor. This mode of operation permits repetitive use of enzyme compared to batch experiments.

We used Millipore EMD 8400 Amicon stirred cell (Billerica, MA) as our integrated membrane bioreactor. We modified the cell to increase the volume to 1 L. We also used a RZR1 Brinkmann Heidolph mechanical overhead stirrer (Elk Grove Village, IL). Designing an effective mixing pattern in enzymatic hydrolysis reactor is crucial because biomass slurry tends to show non-Newtonian characteristics. Since in our modified reactor, the length-to-diameter ratio was not similar to the reactor design standard values, we modified our Heidolph PR30 pitched blade impeller by adding of a propeller for a better mixing hydrodynamics. During semibatch experiments we loaded the reactor with predetermined amount of buffer, substrate and enzyme. We ran enzymatic hydrolysis for 48 h. Then, reactor contents were filtered and loaded with fresh makeup buffer containing both cellulose and enzyme. We employed this procedure for two consecutive cycles. We used 5 kDa ultrafiltration (UF) and 0.65 μm microfiltration (MF) membranes in our membrane bioreactor. A schematic diagram of our experimental apparatus is shown in Figure 1.

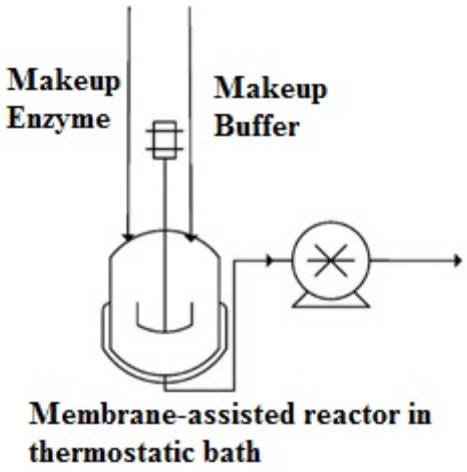

Figure 1: Semibatch process schematic diagram

During the semibatch experiments using 5 kDa UF membrane, we used high pressure nitrogen line to pressurize the cell and filter the reactor contents. We started the filtration with 15 psi, and gradually reached 60 psi by the end of filtration. We were able to remove 210-240 mL of reactor contents after each filtration. In case of membrane bioreactor equipped with polyethersulfone 0.65 μm membrane, we used a peristaltic pump on the permeate side of the membrane to provide the vacuum and filter reactor contents. In case of MF membranes, we removed larger amount of permeate (250 mL) after each filtration. Cellulose conversion can be either calculated using some basic calculations or estimated using the experimental method. If we assume that any density change is due to hydrolysis of cellulose to soluble glucose, then the cellulose conversion (X) can be calculated as followed:

$$X = \frac{m_{glucose}}{1.11\ m_{cell,0}} \tag{3}$$

where $m_{glucose}$ is total glucose mass and $m_{cell,0}$ is total initial cellulose mass [32]. To measure cellulose conversion experimentally, we collected 4 mL samples of reactor contents in several time

intervals. Samples were quickly filtered in Corning Costar Spin-X centrifuge tube filters (Sigma Aldrich, St. Louis, MO) spinning at 10,000 rpm for 2 minutes. Contents of each filter was washed with 1 mL of DI water, followed by spinning at 10,000 rpm for 5 minutes. We repeated the washing procedure for 3 times. Then, the insert filters were dried in a VWR Symphony Vacuum Oven (Radnor, PA) at 35 ˚C overnight. The total suspended solid (TSS) content was calculated using the equation (4).

$$X = \frac{m_{filter,AD} - m_{filter,0}}{V_0} \quad (4)$$

in which $m_{filter,AD}$ and $m_{filter,0}$ are the total weight of filter after drying in the oven and before loading with sample, respectively. V_0 is the volume of the sample loaded in the centrifuge tube. Weiss et al. [57] have studied the measurement of insoluble solids in biomass slurries in detale.

We also collected some samples at different time intervals to measure the amount of liberated glucose and cellubiose. The samples were filtered using 0.22 μm syringe filters and then analyzed using HPLC. We added 25-50 mL of DI water after each 20 hours to compensate for the amount of evaporation from the cell, and adjusted the cell contents level to the predetermined amount. All semibatch tests were carried out at 50 ˚C and 100 rpm.

4.3. Continuous Experiments

Continuous experiments were also run. Continuous addition of buffer containing cellulose + enzyme and removal of solvent containing dissolved sugar (glucose) was investigated, A challenging barrier remains pumping of cellulose. As it is shown in Figure 2, we used 2 pumps to inject cellulose+buffer and enzyme+buffer in the feed side and one pump in the permeate side of the reactor to remove the sugar stream with a constant flux.

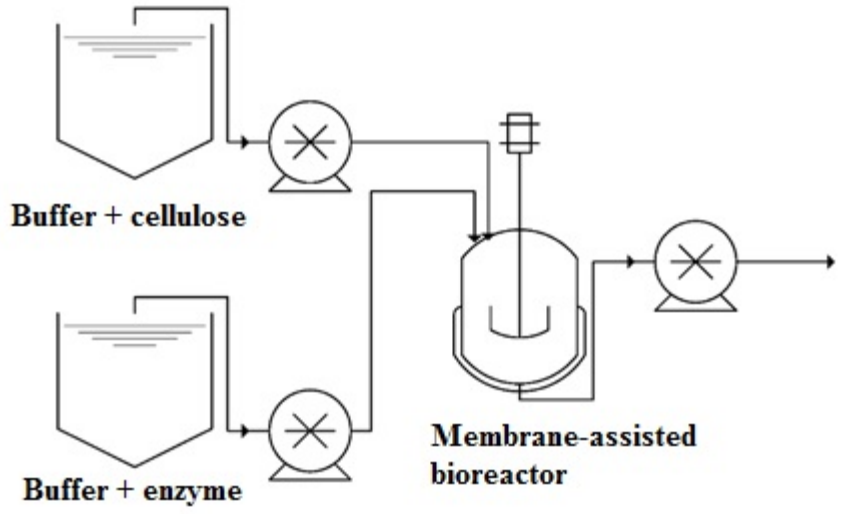

Figure 2: Continuous process schematic diagram

Handling and transfer of biomass slurry is challenging. Cellulose tends to settle, agglomerate and block the tubing. To ease the process of pumping of makeup biomass solution into the membrane bioreactor we placed the cellulose+buffer tank and pump in an altitude to take advantage of gravity. In this set of experiments we only employed MF membrane since it was easier to operate and required lower vacuum pressure on the permeate side. We could provide this vacuum pressure using a peristaltic pump. The parameters that we investigated during continuous enzymatic hydrolysis experiments were residence time inside the reactor, pre-holding time and cellulose loading. The higher the reactor residence time, the higher is the concentration of glucose in hydrolysate and the higher is enzyme inhibition. Also, pre-holding time was an influential parameter. We followed the same procedure for soaking and loading of enzyme and substrate, as mentioned in batch and semibatch experiments. After addition of enzyme, we started to inject the feed to the system and take the permeate side with a constant flux for experiments with pre-holding time equal to zero. For experiments with pre-holding time more than zero (half of retention time),

we let the enzymatic hydrolysis take place for the pre-holding time and then started to inject the feed and take permeate. All continuous tests were carried out at 50 ˚C and 100 rpm.

5. Results and Discussions

5.1. Effect of Temperature, pH, and Hydrolysis Time

We ran batch tests inside the centrifuge tubes for 2 and 4 days. The aim was to understand the effect of temperature, pH and hydrolysis time on performance of Cellic CTec2 and the enzymatic saccharification process. At the end of each batch test, we took a 2 mL sample for HPLC analysis. Samples were prefiltered using a 0.2 μm syringe filter to remove all the particulate matter. Figure 3 is showing the results of batch experiments in centrifuge tubes. Here the glucose concentration after 2 days of hydrolysis, as shown. HPLC analysis showed the cellobiose concentration was negligible after 2 days of hydrolysis. This is due to sufficient activity of beta glucosidase in Cellic CTec2 cocktail. Results for hydrolysis after 2 and 4 days show that 50 °C is the most optimum temperature for enzymatic saccharification.

Effect of pH was also investigated. Results show that batch enzymatic hydrolysis after 2 days had the highest glucose production (~54 g/L) at pH 4.95. Higher and lower pH resulted in much lower enzymatic activity. Enzymatic activity of cellulose was not significantly changed at lower pH ranges. Comparing Figure 3 a and b shows the effect of hydrolysis time. It is clear that more reaction time results in higher glucose production. The highest glucose production was 75 g/L obtained at pH 4.75 and 50 °C after 4 days of hydrolysis. It is interesting to notice the hydrolysis rates at 30 and 60 °C after 2 and 4 days. Glucose production after 2 days is higher at higher temperature (60 °C). However, 4-day results show that the production rate decreases

significantly. For example, comparison of results at pH 4.95 (2-day hydrolysis) and 4.9 (4-day hydrolysis) and 40 °C shows that glucose production has increased by 90% from day 2 to day 4.

However, this increase is significantly lower (~5%) for glucose production at 60 °C. This is maybe due to the faster deactivation of cellulose enzyme at higher temperature.

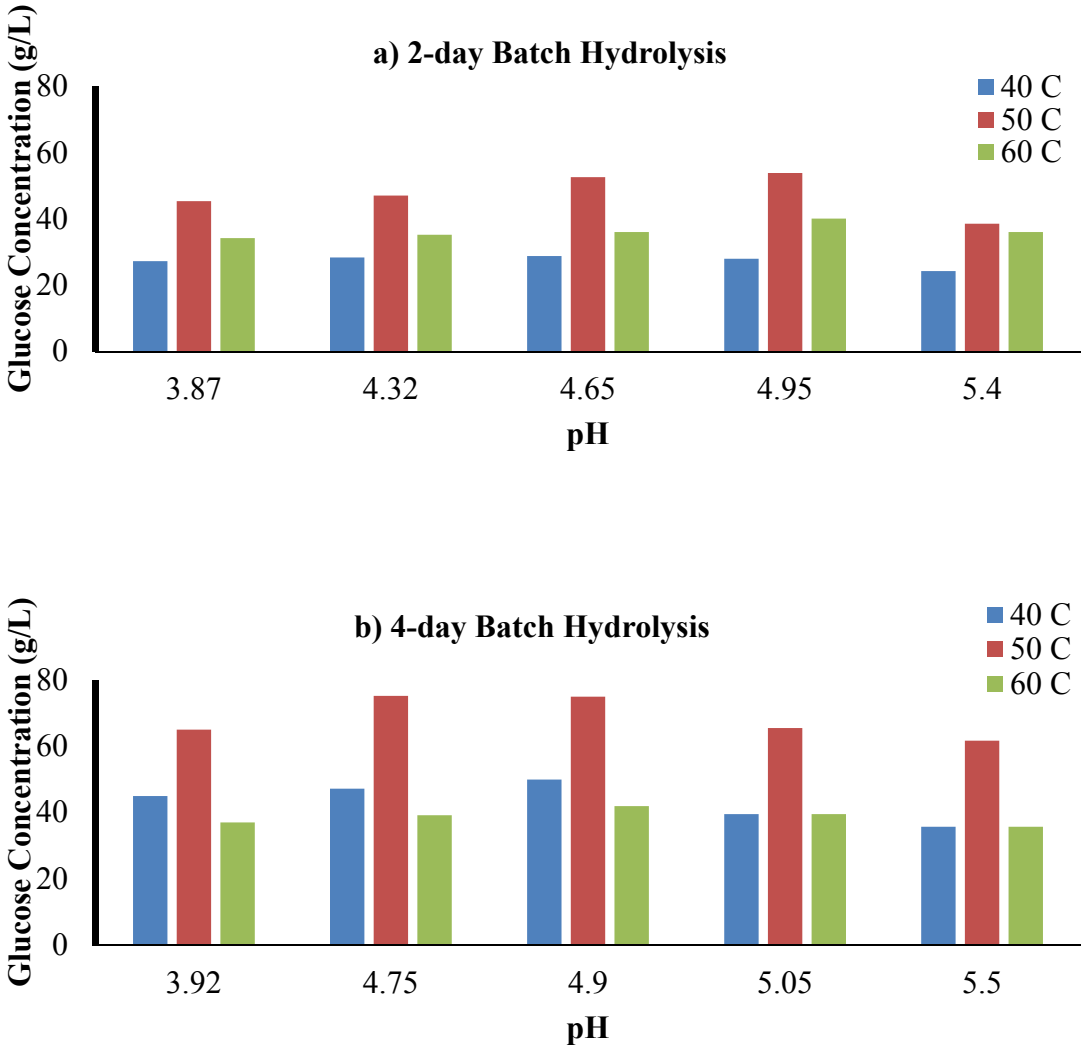

Figure 3: Enzymatic hydrolysis batch test results in different pH and temperature after 2 and 4 days.

5.2. Batch Experiments

We carried out batch experiments in a 1 L reactor to investigate the effect of solids and enzyme loading, as well as agitation speed. Total solids loading and agitation speed are important parameters since biomass slurries exhibit a non-Newtonian behavior [34,35] and become thick during mixing and transport. As a result power requirements are higher for these fluids at higher agitation speeds.

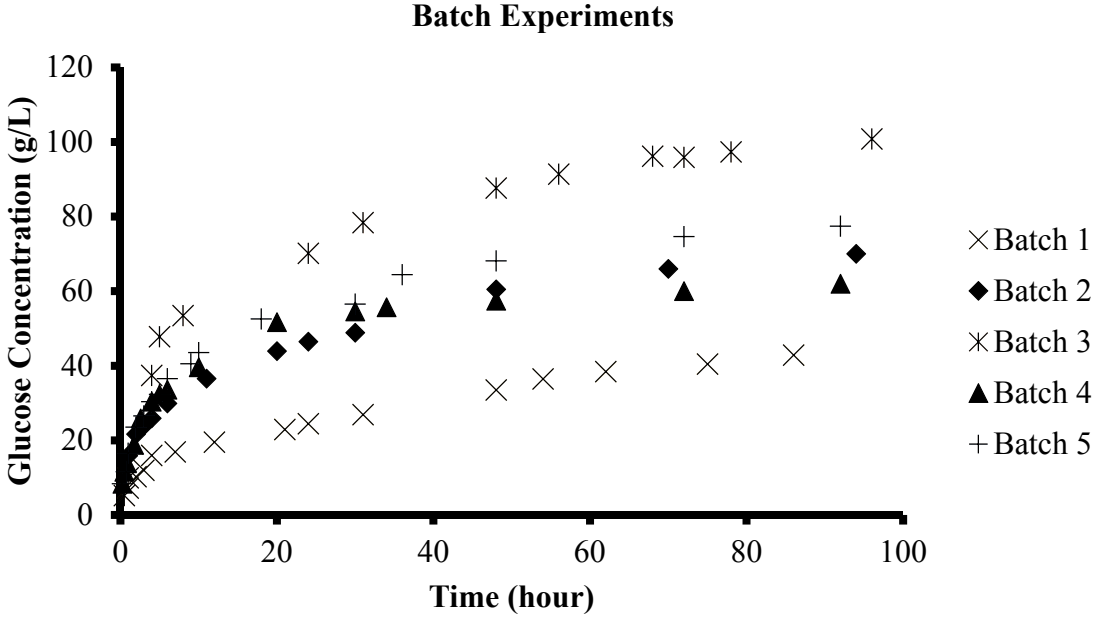

Figure 4: Batch experiments results; reactor size: 1000 ml;

Batch 1: 100 rpm, 100 g/L cellulose , 5 g/L enzyme; Batch 2: 100 rpm, 100 g/L cellulose, 10 g/L enzyme; Batch 3: 600 rpm, 100 g/L cellulose, 10 g/L enzyme; Batch 4: 600 rpm, 100 g/L cellulose, 5 g/L enzyme; Batch 5: 200 rpm, 150 g/L cellulose, 10 g/L enzyme

Figure 4 shows the batch enzymatic hydrolysis results in a 1 L laboratory scale reactor. Increasing cellulase loading from 5 to 10 g/L (Batch 1 and 2) results in about 70% increase in glucose production after 86 hours. Doubling the enzyme loading does not double the rate of glucose production because the enzyme inhibition is more severe at higher glucose concentrations.

Batch 3 shows the effect of increasing the agitation speed by six times. Result show that higher agitation speed leads to higher hydrolysis rates, especially during the first 24 hours. Higher agitation speeds make the slurry more homogenous and cellulose substrate more accessible to the enzyme.

Batch 4 shows that decreasing the cellulase loading by 50% while keeping the agitation speed at 600 rpm, keeps the glucose production almost similar to Batch 2. We also investigated the effect of solids loading in batch experiments. Increasing the cellulose loading by 50% could enhance the rate of glucose production by ~25%. Generally, higher solids loading is favorable for bioconversion process because it will results in higher sugar concentrations and a more economic bioconversion process [36]. However, higher solids loading makes the effective mixing and pumping more difficult and energy-intensive. In addition, batch tests show that the enzyme dosage has a significant effect on hydrolysis rates in our batch tests. Besides, agitation speed is a key parameter in design of enzymatic hydrolysis process due to non-Newtonian behavior of biomass slurry. Cellulose loading is less effective on glucose production rates. This qualitative order of importance of operating parameters is as follows: enzyme dosage>agitation speed>cellulose loading. This qualitative comparison is not in complete agreement with previous study by Mussato et al. [37]. They found out that cellulose loading is more efficacious than agitation speed. They used substrate loadings of 2 to 8 w/v%, which is lower than what we implemented in our

experiments (10 to 15% wt%). It is a fact that viscosity of biomass slurry changes exponentially by increasing the biomass concentration.

5.3. Semibatch Experiments

The experiments we carried out with semibatch tests reactor is summarized in Table 1. We kept the initial cellulose concentration and enzyme loading at 100 g/L and 10 g/L, respectively.

Table 1: List of conducted semibatch experiments and operating condition

Test #	Initial Cellulose loading (g/L)	Initial Cellulase loading (g/L)	Makeup Cellulose (g/L)	Makeup Cellulose (g/L)	Membranes	RPM	Volume Removed (mL)
Semibatch 1	100	10	20	3	UF	100	210
Semibatch 2	100	10	55	3	UF	100	210
Semibatch 3	100	10	66.6	10	UF	100	240
Semibatch 4	100	10	66.6	10	MF	100	250
Semibatch 5	150	5	32	0.75	MF	100	250

We utilized UF and MF membranes in different tests to retain the cellulose and cellulase enzyme. It is reported that Trichoderma reesei cellulases are in the range of 48-65 kDa [38]. However, MF pores are too big to retain the cellulase enzyme. Previous studies show that cellulase enzyme binds to cellulose and lignacious residue [39,40]. As a result, rejection of cellulosic material leads to retention of the cellulase enzyme inside the reactor. We can retain the cellulose and enzyme inside the reactor while removing sugars through the membrane. There is a possibility that some of the enzymes such as β-glucosidase may remain in solution and pass through the

membrane. Comparison of semibacth experiments with UF and MF membranes enable us to understand the passage of Cellic CTec2.

Figure 5 shows the results for semibatch 1 experiment. We started the test with 100 g/L cellulose and 10 g/L of cellulase loading. After 48 h the concentration of glucose in the reactor was 48.6 g/L, which is consistent with our batch results in 1 L reactor. Then, we connected the cell to high pressure nitrogen cylinder and pressurized the cell to 15 psi. We continually increased the pressure until it reached 60 psi. We were able to filter 210 mL of the contents of reactor. Then, we filled the reactor with 210 mL of buffer containing 20 g/L of cellulose and 3 g/L of cellulase.

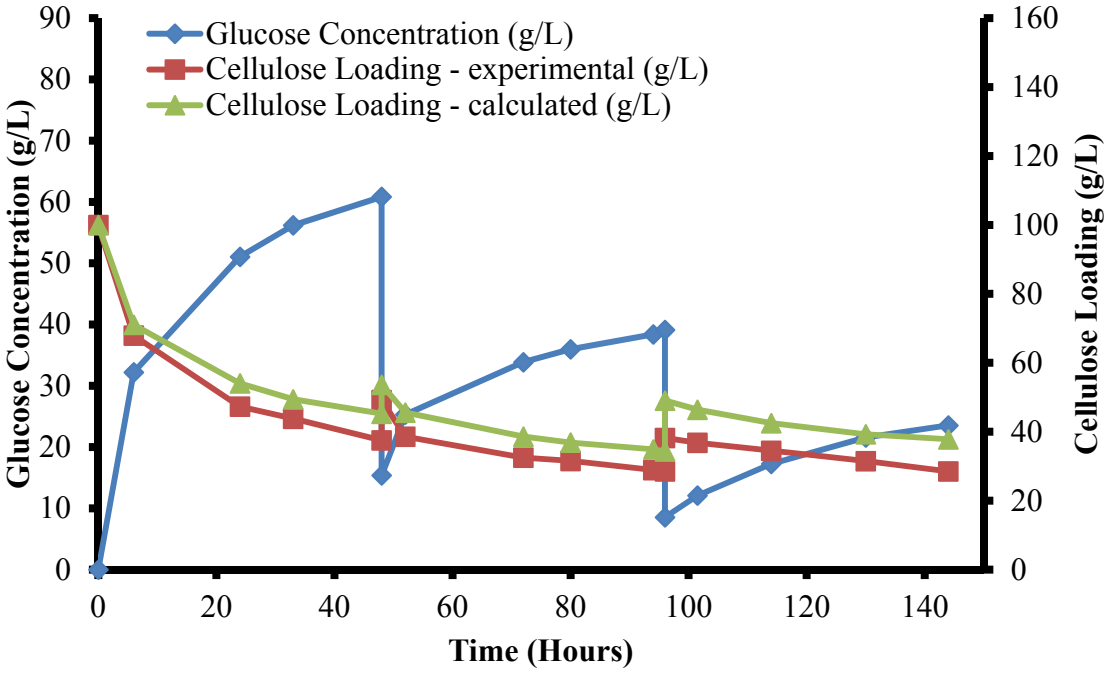

Figure 5: Semibatch 1 in 300 mL reactor, initial enzyme loading: 10 g/L; initial cellulose concentration: 100 g/L; makeup enzyme loading: 3 g/l; makeup cellulose concentration: 20 g/L; filtrate volume after each cycle: 210 mL; membrane: UF

It is apparent from Figure 5 that the rate of glucose production is decreasing after each filtration. After 48, 96 and 144 h, the concentration of glucose in the reactor was 60, 39 and 23 g/L, respectively. Although the reactor is loaded with a smaller amount of cellulase enzyme, we

believe this decreasing trend is due to sudden drop in cellulose concentration inside the reactor. Both experimental and calculated cellulose concentrations depicted in Figure 5 show that we have started the hydrolysis with 100 g/L of cellulose and after 48 h, we see that the cellulose concentration has dropped to ~53 g/L (experimentally). A 50% decrease in cellulose loading results in huge decline in glucose production. Also, the same pattern is followed after the second filtration. That 210 mL of reactor contents was filtered, the reactor was loaded with the same amount of fresh buffer. The declining rate of glucose production was continued after the second filtration. Again, cellulose loading determined experimentally shows that the cellulose concentration during the starting of third step is about 47 g/L, and it decreases to 37 g/L (less than 4 wt%) by the end of the test. This low solids loading results in slower rates of glucose production.

In Semibatch 2 (Figure 6) we tried to increase the cellulose makeup loading after each filtration. We used Equation (3) to roughly calculate the conversion of cellulose. We started the new test as mentioned in Table 1. The difference with semibatch 1 is that we loaded the cell with new buffer containing 55 g/L of cellulose and 5 g/L of cellulase after each filtration. Cellulose concentration curves show that the cellulose concentration drops to 45 g/L after 48 h. Then we loaded the cell with 210 mL of buffer containing 55 g/L of cellulose and 3 g/L of enzyme. This cellulse is compensating for the amount of cellulose which has hydrolyzed during the first 48 h. After loading, cellulose concentration increased to 91 g/L. However, the experimental or calculated values of cellulose concentration still show that we have lower (than 100 g/L) cellulose loading (91 and 93 g/L, respectively). Glucose concentration curves show that we have produced

glucose with 60, 54 and 49 g/L after 48, 96, and 144 h, respectively. We should keep in mind that the reactor was loaded with 30% of the initial fresh enzyme after each 48 h.

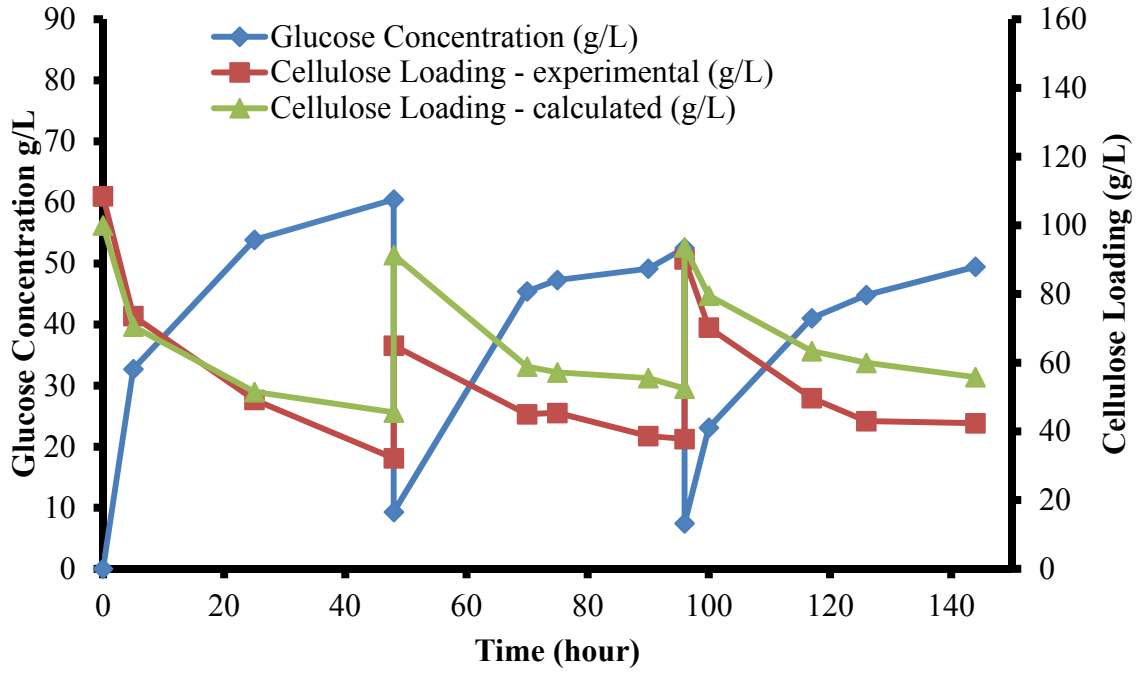

Figure 6: Semibatch 2 in 300 mL reactor, initial enzyme loading: 10 g/L; initial cellulose concentration: 100 g/L; makeup enzyme loading: 3 g/l; makeup cellulose concentration: 55 g/L; filtrate volume after each cycle: 210 mL; membrane: UF

Figure 7 shows the result for Semibatch 3. After each filtration we feed the reactor with fresh makeup buffer containing 66.6 g/L of cellulose and 10 g/L of cellulase enzyme. It is shown that after each 48 h the rate of sugar production is increased at least by 25%. It is interesting to notice that we still keep this increasing trend in very high concentrations of glucose, which is inhibiting the cellulase enzyme. Afer 48, 96, 144 h, we were able to produce 52, 66, and 81 g/L of glucose, respectively. Figure 7 also shows that the cellulose concentration curve is almost similar after each filtration. As a result, we can conclude that this higher hydrolysis rates are because of higher concentration of cellulase in the reactor. Fresh makeup enzyme added after each filtration is increasing the total concentration of enzyme since most enzyme is retained in the

reactor after the filtration. This trend also shows that our membrane bioreactor was successfully rejecting the enzyme and diluting the glucose concentration inside the reactor.

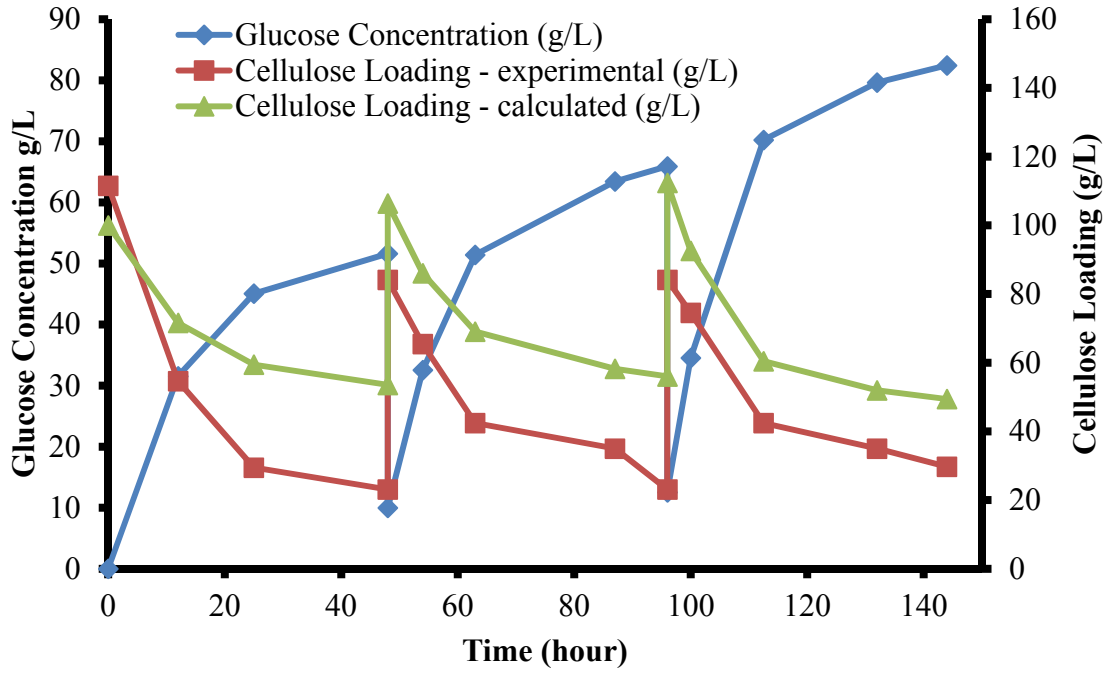

Figure 7: Semibatch 3 in 300 mL reactor, initial enzyme loading: 10 g/L; initial cellulose concentration: 100 g/L; makeup enzyme loading: 10 g/l; makeup cellulose concentration: 66.6 g/L; filtrate volume after each cycle: 240 mL; membrane: UF

Application of 10 kDa polysulfone membranes showed that we could retain the enzymes in the reactor. However, the membrane bioreactor requires to be pressurized up to 60 psi to filter the reactor contents. Higher pressure means higher capital and operating costs. This is why we were interested to test MF membranes in Semibatch and continuous experiments. Knutsen et al. [40] tested UF and MF membranes for retention of cellulase enzymes inside the reactor. Figure 8 shows the Semibatch 4 result for the same operating conditions as Semibatch 3, except we used a 0.65 µm loaded on the membrane bioreactor. We also used a peristaltic pump on the permeate side to extract the permeate stream containing glucose. Lower transmembrane pressure requirements for MF membrane helped us to remove more filtrate out of reactor (250 mL). Results show that

the rate of hydrolysis is not as fast as for Semibatch 3. This is because we have lost some of the enzyme after each filtration while we were able to retain more enzyme using UF membrane. During the MF filtration after 48 and 96 h, we believe most of enzyme is bound to the cellulose and retained. Also, there was no agitation during filtration and a cake layer of cellulose was formed on the membrane. This layer helped to retain more enzyme. However, the enzyme retention was not similar to Semibatch 3, which we implemented UF membrane. We had about 20% decline in the final glucose production rate after each 48 h.

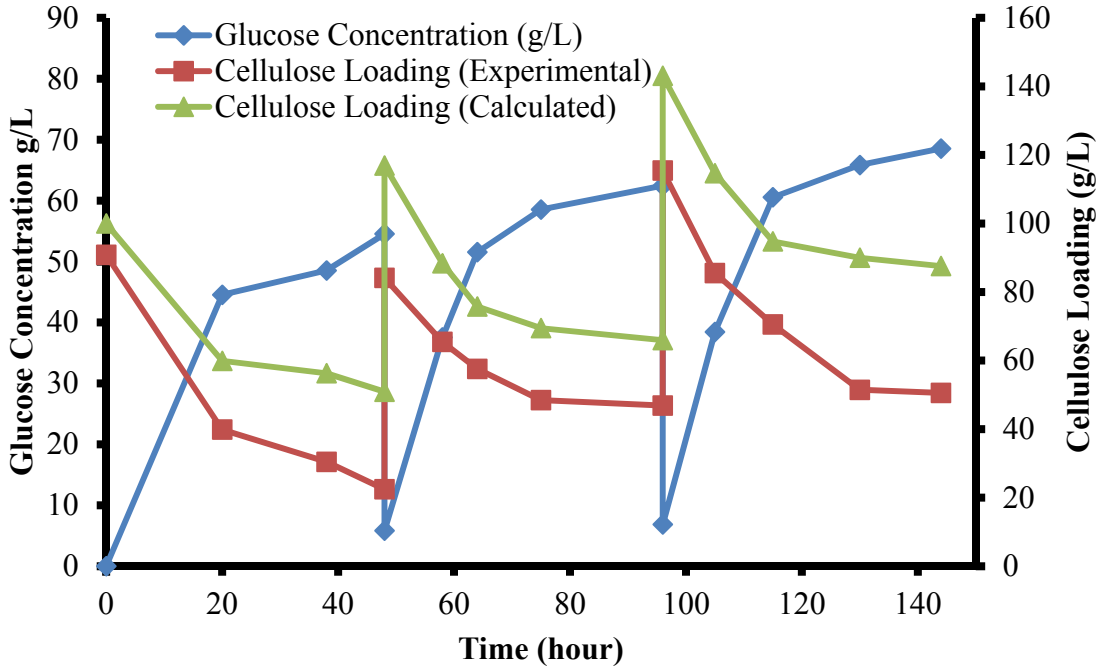

Figure 8: Semibatch 4 in 300 mL reactor, initial enzyme loading: 10 g/L; initial cellulose concentration: 100 g/L; makeup enzyme loading: 10 g/l; makeup cellulose concentration: 66.6 g/L; filtrate volume after each cycle: 250 mL; membrane: MF

Next we tried to find out the optimum procedure to keep the glucose production and solid concentrations similar after each filtration. We used a UF membrane. Figure 9 depicts the results for Semibatch 5. As it is shown, the concentration of glucose after 48, 96 and 144 h is around 30 g/L while we just feed the reactor with 15% of initial enzyme loading after each filtration. Also, we can see that there is a slight increase in cellulose concentration in the reactor. Overall, due to

the lower initial and makeup enzyme loadings, we have lower concentration of glucose and higher concentration of cellulose in the reactor. This higher cellulose concentration helps us to retain more enzyme.

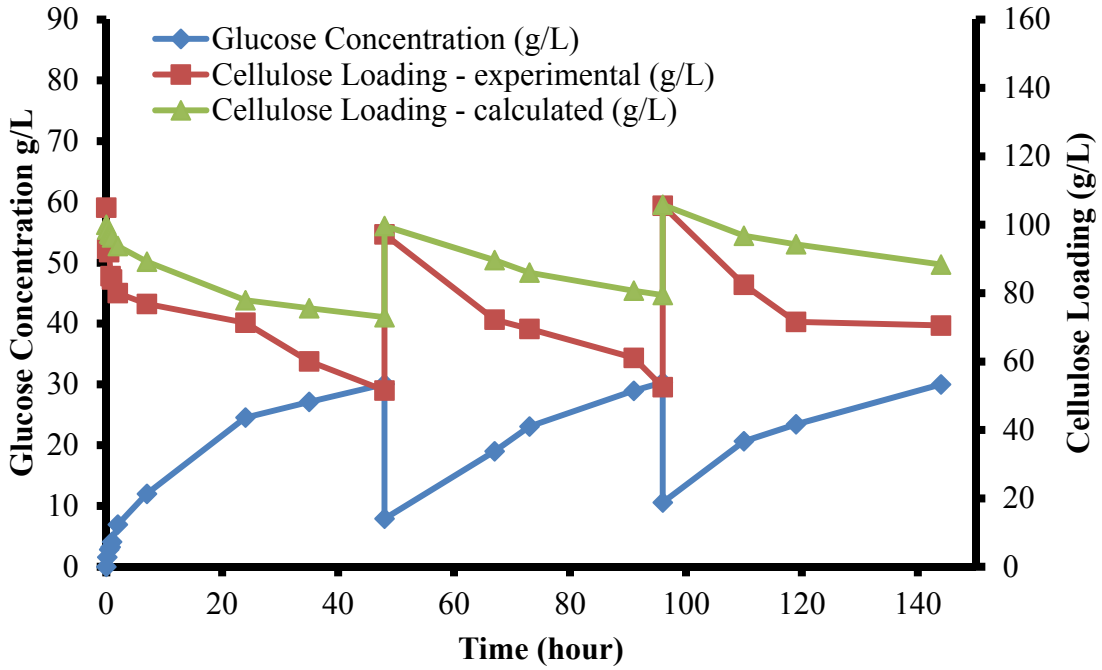

Figure 9: Semibatch 5 in 300 mL reactor, initial enzyme loading: 5 g/L; initial cellulose concentration: 100 g/L; makeup enzyme loading: 0.75 g/l; makeup cellulose concentration: 32 g/L; filtrate volume after each cycle: 250 mL; membrane: UF

5.4. Continuous Experiments

MF membrane was employed for continuous experiments. We investigated the effect of cellulose loading, reactor retention time and pre-holding time on performance of the reactor. List of our experiments is shown in Table 2.

Table 2: List of conducted continuous enzymatic hydrolysis experiments

Test #	Retention Time	Cellulose Loading	Pre-holding Time	Permeate Flux	Reactor Vol.	Permeate Conc.	Glucose Production
	min	g/L	min	mL/min	mL	$mg_{glucose}$/L	$mg_{glucose}$/min
Cont 1	600	100	300	2.5	1000	15.00	37.5
Cont 2	600	100	0	2.5	1000	10.41	26.25
Cont 3	60	100	30	5	300	10.95	54.75
Cont 4	60	100	0	5	300	5.04	25.2
Cont 5	600	150	300	2.5	1000	18.40	46
Cont 6	600	150	0	2.5	1000	14.39	35.97

Figure 10 shows the results for Continuous 1 and 2. The cell was initially loaded with 100 g/L of cellulose and 10 g/L of cellulase, and it was continuously fed with makeup solution containing enzyme and cellulose concentration of 3 and 10 g/L, respectively. The membrane bioreactor retention time was set at 600 min. We adjusted the retention time by decreasing the permeate side flow rate to 2.5 mL/min and increasing the reactor volume to 1000 mL. Adjusting the retention time changes the intensity of inhibition rate. Lower retention time leaded to lower glucose concentration and hydrolysis rates. Results show that we have very small amounts (less than 1.5 g/L) of cellubiose. Although we used MF membrane in continuous mode in which β-glucosidase can easily pass through the membrane and no cake was formed on the membrane we had enough cellubiose hydrolysis to keep its concentration down. Also, it is important to notice that for pre-holding time of 300 minutes (Figure 10 a) we have higher glucose production than the test with 0 minute pre-holding (Figure 10 b). This is due to the fact that 300 minutes pre-holding

gives the enzyme enough time to bind to the cellulose and be rejected with MF membrane. The test with 300 minutes pre-holding time is producing more glucose by 43%.

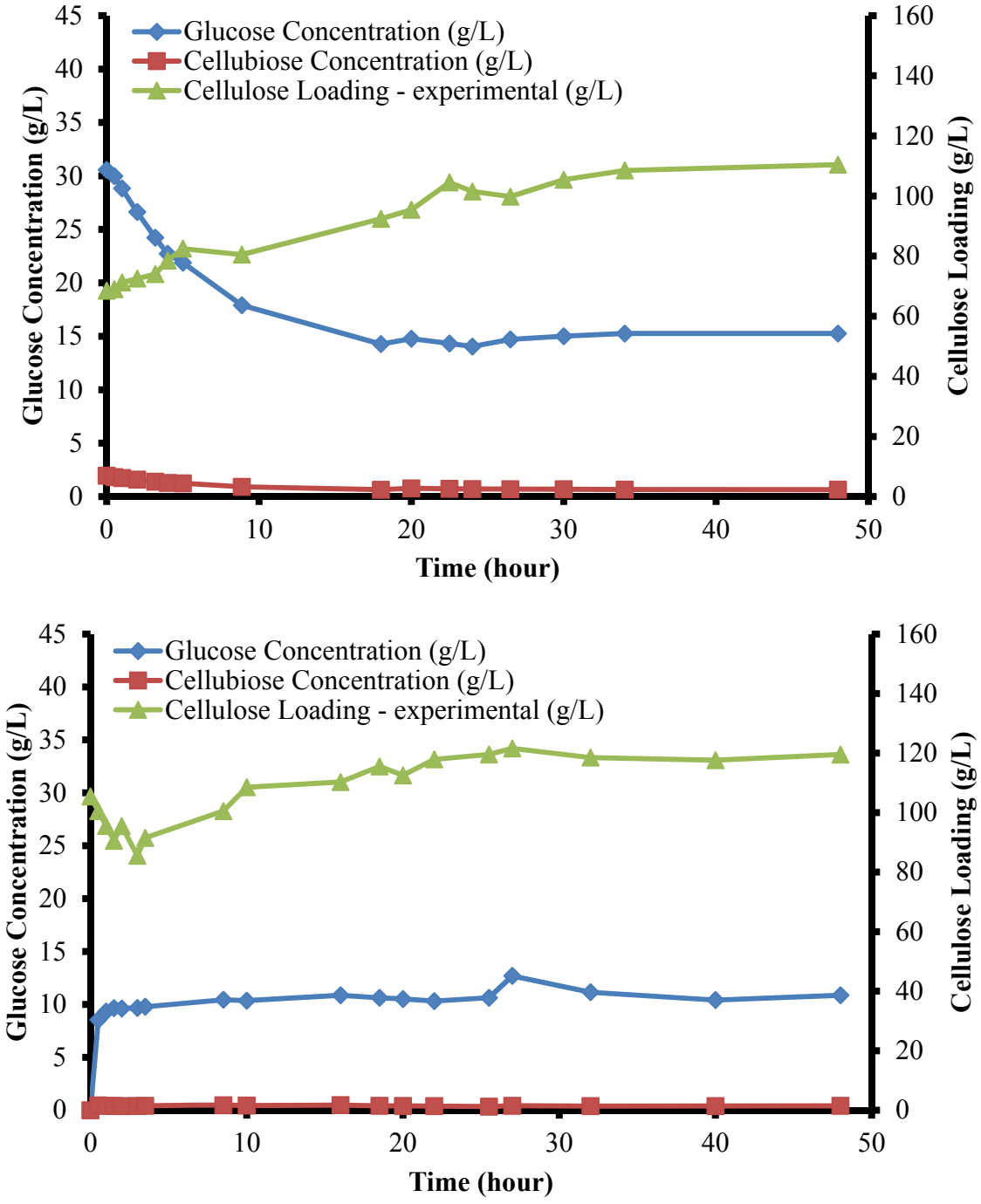

Figure 10: Continuous enzymatic hydrolysis experiments with 600 min retention time and a) 300 min pre-holding time; b) 0 minute pre-holding time

Figure 11 shows the result for Continuous 3 and 4 with 60 minutes retention time, respectively. Pre-holding time was set at 30 minutes (Figure 11 a) and 0 minute (Figure 11 b) for these tests. We increased the permeate flow rate to 5 mL/min and decreased the reactor volume to 300 mL to obtain the retention time of 60 minutes. Results show that the glucose stream on the permeate side of the membrane is containing less glucose than the experiment with 600 minute retention time. Higher glucose concentration inhibits the hydrolysis rate more severe. It is interesting to compare the inhibitory effect of glucose on cellulose hydrolysis and glucose production rate. Glucose production rate of these continuous tests are summarized in Table 2. In Continuous 1, with 600 minutes retention time and 300 minutes pre-holding, we were able to produce 37.5 µg of glucose per minute (permeate flux was 2.5 mL/min and glucose concentration was 12.5 µg/L). For Continuous 3 with 60 minutes retention time and 30 minutes pre-holding time, the glucose production was at 54.75 µg glucose per minute. This results show that by decreasing the concentration of glucose (from 15.25 to 10.60) inside the reactor, we were able to increase the hydrolysis rate (glucose production) by 46%. This increase shows the adverse effect of product inhibition on hydrolysis process. Also, it is important to compare the results from Continuous 2 and 4. Pre-holding period gives enough time to enzyme to bind to cellulose. In Continuous 4, enzymes can leave the membrane bioreactor faster because the retention time is less. Although Continuous 4 has lower glucose concentration (fewer inhibition) it has about 5% decrease in glucose production in comparison with Continuous 2. This result shows that our enzymes are rejected by the membrane only because they are bound to the cellulose. Also, it shows that pre-holding is an important parameter, and there is a tradeoff between glucose concentration and pre-holding time. Continuous 5 and 6 can explain more about the importance of pre-holding time.

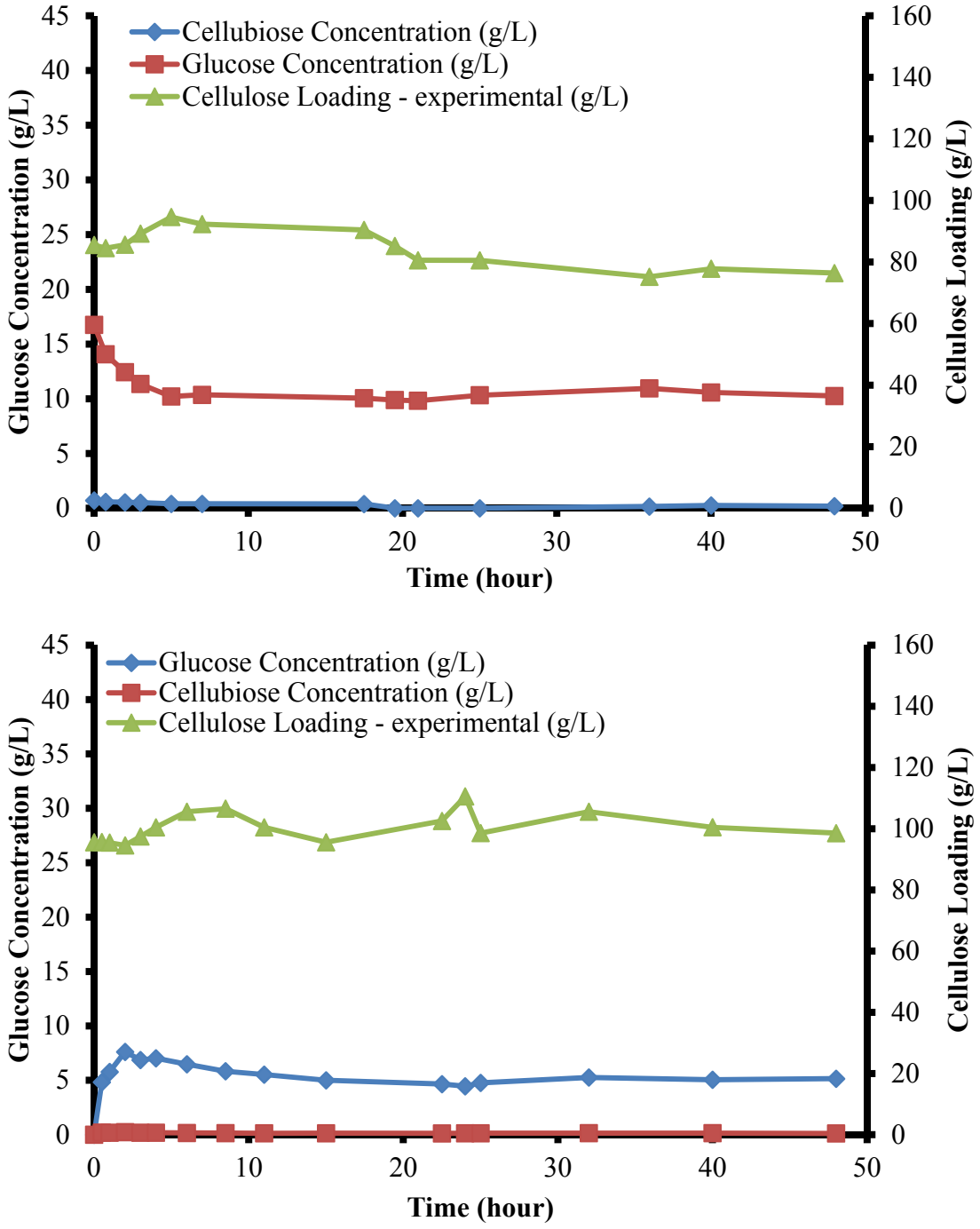

Figure 11: Continuous enzymatic hydrolysis experiments with 60 min retention time and a) 30 min pre-holding time; b) 0 minute pre-holding time

We investigated the effect of cellulose loading on the performance of continuous enzymatic hydrolysis, as well. Reactor was initially loaded with 150 g/L of cellulose and 10 g/L of enzyme, and fed with makeup buffer containing 10 and 3 g/L of cellulose and cellulase, respectively. We

set the retention time at 600 minutes, pre-holding time at 300 minutes. Increasing the solids loading concentration to 150 g/L (50% increase compared to Continuous 1 and 2) has increased the glucose production by 20% and 30% for tests with 300 and 0 minute of pre-holding time, respectively. This results clearly confirm the idea that solid contents of the reactor can retain enzyme inside the reactor. Increasing the cellulose loading has stronger effect on test with 0 minute pre-holding time. For tests with pre-holding time set at 0 h, enzyme can leave the reactor easier, which is disadvantageous for the enzymatic hydrolysis process. We believe higher concentrations of solids leads to more cellulose-cellulase binding and enzyme retention. This is the reason we gained higher hydrolysis improvement in case of 0 minute pre-holding.

Decreasing the pre-holding from 300 to zero minutes (in Continuous 5 and 6) decreases the glucose production by 27%, while for Continuous 1 and 2 this amount was 44%. Although we have the same retention time in both cases, we are having different more severe decrease in glucose production rate. This decrease for Continuous 3 and 4 are more severe (more than 100%). This fact shows the importance of cellulose loading inside the reactor and efficiency MF membranes to reject cellulase at higher cellulose loadings.

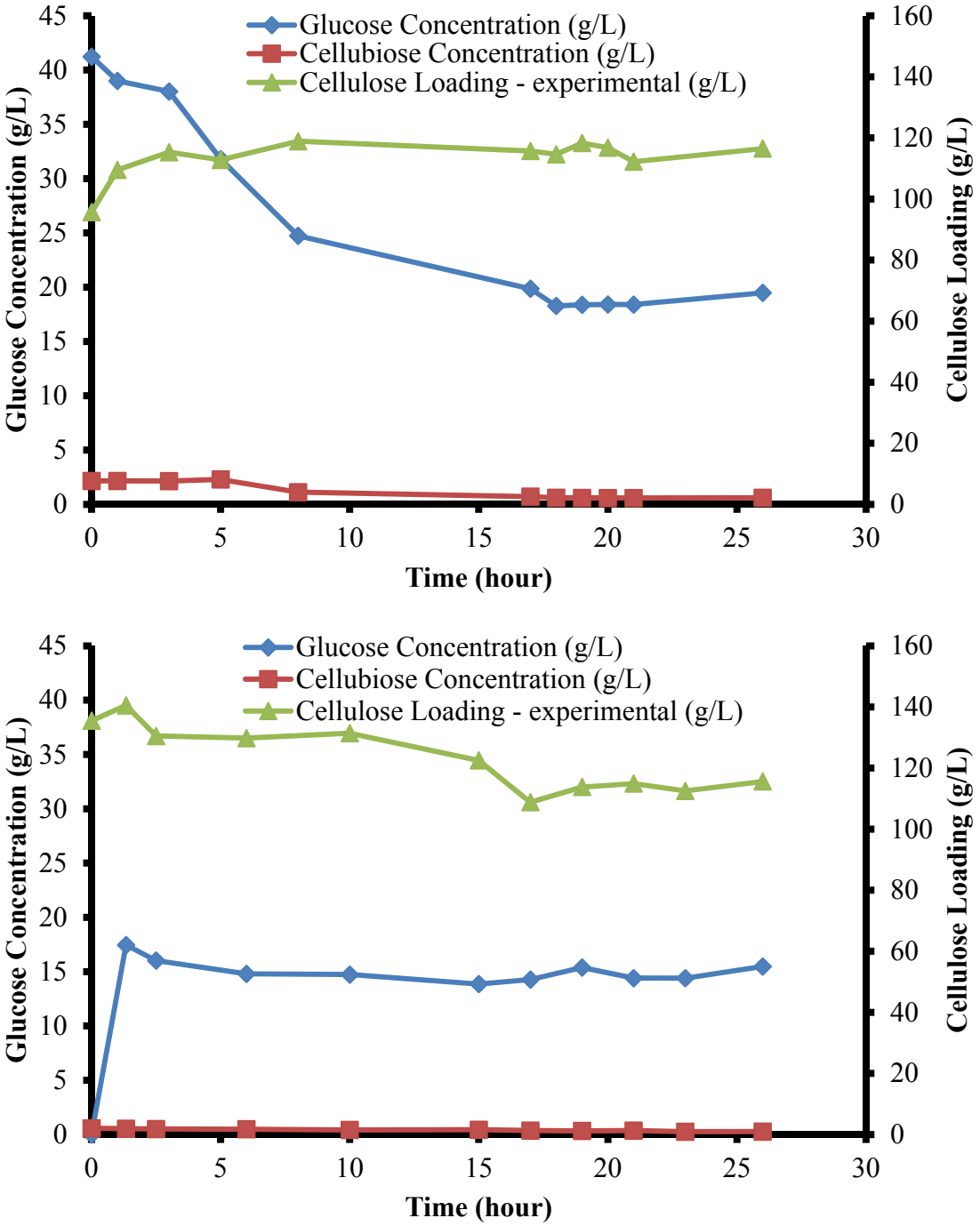

Figure 12: Continuous enzymatic hydrolysis experiments with 600 min retention time and a) 300 min pre-holding time; b) 0 minute pre-holding time

6. Conclusion

We investigated the enzymatic hydrolysis of biomass in batch, semibatch and continuous mode. Effect of temperature, pH and hydrolysis time was studied in batch experiments. MF and UF membranes were employed in membrane bioreactor to run the enzymatic hydrolysis experiments in semibatch and continuous tests. Results showed that both membranes are able to retain cellulose and enzyme inside the bioreactor. Retention of enzymes was possible since the enzyme binds to the cellulosic substrate. Semibatch experiments showed that cellulose loading has a significant effect on hydrolysis process. Agitating speed is also very important. However, we are limited by high viscosity since biomass exhibit non-Newtonian behavior. Higher cellulose loading is also effective. We investigated the effect of reactor retention time, pre-holding time, and cellulose loading during our continuous tests. Results showed that higher retention times leads to higher glucose production. As a result we will have more product inhibition and slower glucose production. There is a tradeoff between retention time and pre-holding time. Pre-holding time is an important processing parameter which gives the enzyme enough time to bind to cellulose. Higher cellulose loading can decrease dependency of continuous experiments on pre-holding time.

7. Reference

[1] G.W. Huber, S. Iborra, A. Corma, Synthesis of transportation fuels from biomass: chemistry, catalysts, and engineering., Chem. Rev. 106 (2006) 4044–98.

[2] C. Wyman, S. Decker, M. Himmel, J. Brady, C. Skopec, L. Viikari, Hydrolysis of Cellulose and Hemicellulose, in: S. Dumitriu (Ed.), Polysaccharides, CRC Press, New York, 2004.

[3] E. Drioli, A. Brunetti, G. Di Profio, G. Barbieri, Process intensification strategies and membrane engineering, Green Chem. 14 (2012) 1561.

[4] D.L. Grzenia, D.J. Schell, S.R. Wickramasinghe, Membrane extraction for removal of acetic acid from biomass hydrolysates, J. Memb. Sci. 322 (2008) 189–195.

[5] M.E. Himmel, S.-Y. Ding, D.K. Johnson, W.S. Adney, M.R. Nimlos, J.W. Brady, et al., Biomass recalcitrance: engineering plants and enzymes for biofuels production., Science. 315 (2007) 804–7.

[6] C.E. Wyman, What is (and is not) vital to advancing cellulosic ethanol., Trends Biotechnol. 25 (2007) 153–7.

[7] P. Andrić, A.S. Meyer, P.A. Jensen, K. Dam-Johansen, Effect and modeling of glucose inhibition and in situ glucose removal during enzymatic hydrolysis of pretreated wheat straw., Appl. Biochem. Biotechnol. 160 (2010) 280–97.

[8] C. Abels, F. Carstensen, M. Wessling, Membrane processes in biorefinery applications, J. Memb. Sci. 444 (2013) 285–317.

[9] R.G. Henley, R.Y.K. Yang, P.F. Greenfield, Enzymatic saccharification of cellulose in membrane reactors, Enzyme Microb. Technol. 2 (1980) 206–208.

[10] F. Alfani, D. Albanesi, M. Cantarella, V. Scardi, A. Vetromile, Kinetics of enzymatic saccharification of cellulose in a flat-membrane reactor, Biomass. 2 (1982) 245–253.

[11] I. Ohlson, G. Trägårdh, B. Hahn-Hägerdal, Enzymatic hydrolysis of sodium-hydroxide-pretreated sallow in an ultrafiltration membrane reactor., Biotechnol. Bioeng. 26 (1984) 647–53.

[12] S. Kinoshita, J.W. Chua, N. Kato, T. Yoshida, H. Taguchi, Hydrolysis of cellulose by cellulases of Sporotrichum cellulophilum in an ultrafilter membrane reactor, Enzyme Microb. Technol. 8 (1986) 691–695.

[13] K. Bélafi-Bakó, A. Koutinas, N. Nemestóthy, L. Gubicza, C. Webb, Continuous enzymatic cellulose hydrolysis in a tubular membrane bioreactor, Enzyme Microb. Technol. 38 (2006) 155–161.

[14] Q. Gan, S. Allen, G. Taylor, Design and operation of an integrated membrane reactor for enzymatic cellulose hydrolysis, Biochem. Eng. J. 12 (2002) 223–229.

[15] W.D. Mores, J.S. Knutsen, R.H. Davis, Cellulase Recovery via Membrane Filtration, Appl. Biochem. Biotechnol. 91-93 (2001) 297–310.

[16] P. Andrić, A.S. Meyer, P.A. Jensen, K. Dam-Johansen, Reactor design for minimizing product inhibition during enzymatic lignocellulose hydrolysis: II. Quantification of inhibition and suitability of membrane reactors., Biotechnol. Adv. 28 (2010) 407–25.

[17] M. Nakajima, T. Shoji, H. Nabetani, Protease hydrolysis of water soluble fish proteins using a free enzyme membrane reactor, Process Biochem. 27 (1992) 155–160.

[18] R.A. Korus, A.C. Olson, Use of glucose isomerase in hollow fiber reactors, J. Food Sci. 42 (1977) 258–260.

[19] F. Sannier, J.-M. Piot, P. Dhulster, D. Guillochon, Stability of a mineral membrane ultrafiltration reactor for peptide hydrolysis of hemoglobin, J. Chem. Technol. Biotechnol. 61 (1994) 43–47.

[20] P. Pasta, G. Carrea, E. Monzani, N. Gaggero, S. Colonna, Chloroperoxidase-catalyzed enantioselective oxidation of methyl phenyl sulfide with dihydroxyfumaric acid/oxygen or ascorbic acid/oxygen as oxidants., Biotechnol. Bioeng. 62 (1999) 489–493.

[21] S. Bouhallab, C. Touzé, Continuous hydrolysis of caseinomacropeptide in a membrane reactor: kinetic study and gram-scale production of antithrombotic peptides, Lait. 75 (1995) 251–258.

[22] M. Prata-Vidal, S. Bouhallab, G. Henry, P. Aimar, An experimental study of caseinomacropeptide hydrolysis by trypsin in a continuous membrane reactor, Biochem. Eng. J. 8 (2001) 195–202.

[23] V. Cauwenberg, P. Vergossen, A. Stankiewicz, H. Kierkels, Integration of reaction and separation in manufacturing of pharmaceuticals: Membrane-mediated production of S-ibuprofen, Chem. Eng. Sci. 54 (1999) 1473–1477.

[24] L. Greiner, D.H. Müller, E.C.D. van den Ban, J. Wöltinger, C. Wandrey, A. Liese, Membrane Aerated Hydrogenation: Enzymatic and Chemical Homogeneous Catalysis, Adv. Synth. Catal. 345 (2003) 679–683.

[25] Y. Isono, H. Nabetani, M. Nakajima, Preparation of lipase-surfactant complex for the catalysis of triglyceride hydrolysis in heterogeneous reaction systems, Bioprocess Eng. 15 (1996) 133–137.

[26] L.-E. Shi, G.-Q. Ying, Z.-X. Tang, J.-S. Chen, W.-Y. Xiong, H. Wang, Continuous enzymatic production of 5′-nucleotides using free nuclease P1 in ultrafiltration membrane reactor, J. Memb. Sci. 345 (2009) 217–222.

[27] L. Wang, T. Khan, K. Mohanty, R. Ghosh, Cascade ultrafiltration bioreactor-separator system for continuous production of F(ab′)2 fragment from immunoglobulin G, J. Memb. Sci. 351 (2010) 96–103.

[28] F. Carstensen, A. Apel, M. Wessling, In situ product recovery: Submerged membranes vs. external loop membranes, J. Memb. Sci. 394-395 (2012) 1–36.

[29] T.K. Ghose, Measurement of cellulase activities, Pure Appl. Chem. 59 (1987) 257–268.

[30] C.M. Roche, C.J. Dibble, J.S. Knutsen, J.J. Stickel, M.W. Liberatore, Particle concentration and yield stress of biomass slurries during enzymatic hydrolysis at high-solids loadings., Biotechnol. Bioeng. 104 (2009) 290–300.

[31] H. Jørgensen, J.B. Kristensen, C. Felby, Enzymatic conversion of lignocellulose into fermentable sugars: challenges and opportunities, Biofuels, Bioprod. Biorefining. 1 (2007) 119–134.

[32] B.T. Smith, J.S. Knutsen, R.H. Davis, Empirical evaluation of inhibitory product, substrate, and enzyme effects during the enzymatic saccharification of lignocellulosic biomass., Appl. Biochem. Biotechnol. 161 (2010) 468–82.

[33] N.D. Weiss, J.J. Stickel, J.L. Wolfe, Q.A. Nguyen, A simplified method for the measurement of insoluble solids in pretreated biomass slurries., Appl. Biochem. Biotechnol. 162 (2010) 975–87.

[34] R.M. Turian, T.W. Ma, F.L.G. Hsu, D.J. Sung, Characterization, settling, and rheology of concentrated fine particulate mineral slurries, Powder Technol. 93 (1997) 219–233.

[35] J.J. Stickel, J.S. Knutsen, M.W. Liberatore, W. Luu, D.W. Bousfield, D.J. Klingenberg, et al., Rheology measurements of a biomass slurry: an inter-laboratory study, Rheol. Acta. 48 (2009) 1005–1015.

[36] A.A. Modenbach, S.E. Nokes, Enzymatic hydrolysis of biomass at high-solids loadings – A review, Biomass and Bioenergy. 56 (2013) 526–544.

[37] S.I. Mussatto, G. Dragone, M. Fernandes, A.M.F. Milagres, I.C. Roberto, The effect of agitation speed, enzyme loading and substrate concentration on enzymatic hydrolysis of cellulose from brewer's spent grain, Cellulose. 15 (2008) 711–721.

[38] A. Suurnäkki, M. Tenkanen, M. Siika-aho, M.-L. Niku-Paavola, L. Viikari, J. Buchert, Trichoderma reesei cellulases and their core domains in the hydrolysis and modification of chemical pulp, Cellulose. 7 (2000) 189–209.

[39] H. Ooshima, D.S. Burns, A.O. Converse, Adsorption of cellulase from Trichoderma reesei on cellulose and lignacious residue in wood pretreated by dilute sulfuric acid with explosive decompression., Biotechnol. Bioeng. 36 (1990) 446–52.

[40] J.S. Knutsen, R.H. Davis, Cellulase retention and sugar removal by membrane ultrafiltration during lignocellulosic biomass hydrolysis., Appl. Biochem. Biotechnol. 113-116 (2004) 585–99.

College of Engineering

Ralph E. Martin Department of Chemical Engineering

Appendix 3A: Multiple Author Documentation

To whom it may concern,

Hereby, I confirm that Mr. Malmali has done more than 51% of the work for chapter 3 of this dissertation. The list of authors is as follow:

Mohammadmahdi Malmali

Jonathan Stickel

S. Ranil Wickramasinghe

S. Ranil Wickramasinghe, PhD

Professor, Ross E Martin Chair in Emerging Technologies
Ralph E Martin Department of Chemical Engineering
University of Arkansas
3202 Bell Engineering Center

Chapter 4: Nanofiltration with Layer-by-layer Polyelectrolyte Deposited Membranes: Fractionation of Sugars in Biomass Slurry

Nanofiltration with Layer-by-layer Polyelectrolyte Deposited Membranes: Fractionation of Sugars in Biomass Slurry

Mohammadmahdi Malmali[*], S. Ranil Wickramasinghe[*3]

[*] Ralph E. Martin Department of Chemical Engineering, University of Arkansas, Fayetteville, AR 72701, USA

1. Abstract

Layer-by-layer deposition of ultra-thin hyperbranched anionic and cationic polyelectrolytes on top of ultrafiltration membranes results in a porous modified membrane showing nanofiltration characteristics. In this study, deposition of polyelectrolyte multilayers on top of the polysulfone membrane substrate is confirmed by ATR-FTIR spectroscopy, SEM images and filtration tests. We investigated modification of 10, 50, and 100 kDa polysulfone membranes with poly (sodium 4-styrenesulfonate)/ poly(diallyldimethylammonium chloride) and poly (acrylic acid)/poly(diallyldimethylammonium chloride) bilayers. We developed different protocols to prepare high-flux, defect-free polyelectrolyte multilayer membranes. SEM images showed that we were able to cover the pores of 100 kDa membranes which had the largest pore size. We carried out several nanofiltration tests with 20 mM sugar feed streams containing sucrose, glucose and xylose with equal concentrations dissolved in 20 mM citric acid-sodium phosphate dibasic buffer at pH 7.5. Results show that these membranes are capable of separating sugars. 50 kDa membranes

[3] Corresponding author: Tel: +1 479 575 8475; Fax: +1 479 575 4940; email: ranil.wickrmasinghe@uark.edu

with 7.5 bilayers of [PSS/PDADMAC] showed the best performance with glucose to sucrose selectivity of more than 11.

Key-words: Dynamic LbL deposition, nanofiltration, fractionation, Biomass slurry, polyelectrolyte

2. Introduction

Nanofiltration (NF) is the newest of the pressure driven filtration processes dating back to the 1970s. This membrane technique was originally developed to enable low-pressure reverse osmosis (RO) filtration [1]. By the 1980s, NF was considered a separate membrane filtration process to RO [2,3]. NF may be characterized by greater than 99% rejection of multivalent ions, low to moderate rejection of monovalent ions (0-70%) and greater than 90% rejection of organic molecules with molecular weights above 150. Today, there are numerous applications for NF including water softening, removal of organic matter and micropollutants from aqueous streams, wastewater polishing and reuse, applications in the food industry, as well as solvent resistant NF for non-aqueous applications [4]. Molecular sieving as well as hydrophilic and hydrophobic interactions are principals of most membrane filtration processes. NF is one of the few filtration processes that exploit charge-charge interactions to separate species since most NF membranes are charged at neutral pHs [5]. The pH during filtration can change the surface conditions of the membrane or the molecule and can lead to lower or higher rejection values. Further, molecular shape and dipole moment of the molecules may also affect the separation.

Today, production of 1st generation biofuels such as bioethanol from sugar cane and corn starch is well established [1]. Manufacturing processes that include the use of membrane-based unit operations have been described [2]. However increasing competition between food and

energy production has led to significant efforts to convert lignocellulosic biomass into 2nd generation biofuels. Unlike 1st generation biofuels, production of 2nd generation biofuels is far more complex. Development of efficient separation and purification operations are essential for production of competitive 2nd generation drop-in biofuels. Membrane based separation processes are attractive as they could lead to significant process intensification and hence reduced operating costs [3].

There are three main strategies practiced for conversion of lignocellulosic biomass into liquid fuels and chemical intermediates: gasification, pyrolysis and hydrolysis [4]. In this study we focus on bioconversion of lignocellulosic biomass. Dilute-acid pretreatment is a well-known technology for initial pretreatment [5]. Dilute sulfuric acid has been shown to effectively hydrolyze the hemicellulose component of the biomass to its monomeric sugars, increase the porosity of the biomass substrate, and enhance the enzymatic digestibility of cellulose [6]. Afterwards, cellulose is enzymatically hydrolyzed to its monomeric sugar, glucose. Enzymatic hydrolysis is followed by fermentation. Prior to fermentation, the hydrolysate is conditioned or detoxified to remove byproducts and sugar degradation products (toxic compounds). Toxic compounds have inhibitory effect on subsequent fermentation of the solubilized sugars [6]. Besides, the maximum glucose concentration is limited by product inhibition during enzymatic hydrolysis.

Abels et al. [6] recently reviewed membrane based separation processes for biorefinery applications. Several investigators have considered the use of ultrafiltration membranes for removal of glucose during enzymatic hydrolysis thus avoiding product inhibition [7-10]. Carstensen et al. [11] have reviewed membrane bioreactors for in situ product recovery. However,

here the focus is the application of membrane-based separation processes to fractionate biomass slurries.

One of the interesting applications of membranes in biofuel production, as well as food industry, is fractionation and concentration of mono- and oligosaccharides. Fractionation of the sugar and larger oligosaccharaide streams has been investigated [12-18]. Among mono- and oligosaccharaids, fractionation of streams containing glucose, xylose, sucrose and fructose is more interesting and challenging. There are different structural carbohydrates such as glucan, xylan, galactan, arabinan, and mannan present in the hydrolysate. Composition of the these carbohydrates is shown in Table 1 [19].

Table 1: Summary of whole stover composition data

Component	Average (dry wt%)	Min	Max	Range
Ethanol Solubles	3.3	1.7	4.1	2.4
Sucrose	3.6	0	10	10
Extractable Inorganics (oil)	2.5	0	4.8	4.8
Other water Extractables	8.6	1.4	15.7	14.2
Total Solubles	17.9	5.7	30.8	25
Glucan	31.9	26.5	37.6	11
Xylan	18.9	14.8	22.7	7.9
Galactan	1.5	0.8	1.9	1.1
Arabinan	2.8	1.6	3.6	2
Mannan	0.3	0	0.7	0.7
Lignin	13.3	11.2	17.8	6.6
Structural Inorganics	3.9	0.8	6.6	5.8
Protein	3.7	1.1	5.4	4.3
Acetyl	2.2	0.9	2.9	2
Estimated Uronic Acids	3.1	2.5	3.7	1.2
Total Structural	81.6	70.4	90.8	20.4
Component Closure	99.5	93.8	104.9	11.1

To reach the vision set by Department of Energy biomass program, considerable improvements in bioconversion of biomass are anticipated. One of these improvements is to have high yields of ethanolic fermentation of hexose and pentose sugars, which is a prerequisite for an economic production of ethanol. Up to 40% of the hydrolysate is containing pentose sugars [20,21].

Currently, Saccharomyces yeast is the most abundant microorganism applied to ferment sugars [22] and tolerant towards toxic compounds produced during pretreatment [23,24]. However, this microorganism is not capable of fermenting xylose and arabinose. There are several other microorganisms capable of fermenting both hexose and pentose sugars; however, either they produce some unwanted compounds, or use xylose as a source of carbon. During the last two decades, there has been abundant research devoted to improve microorganism strains capable of fermenting hexose and pentose sugars with high yields [24,25].

Fermentation of xylose is more complex and challenging. Enteric bacteria and some yeasts are the only strains capable of fermenting pentose sugars, Based on current technology, only a slight ethanol yields is observed during the simultaneous fermentation of hexose and pentose sugars [26]. Pentose fermenting microorganisms are very sensitive to ethanol concentration and inhibitory compounds [27]. Fermentation of pentose sugars happens at higher pHs (neutral) compared to hexose sugars. Also, pentose fermentation is more favorable in aerobic mode. Dutta et al. [19] investigated different fermentation configurations for bioconversion of corn stover. They concluded that separate fermentation of solid and liquid streams (separate xylose and glucose fermentation) is the most viable process.

Fractionation of mono- and oligosaccharides also helps to alleviate the rate of production of toxic compounds. For example, sucrose, one of the components of the hydrolysate stream will

100% hydrolyzes to fructose and glucose during the pretreatment. This reaction is followed by complete degradation of fructose to HMF, which is an inhibitory compound for the fermentation step [19]. As a result, separation of the sugars in the feed stream will result in lower production of toxic compounds, and as a result higher efficiency of the process. Sugars are nonpolar uncharged compounds that have molecular weights within a factor of two. So fractionation of the sugar streams requires careful optimization of the operating conditions.

RO and NF membranes are thin-film composite membranes, consisting of a highly porous support covered by a thin dense layer on top. We can obtain NF membranes with modification of porous substrates that they do not show NF characteristics by nature. After some surface modification or treatment steps, we can produce membranes with molecular weight cut-off in the range of NF membranes. The lower cut-off of modified membrane is due to attachment of an additional layer on the membrane surface. Addition of this layer is designed to be helpful, either to minimize undesired interactions or provide additional interactions. Modification of membrane surface also leads to physiochemical changes in the characteristics of the membrane surface. There are numerous well-known methods such as adsorption, UV irradiation, plasma, high-energy radiation, radical polymerization, and etc. to modify membrane surface [28]. These methods fall into four main categories: 1) heterogeneous reactions; 2) grafting-to reactions; 3) grafting-from reactions; 4) reactive coating [29].

Adsorption is a powerful, viable and simple technique that could be implemented to modify surface of the membrane. By physical addition of another polymeric layer, we can obtain membranes with significantly different characteristics. Layer-by-layer (LbL) deposition of multilayer polyelectrolytes is a relatively new technique dating back to 1997s [30]. Robustness of base membrane and ability to absorb the first layer is a prerequisite for this method. Either,

membranes should have the functional groups capable of making multiple ionic bonds [12], or these groups could be generated on the membrane surface by means of other surface modification techniques [31]. There are numerous articles recently published confirming that LbL polyelectrolyte multilayer deposited on the skin of the membrane support shows NF [31-35], pervaporation [31,36-38] and gas separation [39-42] characteristics.

The deposited film produced through LbL deposition is incredibly thin, in the range of (10-1000 Å). Bruening et al. have modified 0.02 μm porous alumina support using polyelectrolyte multilayer deposition method, and successfully employed the obtained NF substrate for separation of fluoride from multivalent ions [43], purification and separation of textile plant effluent streams [44], and backflushable water treatment membrane with tunable hydrophilicity and charge [45]. They also studied the electrochemical and in situ elipsometric investigation of layered polyelectrolyte films at different pHs [12], and found out that higher pH results in swelling of the polyelectrolyte layer. There are other applications of polyelectrolyte deposited membrane incorporated with polymers, proteins and nanoparticles into coated layer for other specific specifications.

Unique control over permeability and ability to tune the surface characteristics of obtained NF membrane deposited with polyelectrolyte multilayer thin layers [46] exhibits a promising approach for separation and fractionation of sugars and oligosaccharides. LbL deposition of polyanionic and polycationic electrolytes on a porous support showed successful results for separation and fractionation of uncharged molecules such as sugars. Malaisamy et al. [47] modified different polyethersulfone (PES) UF membranes with MWCO of 10, 50, 300, and 500 kDa. They deposited different bilayers of poly (sodium 4-styrenesulfonate)/poly (allylamine hydrochloride) (PSS/PAH) and poly (sodium 4-styrenesulfonate)/poly(diallyldimethylammonium

chloride) (PSS/PDADMAC) to modify the membrane surface. Their results showed to be promising for separation and fractionation of mono- and disaccharides. They were able to obtain 70, 99.2, and 99.7% rejection using 50 kDa PES membranes modified with $[PSS/PAH]_4PSS$ bilayers for glucose, sucrose and raffinose, respectively. The separation factor of 40, and 110 was also obtained for glucose/sucrose and glucose/raffinose feed, respectively. Size-screening transport of these uncharged molecules through the modified membranes is studied, and membrane pores are measured to be of 0.4-0.5 nm. Shi et al. [15] also investigated the application of polyelectrolyte multilayer composite membranes for NF separation of oligosaccharides. They fabricated PAN and PEM UF membranes and deposited $[PAH/PSS]_5$ and $[chitosan/PSS]_5$ bilayers. Membranes' performance showed ~100% rejection of oligosaccharides and 63% rejection for glucose.

In this study, we are going to modified polysulfone ultrafiltration membranes with polyelectrolyte multilayers. We tested these membranes with different mono- and disaccharide mixture model solution to investigate the fractionation of these compounds. Fractionation of saccharides enables us to perform separate fermentation process for hexose and pentose sugars. It also can decrease the production of toxic compounds.

3. Experimental Section

Materials: Unless otherwise noted all chemical were ACS reagent grade. PAA (MW: ~ 100,000), PSS (MW: 70,000), PDADMAC (MW: 100,000-200,000), D-glucose and D-xylose were purchased from Sigma Aldrich (St. Luis, MO). Sodium azide 5% w/v, acetic acid and sulfuric acid were purchased from Seastar Chemicals Inc. (Sidney, BC, Canada). Sodium hydroxide was purchased from J. T. Baker (Philipsburg, NJ). Figure 1 depicts the chemical structure of polyelectrolytes that were used in this study. Deionized water (conductivity < 10 μScm^{-1} and

resistance > 18.5 MΩ) was obtained from a Labconco (Kansas City, MO) water purification system (Water Pro RO and Water Pro PS Polishing Stations). Polysulfone UF membranes with 10, 50, and 100 kDa were purchased from Alfa Laval (Wood Dale, IL).

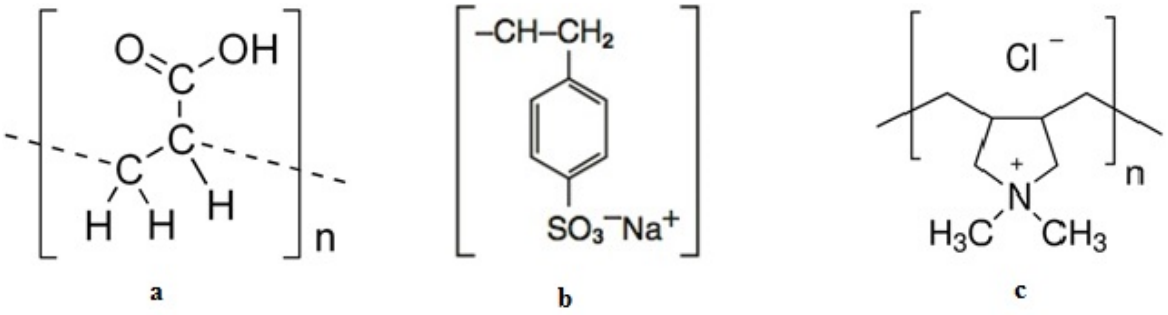

Figure 1: Chemical Structure of polyelectrolyte used in this study: a) PAA ; b) PSS; c) PDADMAC

Film Deposition: Membranes were soaked in DI water for 24 hours, during which the water was changed at least 3 times. Membranes were loaded in a EMD Millipore Amicon stirred cell (Billerica, MA) such that only the functional layer of the membrane was exposed to the polyelectrolyte solution. We used two methods to modify the membranes: static and dynamic LbL deposition. For static film deposition and adsorption of polyelectrolyte layers on membrane support, the cell was (a) loaded with 30 mL of polyanioninc solution and incubated for a predetermined time, (b) rinsed with 30 mL of DI water for 1 minute, (c) loaded with polycationic solution and incubated for a predetermined time. The sequential deposition of polyelectrolyte layer were carried out by repeating steps (a) to (c). The permeate stream was closed during the static LbL deposition. For dynamic LbL deposition, we followed the same steps while we pressurized the cell to 10 psi during each deposition step, and we left the permeate side stream open.

NF membranes are generally used at lower operating pressures in comparison to RO membranes. They are usually categorized as charged membranes due to existence of charged groups on the membrane functional layer. Charged NF membranes are preferable for rejection of

charged species since we can employ Donan exclusion along with sieving effect. NF membranes with more hydrophilic surface are preferred to reduce fouling. All these characteristics of an ideal NF membrane show that multilayer polyelectrolyte membranes are a good candidate to be applied in NF applications. These membranes have different advantages. We can significantly change the characteristics of the membrane surface (such as charge, hydrophilicity, molecular weight cut-off and thickness) by deposition of one or several layers. Polyelectrolytes are water soluble, environmentally friendly, cheap material, and the deposition is happening under ambient conditions, without any specific temperature or pressure requirement. There are two different patterns practiced to modify porous membranes with polyelectrolyte solutions for NF applications. Dip coating 48-50] and adsorption of the polyelectrolyte on one side of the porous support [41,42,46]. In the former one after dipping the membrane in polyelectrolyte solution, we have two layers on the top and bottom of the membrane, and in the later one, we are just forming the deposited layer on one side of the membrane. Different steps and methods to modify porous supports with polyelectrolyte multilayers is depicted in Figure 2. There are several techniques discussed in literature [52] about procedures to modify membranes: 1) static single layer polyelectrolyte deposition; 2) Dynamic single layer deposition ; 3) UV initiated membrane modification; 4) Static LbL adsorption; 5) Dynamic LbL adsorption.

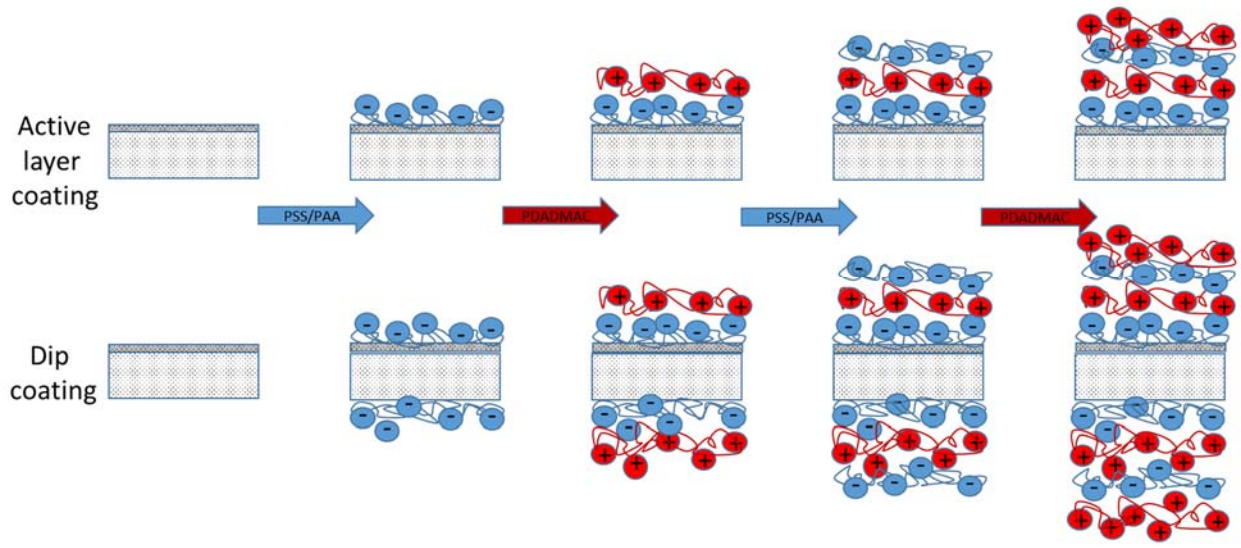

Figure 2: Polyelectrolyte multilayer deposition methods

We started the modification of polysulfone membranes by following the procedure mentioned by Bruening et al. [46,47,52]. Initially we soaked the membranes in DI water for 24 hours, in which the water content was changed at least three times. Then we compressed the membrane at 40 psi and measured the DI water flux at 20 psi. We loaded the washed and compressed membrane in the Amicon stirred cell and started modification by deposition of PSS or PAA as the first layer on the polysulfone support. We started deposition with this solution due to existence of hydrophobic interactions between membrane and PSS. The overall procedure is a sequential repetition of: (a) deposition in polyanionic solution; (b) rinsing with DI water; (c) deposition in polycationic solution. We first performed the adsorption steps for 5 minutes followed by 1 minute DI water rinse, and we used 20 mM polyelectrolyte solutions dissolved in 0.5 M NaCl solution. We did not do pH adjustment for [PSS/PDADMAC] modified membranes. We adjusted the pH of PAA to 4.5 with HCl and NaOH.

Nanofiltration: Nanofiltration experiments were conducted in dead-end flow mode using Millipore Amicon cell 8050 shown schematically in Figure 2. The system was pressurized to 10

psi using a house pressurized air, and the pressure was monitored using a digital gauge. Before starting polyelectrolyte deposition, we compacted membrane at 40 psi. Afterwards, we measured DI water flux at 20 psi to see if the membrane permeability is within the range. The membranes with different DI water permeability were scrapped.

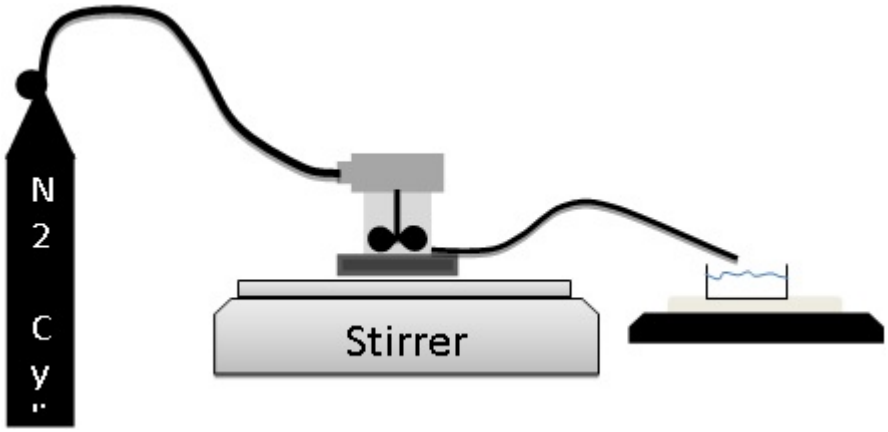

Figure 3: Schematic diagram of filtration cell

Our feed solution consisted of xylose, glucose and sucrose each with concentration of 6.66 mM. The sugars were dissolved in a 20 mM citric acid-sodium phosphate dibasic buffer at pH 7.5. Sugar separation tests were also performed in Amicon stirred cell. 50 mL of feed solution was loaded in the cell and left there to equilibrate for 15 minutes. Afterwards, the cell was pressurized to 10 psi. The stirring speed was set at 150 rpm. Filtration was continued until 10 mL of permeate was obtained. A scale was connected to a computer to record the weight of permeate. After each 2 mL we withdrew 200 µL of permeate to measure the sugar concentration for HPLC analysis.

Samples collected from the permeate stream were analyzed using an Agilent 1200 series HPLC (Agilent Technologies, Palo Alto, CA) equipped with an Agilent 6.5×300 mm Hi-Plex Ca (Duo) column and Agilent refractive index detector (RID). RID sample cell was set at 55 ℃. The mobile phase appropriate for this column was HPLC grade water with flow rate set at 0.6 mL min^{-1}. The auto sampler was set for an injection volume of 15 µL and column was kept at 80℃ using

a thermostatted column compartment. A series of calibration standards and calibration verification standards (CVS) were obtained from Absolute Standards Inc., Hamden, CT. All measurements were taken in triplicate and average results are reported. Sugar rejection was membrane selectivity was calculated using following equation:

$$R = 1 - \frac{C_p}{C_f} \quad (1)$$

$$\alpha_{a/b} = 1 - \frac{C_{a,p}/C_{a,f}}{C_{b,p}/C_{b,f}} \quad (2)$$

in which R is rejection, C_p and C_f are concentration in the permeate and feed side, respectively. $\alpha_{a/b}$ is the selectivity of a to b, $C_{a,p}$, $C_{a,f}$, $C_{b,p}$ and $C_{b,f}$ are concentration of compound a in permeate, concentration of component a in feed, concentration of compound b in permeate and concentration of compound b in feed, respectively.

3.1. Physical and Structural Characterization of Membranes

3.1.1. Attenuated Total Reflectance Fourier Transform Infrared (ATR-FTIR)

ATR-FTIR spectroscopy provides qualitative information on the types of functional groups present at depths between 100 and 1000 nm. A Shimadzu IR Affinity-1 FTIR spectrometer (Columbia, MD) with the wavenumber in the range of 7800 to 350 cm^{-1}, equipped with a deuterated, L-alanine doped triglycine sulfate (DLaTGS) detector with a resolution of 0.5-16 cm^{-1} and germanium-coated potassium bromide (KBr) beam splitter with an incidence angle of 45° was used. The FTIR was equipped with Pike Technologies (Madison, WI) zinc selenide ATR prism. Prior to analysis, the membranes were removed from the zip top bags and rinsed twice with 10 mL DI water. They were then placed in a 100 mL beaker containing 50 mL DI water for 10 min with slow stirring. The membranes were again rinsed twice with 10 mL DI water and air dried

for 15 min and then dried overnight in vacuum oven at 30˚C. ATR-FTIR spectra were averaged over 32 scans and resolution of 0.5 cm^{-1} in the range of 850-1800 cm^{-1}.

3.1.2. Contact Angle Measurements

For physical characterization, static contact angles were measured for all membranes with a contact angle goniometer (Model 100, Rame-Hart Instrument Company, Netcong, NJ) using the sessile drop method at room temperature and pressure. A DI water drop of 3 μL at a rate of 1 μL/s was made on the tip of a microsyringe. The microsyringe was moved down vertically towards the sample to make the contact with the sample. Then, the syringe was moved up while the drop was remained on the sample. The camera recorded the contact angles of the water drop. Using the circle fitting method and curvature baseline, the angle made between the left- and right-side of water drop and the membrane surface was measured every 0.1 seconds for 5 second. Data were collected for 5 seconds at five locations and averaged for each membrane.

4. Result and Discussions

4.1. Thin Film Characterization

4.1.1. ATR-FTIR

ATR-FTIR characterization technique approved that the LbL deposition of polyelectrolyte layers on the porous polysulfone membrane substrate was successful. However, many of the absorbance peaks of the deposited polyelectrolyte layers are obscured due to polysulfone support large absorbance background. So we could not detect many peaks generated by PSS/PDADMAC and PAA/PDADMAC bilayers. The main characteristic peaks of FTIR spectrum for PSS is reported to be found at around 1185, 1130, 1042, 1011, 668 and 639 cm^{-1} [53]. However, comparing the absorbance peaks of PSS and polysulfone substrate shows that most of these peaks are overlaid by polysulfone support adsorbance. Polysulfone does not have any adsorbance at 1034

cm^{-1}, where we can detect the growth of small peaks due to the deposition of polyelectrolyte multilayer. This peak is due to symmetric vibrational adsorption of SO_3^- at around 1034 cm^{-1} in our ATR-FTIR results. Although, there is a slight background absorbance peak at 1010 cm^{-1} due to polysulfone support, we can clearly detect the growth of peak height due to the deposition of PSS layer and in-plane skeleton vibration of benzene ring adsorption peak at around 1010 cm^{-1} [53].

Deposition of more layers on the membrane support leads to an increase in the height of these two peaks. Figure 3 shows that peaks at 1010 cm^{-1} and 1034 cm^{-1} are growing by deposition of more layers on the substrate for 5, 50 and 100 kDa membranes. Figure 3 also shows that there is large peak coming up after deposition of the 3.5 bilayer. However, FTIR spectra of polysulfone membranes modified with n=5.5 and 7.5 are not significantly different. Malaisamy et al. [47] saw the same nonlinear trend in the growth of the peaks. They saw that there is a significant increase in the absorbance at 1010 and 1034 cm^{-1} after the deposition of the fourth layer. We saw this jump after deposition of the third layer because our deposited layer is thicker (due to the technique we have used). Also, it is evident that the background peak heights of polysulfone substrate are decreasing. ATR-FTIR spectra of polysulfone membranes modified with PAA/PDADMAC multilayers did not show us any significant growing peak regarding deposition of PAA or PDADMAC since all the peaks are overlaid by polysulfone adsorbance peaks. It is also evident from Figures 3 a and b that the peaks at 1108 and 1150 cm^{-1} are shrinking due to the coverage of the polysulfone support with the polyelectrolyte multilayers.

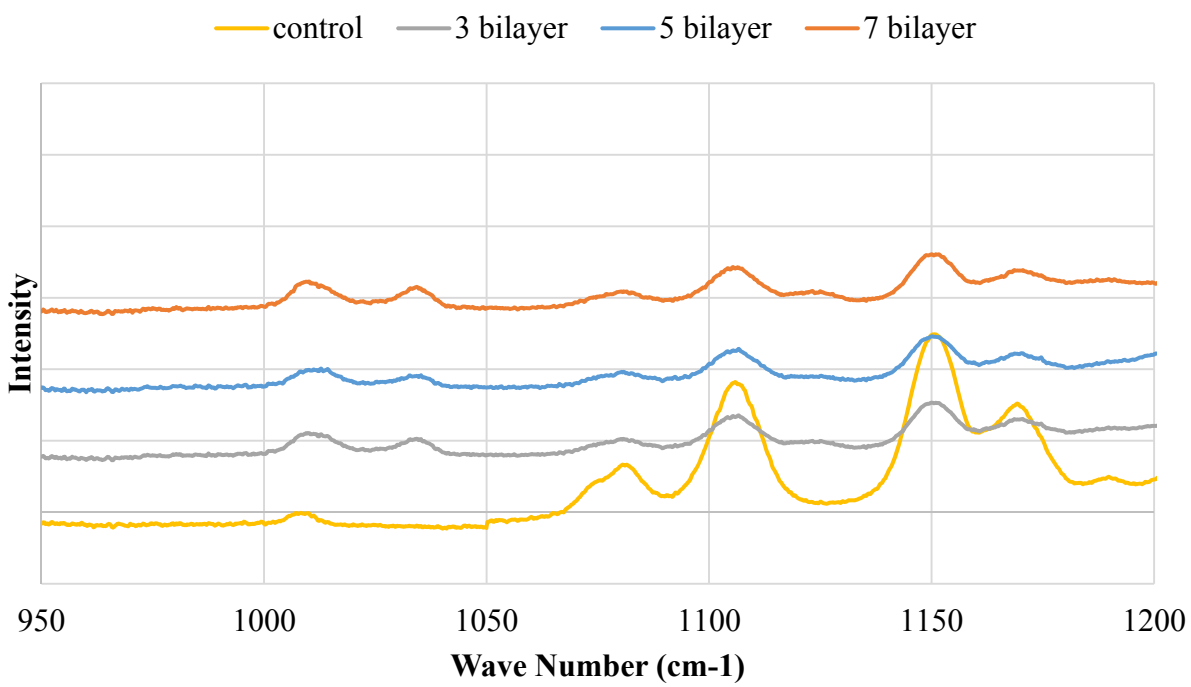

Figure 4a: ATR-FTIR spectra for 5 kDa membranes in the range of 950-1200 cm^{-1}.

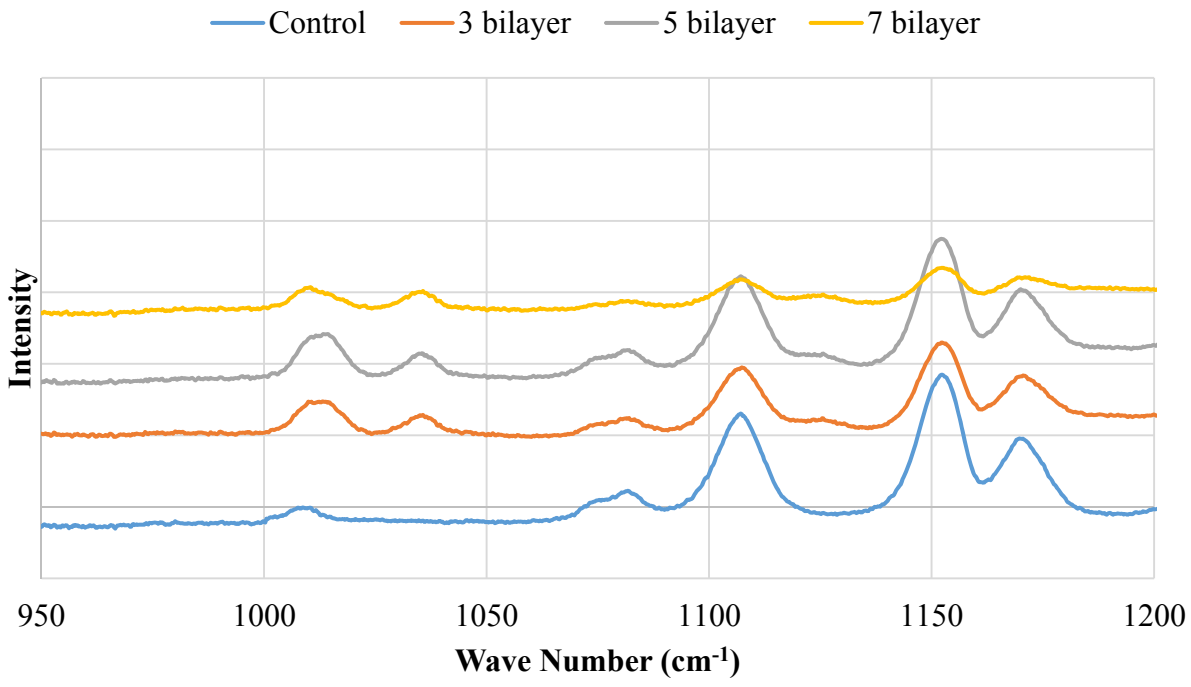

Figure 4 b: ATR-FTIR spectra for 50 kDa membranes in the range of 950-1200 cm^{-1}.

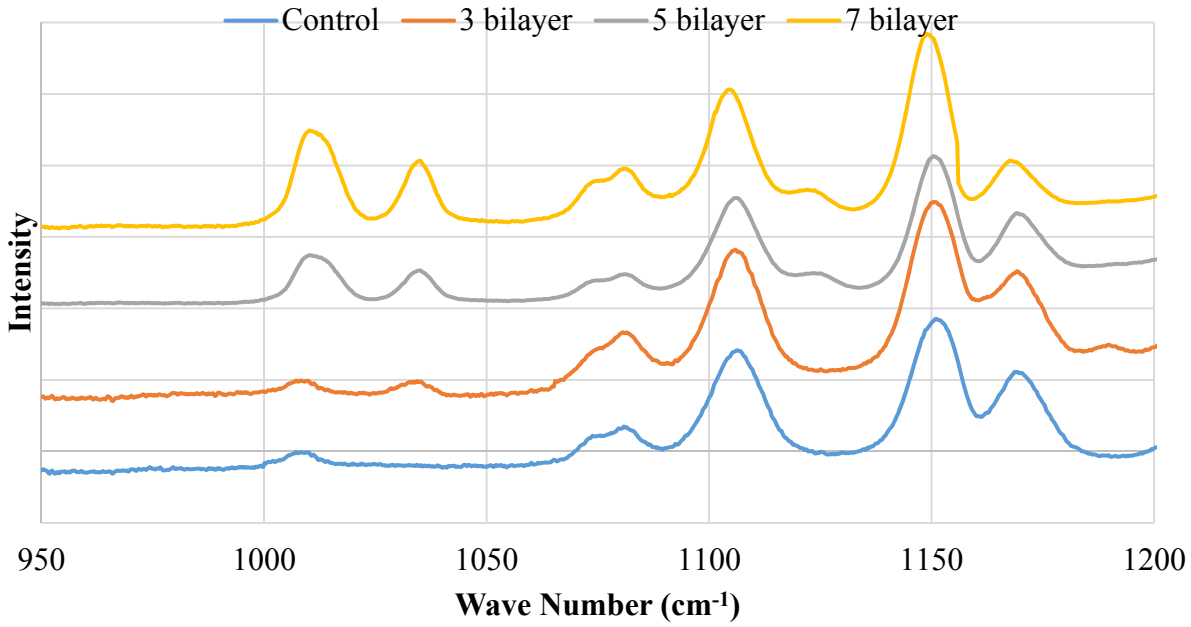

Figure 4c: ATR-FTIR spectra for 100 kDa membranes in the range of 950-1200 cm^{-1}

4.1.2. Contact Angle Measurements

One of the advantages of LbL polyelectrolyte deposition is the excellent control over the fabrication of multilayer surfaces with different wettability. Yoo et al. [54] have studied the parameters affecting the wettability of weak polyelectrolyte multilayer surfaces. They could make surfaces with contact angles from <10 to as high as 50˚ using PAA/poly (allylamine) (PAH) bilayers. We also studied the wettability of the membranes using contact angle measurement method.

It is shown [54,55] that surface contact angle of a polyelectrolyte multilayer surface is obviously controlled by the outermost deposited layer. In our studies, we used three different polyelectrolyte solutions. PAA, PSS and PDADMAC have different degree of hydrophilicity. To have a more permeable membrane and a surface less prone to fouling, it is recommended to have

more hydrophilic surfaces as the outermost layer. This is why we capped the [PSS/PDADMAC] and [PAA/PDADMAC] modified membranes with PSS and PAA, respectively. PAA and PSS could produce surfaces with contact angles less than 25˚ and 50˚. This is in agreement with literature [54] and chemical structure of PAA (aliphatic polyacid) and PSS (aromatic polyacid). On the other hand, PDADMAC is considered hydrophobic. Surfaces modified with PDADMAC as the outermost layer are showing hydrophobic characteristics.

Surface contact angle of polyelectrolyte deposited membrane was measured after each successive layer deposition, and it is shown in Figure 4. [PSS/PDADMAC] modified membranes, with the PSS and PDADMAC as the outer layer, showed contact angle reproducibly between 35-43˚ and 68-79˚ in Figure 4 a, respectively. However, 100 kDa polysulfone membrane showed slightly higher contact angles after the deposition of the first PSS layer. Our hypothesis is that higher contact angle is due to incomplete coverage and uneven surface after the deposition of the first layer. These are because of more porous structure of 100 kDa membrane. This porous structure may results in an uneven deposition. Also, it may be possible that the 100 kDa membrane pores are not fully covered with polyelectrolyte layer. [PAA/PDADMAC] modified membranes, with the PAA and PDADMAC as the outer layer, showed the contact angles reproducibly between 14-27˚ and 64-75 ˚ in Figure 4 a, respectively. Figure 4 b shows that 5 kDa, 50 kDa and 100 kDa polysulfone membranes showed very similar contact angles for up to 15 deposited layers.

The notion of incomplete coverage of bigger pores was mentioned by Malaisamy et al. [47], and they showed membranes with 300 and 500 kDa MWCOs showed lower rejections due to incomplete coverage of large pores. Also, Yoo et al. [54] saw the same trend after the deposition of the PAH layer. In their study of deposition of PAH/PAA multilayers in the absence of

supporting electrolyte, they found that although the outermost layer is dominating layer for wettability of the surface, it takes one complete bilayer to establish a reasonable contact angle.

In our case of PAA/PDADMAC modified membranes, we did not see this lower contact angle of the first PAA deposited layer since deposition of PAA at pH 4.5 may results in high film thickness. We might have had high film thickness after deposition. Due to this thick film deposition on the surface, we have complete coverage of membrane pores. It is interesting that Yoo et al. [54] also did not see any difference in contact angle after deposition of the first PAH layer in the presence of 0.4 M $MgCl_2$ as an electrolyte support. This shows that our hypothesis about thicker modified layer is valid. Lower contact angles due to the uneven surface is clearly seen in contact angle of unmodified 100 kDa membrane (72˚), which is extensively less than the contact angle of unmodified 5 kDa (82˚) and 50 kDa (80˚).

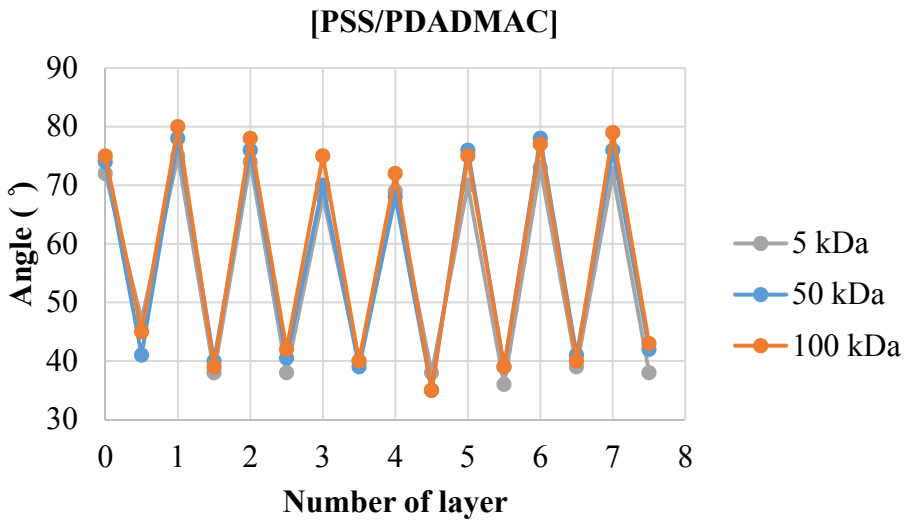

Figure 5a: Contact angle measurements from films containing different number of layers of [PSS/PDADMAC]. Even numbers means that the outermost layer is PDADMAC and odd numbers mean that the outer most layer is coated either with PSS. The final layer for each set is deposited with solution containing 2.5 M NaCl as the electrolyte support

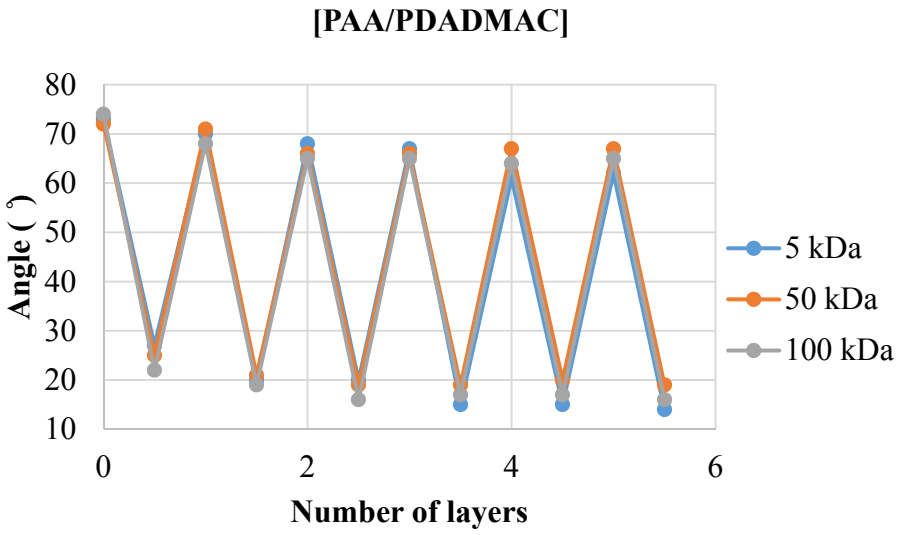

Figure 5b: Contact angle measurements from films containing different number of layers of [PAA/PDADMAC]. Even numbers means that the outermost layer is PDADMAC and odd numbers mean that the outer most layer is coated with PAA. The final layer for each set is deposited with solution containing 2.5 M NaCl as the electrolyte support

In two of our tests, we also modified the 50 kDa polysulfone membrane with same polyelectrolyte solutions mentioned earlier, with different electrolyte supports. We compared the effect of concentration of supporting electrolyte on contact angle of $[PAA/PDADMAC]_5$ modified membranes. Result showed that multilayer polyelectrolyte modified membrane with 0 M NaCl had the lowest (18˚) contact angle. Same membranes with 0.1 M and 0.5 M NaCl supporting electrolyte showed higher and almost the same contact angle (26˚).

4.1.3. Scanning Electron Microscopy

To further verify successful deposition of multilayer polyelectrolyte on polysulfone membranes, we prepared SEM images. Figure 5 a shows the SEM image of an unmodified 100 kDa polysulfone membrane. It shows that the 100 kDa has a surface with uniform pores visible in the range of 0.1-25 nm. Figure 5 b shows the 100 kDa membrane after deposition of 7.5 bilayers. We can see that the pores are fully covered with the deposited polyelectrolyte film. This image shows the successful deposition of PSS/PDADMAC films on the membrane surface. Also, these

images showed us that the deposited film of some membranes had visible cracks due to drying method that we used. The same image was obtained for PAA/PDADMAC deposited films. Regarding 50 kDa and 5 kDa membranes, we were unable to clearly detect any visible pores on the surface.

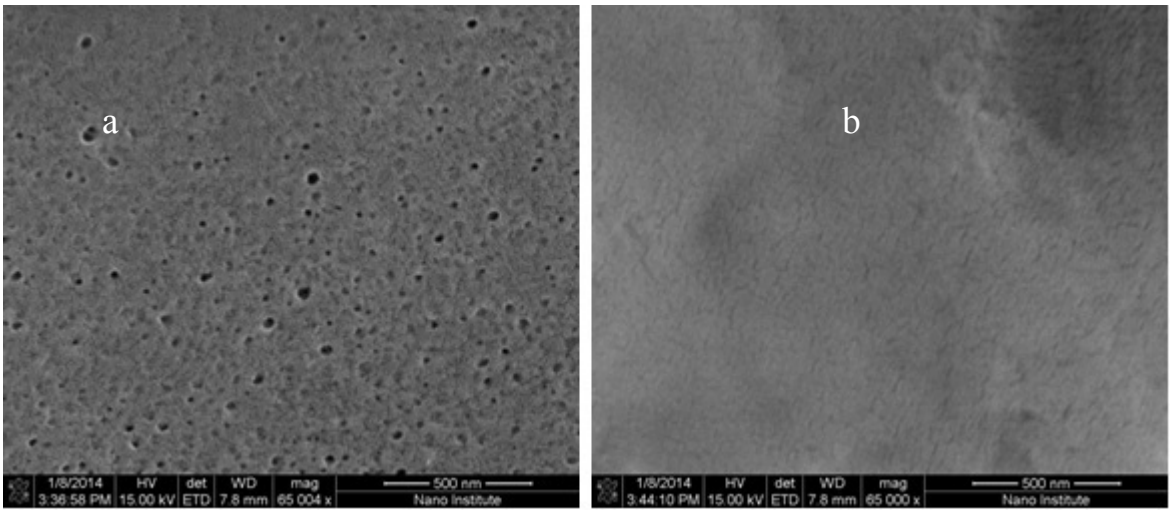

Figure 6: SEM image analysis of unmodified (a) and modified (b) 100 kDa polysulfone membranes. Membrane b is modified with 7.5 bilayers of [PSS/PDADMAC] multilayers. The final layer is deposited at 2.5 NaCl electrolyte support concentration

4.2. Polyelectrolyte Deposition

After deposition of the first PSS/PDADMAC or PAA/PDADMAC bilayer, we saw a sudden drop in membrane DI water permeability (up to 85%). Nevertheless, deposition of subsequent layers did not change the permeability and sugar rejections significantly. For membranes modified with 3.5 to 7.5 bilayers, we had very slight rejection of sugars (less than 15 and 30% for glucose and sucrose, respectively) and very high fluxes. Shiratori et al. [56] and Lvov et al. [57] saw this irregular film growth during their investigations. They found out polyelectrolyte film deposited on the substrate does not grow linearly until after the deposition of 2 or 3 bilayers. In one case, we continued the modification of membranes until 15 bilayers. However, we still had poor sugar separations and rejections. After deposition of 10^{th} bilayer, we had sporadic decrease

and increase in the DI water permeability. Although Kotov et al. [48] performed the polyelectrolyte multilayer deposition for more than 25 bilayers, we believe that for porous polysulfone substrate, deposition of more than 9-10 bilayer with our operating parameters results in an unstable multilayer. This poor result is maybe due to the incomplete coverage of membrane surface with polyelectrolyte multilayers. The NMWCO of the membrane is a very important factor. Bruening et al. [47] found that for spongy and porous substrates that do not have continuous flat surface, full coverage of the membrane surface is not attained, and there may be some pores not fully covered with polyelectrolyte films.

To further improve the deposition of polyelectrolyte multilayer on polysulfone support, we used dynamic LbL polyelectrolyte deposition method. This method was first proposed by Ji et al. [58]. We tried to pressurize the membrane cell containing polyelectrolyte solution, to push the solution through the membrane. This idea could help us to increase the efficiency of film deposition. DI water permeability and model sugar solution fluxes and rejections showed us that this modification was more efficient to cover the polysulfone porous substrate. We also tried to improve the film deposition by adjusting the pH of the polyelectrolyte solution (in case of [PAA/PDADMAC]) and changing the electrolyte support concentrations. Tjipto et al. [49] investigated the effect of pH and salt contents on deposition of polyelectrolytes. They found out that salt and pH changes the orientation and assembly of polyelectrolyte films.

Table 2 . Effect of different operating conditions of separation of sugars with modified membranes. The final layer is deposited with NaCl concentration of 2.5 M.

n	Deposited Polyelectrolytes	Support Concentration	Contact Time	Polyelectrolyte Concentration	Rejection			Selectivity		
					Xylose	Glucose	Sucrose	Xylose/ Sucrose	Glucose/ Sucrose	Xylose/ Glucose
3.5	PSS/PDADMAC	0.5	5	20	5.41	8.86	24.8	1.25	1.21	1.03
3.5	PSS/PDADMAC	1.5	5	20	6.42	9.10	25.7	1.25	1.22	1.02
4.5	PSS/PDADMAC	0.5	5	20	4.35	5.21	13.61	1.10	1.09	1.00
5.5	PSS/PDADMAC	0.5	5	20	7.51	10.21	27.80	1.28	1.24	1.03
5.5	PSS/PDADMAC	0.5	30	20	7.45	12.38	28.74	1.29	1.22	1.05
5.5	PSS/PDADMAC	0.5	30	100	4.51	9.51	26.83	1.30	1.23	1.05
5.5	PSS/PDADMAC*	0.5	30	80	36.92	48.08	85.76	4.42	3.64	1.21
5.5	PAA/PDADMAC	0.5	30	20	3.52	6.56	19.4	1.19	1.15	1.03
5.5	PAA/PDADMAC	0.5	30	40	4.58	7.03	20.1	1.19	1.16	1.02

*Modified using dynamic LbL deposition

We gradually increased the concentration of polyelectrolyte solutions from 20 mM to 80 mM. The final protocol we obtained was to modify the polysulfone substrate by dynamic LbL deposition of 80 mM of polyelectrolyte solution dissolved in 0.5 M NaCl for 30 minutes. After each deposition, we rinsed the cell with 30 mL of DI water for 5 minutes. We will discuss the experimental results in the following discussions. SEM images showed us that our polysulfone unmodified membrane has a very uneven surface with multitude scratches on the surface. This is maybe the reason we should have used higher concentrations of polyelectrolytes with higher contact times.

4.3. PSS/PDADMAC Modified Membranes

As discussed earlier, we tested different methods to modify the surface of polysulfone membranes with polyelectrolyte multilayers. In our experiments, we first started with static LbL adsorption. Polyelectrolyte solutions were containing 20 mM of each polyelectrolyte dissolved in 0.5 mM of NaCl. For the final layer we increased the concentration of support electrolyte to 2.5 M. However, we could not see significant changes in performance of membranes with 3.5, 5.5 and 7.5 bilayers. To improve the deposition of polyelectrolyte films and improve the sugar rejections, we had the option to change the deposition conditions. First, we tried to increase the electrolyte support concentration. Then, we tried to increase the contact time and polyelectrolyte concentration as well. Some of the results are reported in Table 2. Changing these parameters was not very effective to improve the separation characteristics of our membranes. In one of the test we used dynamic LBL deposition (tagged with * in Table 2). This membrane showed better performance compared to other membranes. In one of the tests we also increased the electrolyte support concentration to 1.5 M NaCl, and continued the deposition to 3.5 bilayers. The aim was to increase the concentration of electrolyte support for the first layer in order to enhance the

deposition of polyelectrolyte. However, the performance of the membrane was not improved. We could see slight increases in sugar rejections and separations. Table 2 shows some of the results for sugar rejections and selectivity for [PSS/PDADMAC] modified with static LbL deposition. Longer deposition time also was not very effective. As can be seen, we had a very slight improvement in separation of sugars. Generally, we believe the deposition of the first layer was successful since we had about at least 50% decrease in DI water fluxes after the deposition of the first bilayer. However, this trend was not seen in the subsequent bilayer depositions.

We followed our experiments with dynamic LbL deposition of polyelectrolytes. Table 3, 4 and 5 show the DI water fluxes and sugar rejections and separations for 5 kDa, 50 kDa and 100 kDa membranes, respectively. As shown in Table 4, the 50 kDa membrane deposited with 7.5 bilayers of [PSS/PDADMAC] displayed the best performance. It could reject xylose, glucose and sucrose with 23, 63 and 97%, and selectivity of glucose to sucrose of 11. Addition of extra layers on the membrane surface could result in higher rejections and separation factors, while decreasing the flux through the membrane. Better performance of 50 kDa membrane may be due to the larger pore sizes of this membrane. Larger pores results in pores filled with polyelectrolytes, and better rejection.

Table 3: Solution Fluxes, Solute Rejections, and Selectivities in NF (20 psi) of 20 mM sugar solution through Membranes Composed of [PSS/PDADMAC]n PSS Deposited on Ultrafiltration Supports with 100 kDa MWCO. Membranes were capped with 80 mM PSS with 2.5 M NaCl electrolyte

n	**Sugar Flux (L.M.H) @ 20 psi**	**Solute Rejection**			**Selectivity**		
		Xylose Rejection	Glucose Rejection	Sucrose Rejection	Xylose/ Glucose	Xylose/ Sucrose	Glucose/ Sucrose
3.5	4.59	21.27	48.78	82.24	1.54	4.43	2.88
5.5	3.95	34.05	58.34	87.64	1.58	5.33	3.37
7.5	3.13	38.75	60.61	89.35	1.60	5.11	4.55

Table 4: Solution fluxes, solute rejections, and selectivities in NF (20 psi) of 20 mM sugar solution through membranes composed of [PSS/DADMAC]n PSS deposited on ultrafiltration supports with 50 kDa MWCO. Membranes were capped with 80 mM PSS with 2.5 M NaCl electrolyte.

n	**Sugar Flux (L.M.H) @ 20 psi**	**Solute Rejection**			**Selectivity**		
		Xylose Rejection	Glucose Rejection	Sucrose Rejection	Xylose/ Glucose	Xylose/ Sucrose	Glucose/ Sucrose
3.5	4.51	22.73	44.72	85.58	1.40	5.36	3.83
5.5	3.56	19.47	49.91	91.38	1.61	9.35	5.81
7.5	2.88	23.15	63.29	96.67	2.09	23.05	11.01

Table 5: Solution fluxes, solute rejections, and selectivities in NF (20 psi) of 20 mM sugar solution through membranes composed of [PSS/PDADMAC]n PSS deposited on ultrafiltration supports with 5 kDa MWCO. Membranes were capped with 80 mM PSS with 2.5 M NaCl electrolyte.

n	Sugar Flux (L.M.H) @ 20 psi	Solute Rejection			Selectivity		
		Xylose Rejection	Glucose Rejection	Sucrose Rejection	Xylose/Glucose	Xylose/ Sucrose	Glucose/ Sucrose
3.5	4.47	21.28	48.78	82.24	1.54	4.43	2.88
5.5	3.90	25.47	58.91	91.38	1.81	8.65	4.77
7.5	3.19	34.15	61.33	95.67	1.70	15.19	8.92

We also investigated the effect of capping layer with high concentration of NaCl. We modified 5 kDa membranes with 5 bilayers of [PSS/PDADMAC] polyelectrolytes. One of the membranes was capped with PSS layer with 2.5 M NaCl as the supporting electrolyte, and we performed filtration tests with these membranes. Results showed that the membrane capped with final PSS layer at high supporting electrolyte concentration showed much higher selectivity of glucose/sucrose while having smaller flux. Capped membrane also showed sugar separation flux of 3.90 L. M^{-2}. h^{-1} while the uncapped one showed 12.55 L. M^{-2}. h^{-1}. Miller et al. [46] suggested that this phenomena is due to the swelling characteristics of PDADMAC coating.

4.4. PAA/PDADMAC Modified Membranes

We followed the same approach to modify the polysulfone substrate with multilayer polyelectrolytes. First, we started the modification using static LbL deposition. After deposition of the first bilayer, we had a significant drop in the permeability of the membranes. However, we

had the same problem with deposition of subsequent bilayers. Addition of more bilayers on the membrane did not lead to full deposition of multilayer polyelectrolytes. We also tried to adjust the pH of polyelectrolyte solution between 2-5. Based on Shiratori et al. [56], the highest thickness of the deposited polyelectrolyte is attained at pH 5. We had still very slight decrease in the DI water flux and increase in sugar rejections and separations with PAA solutions at pH 5. Then, we tried to modify polysulfone membranes by dynamic LbL deposition. During the dynamic LbL deposition of PAA/PDADMAC multilayers, we could not make significant change in separation of sugars by deposition of layers on the membrane substrate. Changing deposition time, adjusting pH, and addition of more bilayers on the membrane resulted in separation of glucose from sucrose with the factor of 1.77, which is shown in Table 7. At these specific test, we modified the 50 kDa membrane with 5.5 bilayers of PAA/PDADMAC polyelectrolyte multilayers.

Table 6: Solution fluxes, solute rejections, and selectivities in NF (20 psi) of 20 mM sugar solution through membranes composed of [PAA/PDADMAC]3 PAA deposited on ultrafiltration supports.

N	MWCO	Sugar Flux (L.M.H) @ 20 psi	Solute Rejection			Selectivity		
			Xylose Rejection	Glucose Rejection	Sucrose Rejection	Xylose/Glucose	Xylose/ Sucrose	Glucose/ Sucrose
3.5	5	5.55	3.92	6.82	11.43	1.03	1.08	1.05
3.5	50	10.2	3.79	9.01	16.59	1.05	1.15	1.09
3.5	100	25.2	68.44	79.16	84.12	1.51	1.98	1.31

Table 7: Solution fluxes, solute rejections, and selectivities in NF (20 psi) of 20 mM sugar solution through membranes composed of [PAA/PDADMAC]n PAA deposited on ultrafiltration supports with 50 kDa MWCO.

n	Supporting Electrolyte Concentration (M)	Sugar Flux (L.M.H) @ 20 psi	Solute Rejection			Selectivity		
			Xylose Rejection	Glucose Rejection	Sucrose Rejection	Xylose/Glucose	Xylose/Sucrose	Glucose/Sucrose
3.5	0.2	6.89	16.52	33.09	52.78	1.24	1.76	1.41
5.5	0.2	4.18	15.14	33.08	60.87	1.26	2.16	1.71

Table 8: Solution Fluxes, solute rejections, and selectivities in NF (20 psi) of 20 mM sugar solution through membranes composed of [PAA/PDADMAC] 5 PAA deposited on ultrafiltration supports with 50 kDa MWCO.

n	Polyelectrolyte Concentration (mM)	Sugar Flux (L.M.H) @ 20 psi	Solute Rejection			Selectivity		
			Xylose Rejection	Glucose Rejection	Sucrose Rejection	Xylose/Glucose	Xylose/Sucrose	Glucose/Sucrose
3.5	80	5.65	40.34	56.32	72.74	1.36	2.18	1.60
5.5	40	6.89	16.524	33.09	52.78	1.24	1.76	1.41

4.5. Comparison of Polyelectrolyte Multilayer Modified Membranes with NF270/NF90 Rejections and Fluxes

To compare the performance of polyelectrolyte multilayer deposited membrane with commercially available membranes, we did model sugar filtration tests with NF90 and NF270 (Dow Filmtech, Edina, MN). We used a HP4750 Sterlitech (Kent, WA) NF stirred cell loaded with

these membranes. The membrane was soaked in DI water for 24 hours prior to filtration tests, in which the water was changed at least for 3 times. Afterwards, the membrane was loaded in the cell and pressurized to 45 psi to compact the membrane, following with DI water permeability measurement. The stirring speed was 300 rpm. We prepared the same sugar feed solution with citric acid in 20 mM citric acid-sodium phosphate dibasic buffer at pH 7.5 and loaded the cell with 150 mL of this solution and pressurized the cell to 45 psi. We collected permeate until it reached 25 mL and, and collected 1 mL of permeate after each 5 mL. The reported fluxes, rejection and selectivities are the average of three points. The highest glucose/sucrose separation factor we obtained was 1.15 at pH 7.5. Also, it is interesting to compare the rejection and flux values for the commercial and polyelectrolyte multilayer membranes. NF270 was able to reject xylose, glucose and sucrose with 19, 26 and 68%, respectively. Permeate flux was measured to be 7.66 L m^{-2} h^{-1} bar^{-1}. NF90 is a tighter nanofiltration membrane and rejected xylose, glucose and sucrose with more than 98, 99 and 99%. It also showed much lower fluxes 1.68 L m^{-2} h^{-1} bar^{-1}. The highest separation and rejection for sugars using polyelectrolyte multilayer modified membranes obtained with 50 kDa polysulfone membranes deposited with 7.5 PSS/PDADMAC bilayers. Membrane had 61% and 96% rejection for glucose and sucrose with permeability of 2.11 L m^{-2} h^{-1} bar^{-1}. We should also keep in mind that higher operating pressures results in higher rejections of sugars [59]. NF filtration using commercial NF270 membrane was performed at 3.1 bar, which means at lower pressures the rejection and separation factors can be poorer. This comparison shows us that the excellent control over the polysulfone membranes results in production of a highly permeable defect-free membrane. The high flux is due to deposition of ultrathin layer on porous support.

5. Conclusion

Application of membrane-based separations in future biorefineries may results in better economic bioconversion process. Fractionation of biomass slurry is an option. We can perform separate fermentation for hexose and pentose sugars. Separate fermentation is more economic and effective. Also fractionation can help us to diminish the degradation of some of the hydrolysate compounds such as sucrose. Here, we studied the modification of polysulfone membranes for separation and fractionation of mono- and di-saccharide present in our model sugar feed solution. We could successfully modify 5, 50, and 100 kDa polysulfone membranes with [PSS/PDADMAC] polyelectrolytes. We used static LbL deposition, as well as dynamic deposition. These modified membranes were able to separate glucose and sucrose with selectivity in the range of 5-11. We also tried to modify polysulfone membranes with [PAA/PDADMAC] polyelectrolytes. However, both static and dynamic LbL deposition were not successful for modification of polysulfone membranes with [PAA/PDADMAC] polyelectrolytes. We investigated the effect of different parameters such as contact time, polyelectrolyte concentration, electrolyte support concentration, membrane MWCO, and number of deposited layers. We also investigated the effect of pH for [PAA/PDADMAC] modified membranes.

6. References

[1] T. Uemura, H. Masahiro, Thin-film composite membranes for reverse osmosis, in: N.N. Li, A.G. Fane, W.S.W. Ho, T. Matsuura (Eds.), Adv. Membr. Technol. Appl., John Wiley & Sons, Inc., Hoboken, NJ, USA, 2008.

[2] P. Eriksson, Nanofiltration extends the range of membrane filtration, Environ. Prog. 7 (1988) 58–62.

[3] W.J. Conlon, S.A. McClellan, Membrane softening: a treatment process comes of age, J. Am. Water Work. Assoc. 81 (n.d.) 47–51.

[4] B. Van der Bruggen, J. Geens, Nanofiltration in advanced membrane technology and applications, in: N.N. Li, A.G. Fane, W.S.W. Ho, T. Matsuura (Eds.), Adv. Membr. Technol. Appl., Hoboken, NJ, USA, 2008.

[5] G. Murthy, S. Sridhar, M. Shyamsunder, B. Shankaraiah, M. Ramkrishna, Concentration of xylose reaction liquor by nanofiltration for the production of xylitol sugar alcohol, Sep. Purif. Technol. 44 (2005) 221–228.

[6] C. Abels, F. Carstensen, M. Wessling, Membrane processes in biorefinery applications, J. Memb. Sci. 444 (2013) 285–317.

[7] Q. Gan, S.. Allen, G. Taylor, Design and operation of an integrated membrane reactor for enzymatic cellulose hydrolysis, Biochem. Eng. J. 12 (2002) 223–229.

[8] S. Kinoshita, J.W. Chua, N. Kato, T. Yoshida, H. Taguchi, Hydrolysis of cellulose by cellulases of Sporotrichum cellulophilum in an ultrafilter membrane reactor, Enzyme Microb. Technol. 8 (1986) 691–695.

[9] I. Ohlson, G. Trägårdh, B. Hahn-Hägerdal, Enzymatic hydrolysis of sodium-hydroxide-pretreated sallow in an ultrafiltration membrane reactor., Biotechnol. Bioeng. 26 (1984) 647–53.

[10] K. Bélafi-Bakó, A. Koutinas, N. Nemestóthy, L. Gubicza, C. Webb, Continuous enzymatic cellulose hydrolysis in a tubular membrane bioreactor, Enzyme Microb. Technol. 38 (2006) 155–161.

[11] F. Carstensen, A. Apel, M. Wessling, In situ product recovery: Submerged membranes vs. external loop membranes, J. Memb. Sci. 394-395 (2012) 1–36.

[12] J.J. Harris, J.L. Stair, M.L. Bruening, Layered Polyelectrolyte Films as Selective, Ultrathin Barriers for Anion Transport, Chem. Mater. 12 (2000) 1941–1946.

[13] E. Tsakalidou, E. Alichanidis, D.L. Oliveira, R.A. Wilbey, A.S. Grandison, L.C. Duarte, et al., Separation of oligosaccharides from caprine milk whey, prior to prebiotic evaluation, Int. Dairy J. 24 (2012) 102–106.

[14] N. V. Patil, A.E.M. Janssen, R.M. Boom, The potential impact of membrane cascading on downstream processing of oligosaccharides, Chem. Eng. Sci. 106 (2014) 86–98.

[15] J. Shi, W. Zhang, Y. Su, Z. Jiang, Composite polyelectrolyte multilayer membranes for oligosaccharides nanofiltration separation, Carbohydr. Polym. 94 (2013) 106–113.

[16] C. Nobre, J.A. Teixeira, L.R. Rodrigues, New trends and technological challenges in the industrial production and purification of fructo-oligosaccharides, Crit. Rev. Food Sci. Nutr. (2013) 131011062919009.

[17] A. Giacobbo, A.M. Bernardes, M.N. de Pinho, Nanofiltration for the Recovery of Low Molecular Weight Polysaccharides and Polyphenols from Winery Effluents, Sep. Sci. Technol. 48 (2013) 2524–2530.

[18] H.H. Himstedt, H. Du, K.M. Marshall, S.R. Wickramasinghe, X. Qian, pH Responsive Nanofiltration Membranes for Sugar Separations, Ind. Eng. Chem. Res. 52 (2013) 9259–9269.

[19] A. Dutta, N. Dowe, K.N. Ibsen, D.J. Schell, A. Aden, An economic comparison of different fermentation configurations to convert corn stover to ethanol using Z. mobilis and Saccharomyces., Biotechnol. Prog. 26 (n.d.) 64–72.

[20] B.L. Boynton, J.D. McMillan, High-yield shake-flask fermentation of xylose to ethanol, Appl. Biochem. Biotechnol. 45-46 (1994) 509–514.

[21] T. Lindén, B. Hahn-Hägerdal, Fermentation of lignocellulose hydrolysates with yeasts and xylose isomerase, Enzyme Microb. Technol. 11 (1989) 583–589.

[22] B. Hahn-Hägerdal, H. Jeppsson, K. Skoog, B.A. Prior, Biochemistry and physiology of xylose fermentation by yeasts, Enzyme Microb. Technol. 16 (1994) 933–943.

[23] B. Hahn-Hägerdal, K. Karhumaa, C. Fonseca, I. Spencer-Martins, M.F. Gorwa-Grauslund, Towards industrial pentose-fermenting yeast strains., Appl. Microbiol. Biotechnol. 74 (2007) 937–53.

[24] B. Hahn-Hägerdal, M. Galbe, M.F. Gorwa-Grauslund, G. Lidén, G. Zacchi, Bio-ethanol – the fuel of tomorrow from the residues of today, Trends Biotechnol. 24 (2006) 549–556.

[25] R. Huang, R. Su, W. Qi, Z. He, Bioconversion of Lignocellulose into Bioethanol: Process Intensification and Mechanism Research, BioEnergy Res. 4 (2011) 225–245.

[26] Y. Lin, S. Tanaka, Ethanol fermentation from biomass resources: current state and prospects., Appl. Microbiol. Biotechnol. 69 (2006) 627–42.

[27] J. Zaldivar, J. Nielsen, L. Olsson, Fuel ethanol production from lignocellulose: a challenge for metabolic engineering and process integration, Appl. Microbiol. Biotechnol. 56 (2001) 17–34.

[28] D. Wandera, S.R. Wickramasinghe, S.M. Husson, Stimuli-responsive membranes, J. Memb. Sci. 357 (2010) 6–35.

[29] M. Ulbricht, Advanced functional polymer membranes, Polymer (Guildf). 47 (2006) 2217–2262.

[30] G. Decher, Fuzzy Nanoassemblies: Toward Layered Polymeric Multicomposites, Science (80-.). 277 (1997) 1232–1237.

[31] J. Meier-Haack, M. Müller, Use of polyelectrolyte multilayer systems for membrane modification, Macromol. Symp. 188 (2002) 91–104.

[32] R.H. Lajimi, A. Ben Abdallah, E. Ferjani, M.S. Roudesli, A. Deratani, Change of the performance properties of nanofiltration cellulose acetate membranes by surface adsorption of polyelectrolyte multilayers, Desalination. 163 (2004) 193–202.

[33] A.M. Hollman, D. Bhattacharyya, Pore Assembled Multilayers of Charged Polypeptides in Microporous Membranes for Ion Separation, Langmuir. 20 (2004) 5418–5424.

[34] X. Liu, M.L. Bruening, Size-Selective Transport of Uncharged Solutes through Multilayer Polyelectrolyte Membranes, Chem. Mater. 16 (2004) 351–357.

[35] B.W. Stanton, J.J. Harris, M.D. Miller, M.L. Bruening, Ultrathin, Multilayered Polyelectrolyte Films as Nanofiltration Membranes, Langmuir. 19 (2003) 7038–7042.

[36] W. Lenk, J. Meier-Haack, Polyelectrolyte multilayer membranes for pervaporation separation of aqueous-organic mixtures, Desalination. 148 (2002) 11–16.

[37] J. Meier-Haack, W. Lenk, D. Lehmann, K. Lunkwitz, Pervaporation separation of water/alcohol mixtures using composite membranes based on polyelectrolyte multilayer assemblies, J. Memb. Sci. 184 (2001) 233–243.

[38] P.M. Budd, N.M.P.S. Ricardo, J.J. Jafar, B. Stephenson, R. Hughes, Zeolite/Polyelectrolyte Multilayer Pervaporation Membranes for Enhanced Reaction Yield, Ind. Eng. Chem. Res. 43 (2004) 1863–1867.

[39] J.-M. Leväsalmi, T.J. McCarthy, Poly(4-methyl-1-pentene)-Supported Polyelectrolyte Multilayer Films: Preparation and Gas Permeability 1, Macromolecules. 30 (1997) 1752–1757.

[40] W. Chen, T.J. McCarthy, Layer-by-Layer Deposition: A Tool for Polymer Surface Modification, Macromolecules. 30 (1997) 78–86.

[41] D.M. Sullivan, M.L. Bruening, Ultrathin, Gas-Selective Polyimide Membranes Prepared from Multilayer Polyelectrolyte Films, Chem. Mater. 15 (2003) 281–287.

[42] K.P. Xiao, J.J. Harris, A. Park, C.M. Martin, V. Pradeep, M.L. Bruening, Formation of Ultrathin, Defect-Free Membranes by Grafting of Poly(acrylic acid) onto Layered Polyelectrolyte Films, Langmuir. 17 (2001) 8236–8241.

[43] S.U. Hong, R. Malaisamy, M.L. Bruening, Separation of fluoride from other monovalent anions using multilayer polyelectrolyte nanofiltration membranes., Langmuir. 23 (2007) 1716–22.

[44] S.U. Hong, M.D. Miller, M.L. Bruening, Removal of Dyes, Sugars, and Amino Acids from NaCl Solutions Using Multilayer Polyelectrolyte Nanofiltration Membranes, Ind. Eng. Chem. Res. 45 (2006) 6284–6288.

[45] W. Shan, P. Bacchin, P. Aimar, M.L. Bruening, V. V. Tarabara, Polyelectrolyte multilayer films as backflushable nanofiltration membranes with tunable hydrophilicity and surface charge, J. Memb. Sci. 349 (2010) 268–278.

[46] M.D. Miller, M.L. Bruening, Controlling the nanofiltration properties of multilayer polyelectrolyte membranes through variation of film composition., Langmuir. 20 (2004) 11545–51.

[47] R. Malaisamy, M.L. Bruening, High-flux nanofiltration membranes prepared by adsorption of multilayer polyelectrolyte membranes on polymeric supports., Langmuir. 21 (2005) 10587–92.

[48] N.A. Kotov, S. Magonov, E. Tropsha, Layer-by-Layer Self-Assembly of Alumosilicate−Polyelectrolyte Composites: Mechanism of Deposition, Crack Resistance, and Perspectives for Novel Membrane Materials, Chem. Mater. 10 (1998) 886–895.

[49] E. Tjipto, J.F. Quinn, F. Caruso, Assembly of multilayer films from polyelectrolytes containing weak and strong acid moieties., Langmuir. 21 (2005) 8785–92.

[50] W. Jin, A. Toutianoush, B. Tieke, Use of Polyelectrolyte Layer-by-Layer Assemblies as Nanofiltration and Reverse Osmosis Membranes, Langmuir. 19 (2003) 2550–2553.

[51] L.Y. Ng, A.W. Mohammad, C.Y. Ng, A review on nanofiltration membrane fabrication and modification using polyelectrolytes: effective ways to develop membrane selective barriers and rejection capability., Adv. Colloid Interface Sci. 197-198 (2013) 85–107.

[52] W. Shan, P. Bacchin, P. Aimar, M.L. Bruening, V. V. Tarabara, Polyelectrolyte multilayer films as backflushable nanofiltration membranes with tunable hydrophilicity and surface charge, J. Memb. Sci. 349 (2010) 268–278.

[53] J.C. Yang, M.J. Jablonsky, J.W. Mays, NMR and FT-IR studies of sulfonated styrene-based homopolymers and copolymers, Polymer (Guildf). 43 (2002) 5125–5132.

[54] D. Yoo, S.S. Shiratori, M.F. Rubner, Controlling Bilayer Composition and Surface Wettability of Sequentially Adsorbed Multilayers of Weak Polyelectrolytes, Macromolecules. 31 (1998) 4309–4318.

[55] M. McCormick, R.N. Smith, R. Graf, C.J. Barrett, L. Reven, H.W. Spiess, NMR Studies of the Effect of Adsorbed Water on Polyelectrolyte Multilayer Films in the Solid State, Macromolecules. 36 (2003) 3616–3625.

[56] S.S. Shiratori, M.F. Rubner, pH-Dependent Thickness Behavior of Sequentially Adsorbed Layers of Weak Polyelectrolytes, Macromolecules. 33 (2000) 4213–4219.

[57] Y. Lvov, G. Decher, H. Moehwald, Assembly, structural characterization, and thermal behavior of layer-by-layer deposited ultrathin films of poly(vinyl sulfate) and poly(allylamine), Langmuir. 9 (1993) 481–486.

[58] S. Ji, G. Zhang, Z. Liu, Y. Peng, Z. Wang, Evaluations of polyelectrolyte multilayer membranes assembled by a dynamic layer-by-layer technique, Desalination. 234 (2008) 300–306.

[59] E. Sjöman, M. Mänttäri, M. Nyström, H. Koivikko, H. Heikkilä, Separation of xylose from glucose by nanofiltration from concentrated monosaccharide solutions, J. Memb. Sci. 292 (2007) 106–115.

College of Engineering

Ralph E. Martin Department of Chemical Engineering

Appendix 4 A: Multiple Author Documentation

To whom it may concern,

Hereby, I confirm that Mr. Malmali has done more than 51% of the work for chapter 4 of this dissertation. The list of authors is as follow:

Mohammadmahdi Malmali

S. Ranil Wickramasinghe

S. Ranil Wickramasinghe, PhD

Professor, Ross E Martin Chair in Emerging Technologies
Ralph E Martin Department of Chemical Engineering
University of Arkansas
3202 Bell Engineering Center

Conclusion

Concluding Remarks

Dead-end filtration experiments have been conducted using model and real hydrolysates to screen a number of commercially available membranes under a range of conditions. Design of experiments software enabled minimization of the number of experiments while yet indicating the effect of the various variables that were investigated on membrane performance. This work highlights the fact that nanofiltration could be a viable process for sugar concentration in biomass hydrolysates while reducing the load of toxic compounds prior to fermentation. Often selection of an appropriate membrane and optimum operating conditions is complex and time consuming. The method developed here could be used to quickly screen membranes. Promising membranes and operating conditions could then be more rigorously tested in tangential flow operation.

We investigated the enzymatic hydrolysis of biomass in batch, semibatch and continuous mode. Effect of temperature, pH and hydrolysis time was studied in batch experiments. MF and UF membranes were employed in membrane bioreactor to run the enzymatic hydrolysis experiments in semibatch and continuous tests. Results showed that both membranes are able to retain cellulose and enzyme inside the bioreactor. Retention of enzymes was possible since the enzyme binds to the cellulosic substrate. Semibatch experiments showed that cellulose loading has a significant effect on hydrolysis process. Agitating speed is also very important. However, we are limited by high viscosity since biomass exhibit non-Newtonian behavior. Higher cellulose loading is also effective. We investigated the effect of reactor retention time, pre-holding time, and cellulose loading during our continuous tests. Results showed that higher retention times leads to higher glucose production. As a result we will have more product inhibition and slower glucose production. There is a tradeoff between retention time and pre-holding time. Pre-holding time is

an important processing parameter which gives the enzyme enough time to bind to cellulose. Higher cellulose loading can decrease dependency of continuous experiments on pre-holding time.

Application of membrane-based separations in future biorefineries may results in better economic bioconversion process. Fractionation of biomass slurry is an option. We can perform separate fermentation for hexose and pentose sugars. Separate fermentation is more economic and effective. Also fractionation can help us to diminish the degradation of some of the hydrolysate compounds such as sucrose. Here, we studied the modification of polysulfone membranes for separation and fractionation of mono- and di-saccharide present in our model sugar feed solution. We could successfully modify 5, 50, and 100 kDa polysulfone membranes with [PSS/PDADMAC] polyelectrolytes. We used static LbL deposition, as well as dynamic deposition. These modified membranes were able to separate glucose and sucrose with selectivity in the range of 5-11. We also tried to modify polysulfone membranes with [PAA/PDADMAC] polyelectrolytes. However, both static and dynamic LbL deposition were not successful for modification of polysulfone membranes with [PAA/PDADMAC] polyelectrolytes. We investigated the effect of different parameters such as contact time, polyelectrolyte concentration, electrolyte support concentration, membrane MWCO, and number of deposited layers. We also investigated the effect of pH for [PAA/PDADMAC] modified membranes.